CORE–SHELL PVA/GELATIN NANOFIBROUS SCAFFOLDS USING MULTINOZZLE AQUEOUS ELECTROSPINNING

by

Mustafa Şengör

B.S., Mechanical Engineering, Boğaziçi University, 2010

M.S., Mechanical Engineering, Boğaziçi University, 2013

Submitted to the Institute for Graduate Studies in
Science and Engineering in partial fulfillment of
the requirements for the degree of
Doctor of Philosophy

Graduate Program in Mechanical Engineering

Boğaziçi University

2019

This thesis is dedicated to my beloved wife

ACKNOWLEDGEMENTS

I would like to express my sincere gratitude to my thesis supervisor Prof. Dr. Sabri ALTINTAŞ for his invaluable guidance and help during the preparation of this dissertation. I would like to mention his patience, giving me inspiration and motivation.

Besides my advisor, I would like to thank my thesis committee member, Prof H. Bedir, Assoc. Prof. B. Garipcan, Assist Prof. M. İpekoğlu, Assist Prof. G. Vardar, Assoc. Prof. E. Alaca for their encouragement and astute comments.

Also I would like to thank Assoc. Prof. M. Çelik separately due to helping me at critical times without any expectation.

It is impossible for me to thank my parents Melihat and Nurettin Şengör enough for supporting me during my life. I also would like to thank especially to my dear brothers Arif, Sinan, Ömer and sister Gülseda, because sometimes human-beings require empathy more than a physical or mental support.

My wife and daughters are the columns of this thesis. I would also like to thank my mother-in-law and father-in-law for their blessings.

I would like to thank Fatih Öz, Amin and his precious wife Sedef for their kind supports.

It is impossible to state my friends one by one. But precious friends of "Last 8-horses" are still holding an important place in my life therefore in this thesis.

ABSTRACT

CORE–SHELL PVA/GELATIN NANOFIBROUS SCAFFOLDS USING MULTINOZZLE AQUEOUS ELECTROSPINNING

Biological scaffolds have been used in the reconstruction of the damaged tissues. They have similar morphology and structure to the host tissues. However, they can be produced using materials that can be harmful to humans and the environment. In this context, core-shell nanofiber based scaffolds, whose mechanical strengths are provided by PVA(poly vinyl alcohol) and recognition sites are provided by gelatin, were fabricated in a non-woven manner using multiple nozzles of electrospinning technique. Instead of widely used toxic, acidic or salt-based ionic solvents, deionized "water" was used as the only solvent for both polymers. Firstly, nanofibers were produced from 8 % (w / w) gelatin and 8%(w / w) PVA solutions individually. Limits were determined for parameters such as voltage, feed rate, temperature and polymer concentrations. Although pure gelatin nanofibers have diameters of less than 50 nm, they have beaded structure and have lower mechanical strengths. Smooth fibers were obtained from 8% PVA. Fibers with PVA: gelatin core shell morphology were then produced at different feed rate ratios (FRR). Based on the fiber diameter, the optimal FRR with a 15 kV voltage magnitude and 15 cm electrode distance was found to be 1: 1 with an average diameter of 280 nm. The ratio of 1: 3 and 1: 4 was seen as the formation of "beaded" fibers and the pealing limit of gelatin over PVA, respectively. Mechanical and water resistance of the produced scaffolds was further improved by cross-linking. Core - shell morphology was demonstrated by TEM, SEM, EDS analysis. The secondary structure of the gelatin from collagen and the effects of the electrospinning were revealed by FTIR and DSC. Approximately 60% of all cross-linked scaffolds were degraded in solution using lysozyme enzyme up to day 14.

ÖZET

SU BAZLI, ÇOKLU NOZÜL ELEKTROEĞİRME YÖNTEMI İLE EŞ EKSENLİ PVA/JELATİN NANOFİBER İSKELELERİN ÜRETİMİ

Zarar görmüş dokuların iyileşmesinde kullanılan, ev sahibi doku ile yakın içerik ve morfolojiye sahip biyolojik iskeleler kullanılmaktadır. Fakat, iskelelerin imalatları esnasında sağlığına ve doğaya zararlı maddeler de kullanılabiliyor. Bu çalışmada üretim esnasında sağlığa ve çevreye zararsız, "su"dan elde edilmiş, elektro-eğirme yöntemiyle üretilmiş, eş eksenli, nanofiber bazlı iskelelerin üretimi ele alınmıştır. Bu bağlamda mekanik dayanımı polivinil alkol (PVA)' dan sağlayan, hücreler tarafından tanınma özelliğini de jelatinden alan eş eksenli nanofiberler çoklu nozül kullanılarak üretildi. Genel olarak kullanılan toksik, asidik ya da tuz bazlı iyonik çözücüler yerine, iki polimer için de çözücü olarak deiyonize "su" kullanıldı. Önce tekil olarak %8 (a/a) jelatin ve %8 (a/a) PVA çözeltilerinden nanofiberler üretildi. Voltaj, elektrod mesafesi, besleme hızı, sıcaklık, konsantrasyon gibi parametreler ile sınırlar belirlendi. Saf jelatin nanofiberleri 50 nm den az çapa sahip olsalar da boncuklu yapıya sahipler ve tek başlarına mekanik olarak dayanımları düşüktü. %8 PVA fiberleri kendi başlarına pürüzsüz olarak üretildi. Daha sonra farklı besleme hız oranlarında (BHO) PVA:jelatin çekirdek kabuk morfolojili fiberler üretildi. Fiber çapı baz alınarak, 15 kV voltaj büyüklüğünde, 15 cm elektrod mesafesinde en uygun BHO'nun 280 nm ortalama çap ile 1:1 oranı olduğu görüldü. 1:3 ve 1:4 oranları ise "bead"li fiber oluşumu ve jelatinin PVA'nın üzerinden sıyrılma limiti olarak görüldü. Üretilen iskelelerin mekanik ve suya karşı dayanımları, çapraz bağlama ile daha da geliştirildi. Çekirdek – kabuk morfolojisi TEM, SEM, EDS analizleri ile gösterildi. Jelatinin kolajenden miras kalmış, ikincil yapısı ve elektro-eğirmenin etkileri FTIR, DSC ile açıklandı. Çapraz bağlanmış bütün iskelelerin yaklaşık olarak %60'ı 14 günde, lysozyme enzimi kullanılan çözeltinin içerisinde bozunuma uğradı.

TABLE OF CONTENTS

LIST OF FIGURES

LIST OF TABLES

LIST OF SYMBOLS

w_i	Initial Weight
w_f	Final Weight

LIST OF ACRONYMS/ABBREVIATIONS

AC	Alternative Current
ASTM	American Society for Testing and Materials
CS	Core Shell
DC	Direct Current
DHT	Dehydrothermal Treatment
DMF	N,N dimethylformamide
DMSO	Dimethyl sulfoxide
DSC	Differential Scanning Calorimetry
ECM	Extra Cellular Matrix
EDC	1-ethyl-3-(3-dimethyl-aminopropyl)-1- carbodiimide hydrochloride
EDS	Energy Dispersive Spectroscopy
ES	Electrospinning
FDA	Food and Drug Administration
FR	Feed Rate
FRR	Feed Rate Ratio
FTIR	Fourier-transform Infrared Spectroscopy
GA	Glutaraldehyde
HA	Hyaluronic acid
HAp	Hydroxyapatite
HFIP	(1,1,1,3,3,3-hexafluoro-2-propanol)
ICH	International Council for Harmonisation of Technical Requirements for Registration of Pharmaceuticals for Human Use
NFES	Near Field Electrospinning
NHS	N- hydroxysuccinimide
PAA	poly (acylic acid)
PAN	poly (acrylonitrile)
PBS	Phosphate-buffered Saline
PCL	poly (caprolactone) (PCL),

PEG	poly (ethylene glycol)
PEO	poly (ethylene oxide)
PID	Proportional-Integral-Derivative
PLA	poly (lactic acid)
PLGA	poly (lactic-co-glycolic acid)
PLS	Pulsed Inductively Coupled Plasma
PU	poly (urethane)
PVA	poly(vinyl alcohol)
RGD	The tripeptide Arg-Gly-Asp
SEM	Scanning Electron Microscopy
TEM	Transmission Electron Microscopy
TG	Transglutaminase
TIPS	Thermally induced phase separation
TFE	Fluorinated Alcoholic Solvent of 2,2,2-trifluoroethanol
UV	Ultraviolet
WAXS	Wide-angle X-ray scattering
Wrt	With Respect To
ZnO	Zinc oxide

1. INTRODUCTION

1.1. Tissue Engineering

Tissue engineering is a discipline that appoints the principles of engineering to reproduce required signals to cells that are responsible from healing of damaged area or creating a fresh tissue. One of the essential control mechanisms of cell activities is the utilization of physical, chemical and mechanical properties of the ECM (extra-cellular matrix) which contains cues of information needed to modulate adhesion, growth, proliferation and differentiation factors [1].

Tissue transplants have been made in the world for centuries. The first attempts to transplant bone and skin goes back to the Middle Ages described by ancient documents. First proven tooth transplantation was practiced in ancient Egypt by forcing slaves to donate their masters [2]. Although different methods are used in surgeries whose quality and quantity develops as time progresses, the logic in general has remained the same and can be examined in three different categories: (i) autograft, (ii) allograft (patch from another individual of the same species), (iii) synthetic tissue patch. Autografts have many advantages in itself. Because taken graft belongs to the body itself, the tissues in the area where the transplant is performed quickly recognize the guest tissue and the risk of side effects is low [3]. However, this technique only opens a new site in the body that needs to be treated and can be applied for a limited number of operations. The second option allograft is more practical than the first case. But, it also includes problems such as tissue adaptation, not being accepted by the immune system, availability and transfer of diseases [4]. Along with these adversities, the increasing standard of living and the expectation of a faster recovery of the diseases channel the scientific world of today into the third option, synthetic tissue transplantations. It is possible to produce an imitation of a less complicated tissue with engineering. For instance, cardiovascular disease is one of the most common diseases in the world. Vascular autografts with limited availability are gradually replaced by synthetic artistic vessels in this area [5].

Synthetic tissues may vary depending on the treatment method. Required tissue can be produced synthetically and stays on the damaged area permanently as a part of the body like implants or artificial scaffolds where tissue cells can grow on it and can be degraded over time. As an example, in micro-fracture method [6], which is a method used in the treatment of articular cartilage, the cells are transported to the damaged area with a channel opening into the bone marrow. With this technology, which has been started to be used especially in recent years, bio-compatible, biodegradable artificial scaffolds are placed in the damaged area for the stem cells to locate on the cartilage and expected to repair this area.

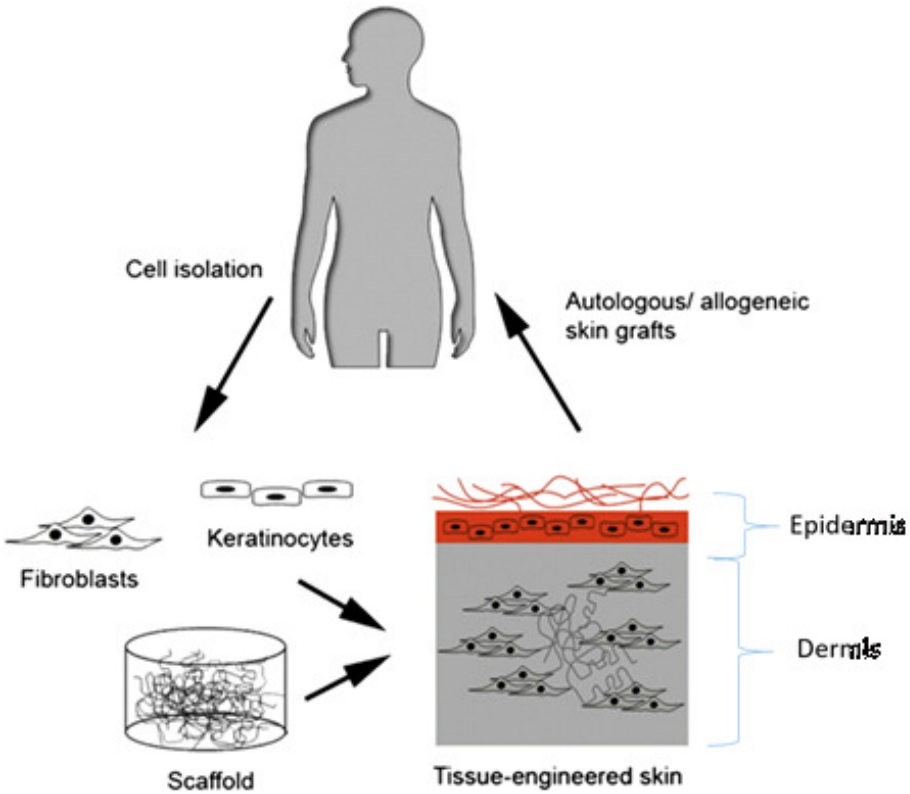

Figure 1.1. Schematic illustration of principles of skin tissue engineering (adapted from [7])

Tissue engineers in various sub-fields are trying to produce biological scaffolds on which cells can grow and infiltrate inside effectively. As shown in Figure 1.1, these platforms can serve different purposes. Polymer based scaffold should show both the mechanical properties of the original tissue as well as the biological content, so that

the host tissue cells do not define the scaffold as foreigners. For faster progress of the process, the scaffold can be fed with the cells. This is done by isolating keratinocytes and fibroblasts from donor tissue, which are then *in vitro* cultured and seed onto scaffold. For a full-thickness skin substitute, fibroblasts are first planted on the scaffold to form dermis which then seeded with keratinocytes to establish epidermis.

1.2. Skin Structure and Wound Healing

Skin is the largest organ and constituting 8% of the whole body weight. The outer shell of the skin is epidermis, which is mainly comprised of keratinocytes, protects body from external environment and prevents loss of moisture. Epidermis is divided into 4 or 5 layers through which keratinocytes gradually enlarge and flatten till the surface where the migration ends and sloughing begins [8, 9]. Calcium is the key component in the formation and differentiation of the keratinocytes. As calcium concentration increases keratinocyte differentiation increases. Other cells of the epidermis are melanocytes and Langerhans' cells where the former one responsible from tone of the skin and latter one responsible from the skin immune system [10, 11].

The dermis, just below the epidermis is a relatively thick, fibrous and elastic layer of the skin which is formed by

(i) Vascular plexus, present at that region to nourish the tissue;
(ii) Nerve endings, sense touch, pain, temperature and pressure
(iii) Cells, are mainly fibroblasts, histiocytes, mast cells, plasma cells and some dendritic cells comprise approximately 10% of the dermal content [13]. The most abundant fibroblasts are considered to be the fabrication sites of the other dermal components. Other cells are generally responsible from immunocompetence [12].
(iv) ECM, consists of different type collagen fibrils and elastic fibers, embedded in a gelatinous substance of proteoglycans. While upper ECM contains randomly distributed collagen fibers, lower part contains collagen fibers aligned parallel to the surface of the skin. (Figure 1.2)

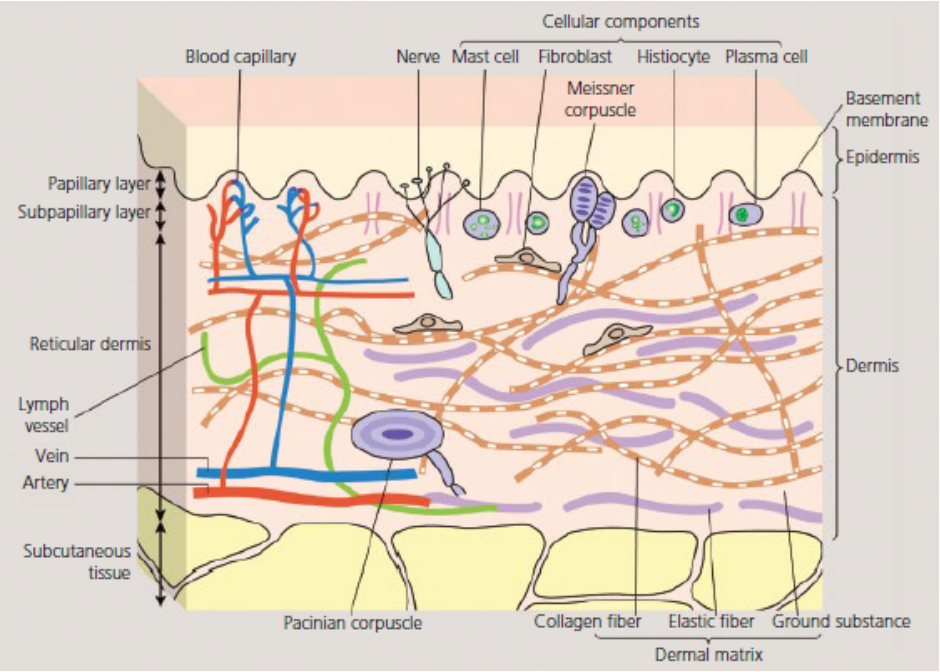

Figure 1.2. Structure of Dermis [12]

Collagens and elastin are the major elements of the skin matrix providing tensile strength and elasticity. In case of any destruction on the epidermis or dermis, platelets go to the damaged area to stop bleeding by sealing blood vessels. The platelets adhere to the exposed type 1 collagen. They induce activation signals and secrete adhesive glycoproteins, leading to platelet reformation and coagulation [14]. Fibrin derived from fibrinogen crosslinks platelets forming a barrier against microorganisms, establishes the temporary medium for cell migration via activation of thrombin enzyme and other released factors which will finally ends hemostasis stage and initiates further healing stage of inflammatory stage. At this stage cells responsible for the digestion of debris and bacteria is formed and afterwards they die and releases enzymes that break fibrins. Departed fibrins attract fibroblasts to create new matrix and other mast cells which secrete cytokines [15]. Cytokines are soluble proteins that establishes communication between cells and growth factors send information of required collagen synthesis and cell proliferation. Also ECM contains groups that interacts with integrin which is a transmembrane receptor, directing to platelet activation, epithelial migration and fibroblast movement [16]. Macrophages occurred by differentiation of monocytes phagocytose

bacteria and secretes enzymes to degrade necrotic tissue. They also release specific cytokines and growth factors that leads to the next stage of healing [17]. Proliferation is the third stage of healing. In this stage, specialized fibroblasts create scaffolds to build frames of collagen. Proliferation stage is formed by granular tissue growth, wound contraction and epithelialization. Through the end of this stage keratinocytes grow and close the top of wound. Remodeling stages will start soon and sometimes it takes two years to remodel under the surface by decreasing the density of cells and reproducing other components [18].

Apart from acute wounds, chronic wounds have problems at one of the healing stages especially proliferation stage. Chronic wound fluid was investigated as an inhibitory to epithelialization and impediment to keratinocyte migration and unbalanced protease (enzyme degrades proteins) activity than acute wounds [19].

1.3. Objective of the Study

Purpose of this thesis is to produce scaffolds which take their high mechanical strengths from the organization of nanofibers that are synthesized by using environment friendly solvents. Planned scaffolds will be biocompatible, biodegredable and employed in skin tissue engineering applications. To achieve this, core-shell morphology at nano scale is aimed to reach by electrospinning of organic and synthetic polymers where the former one supplies recognition sites for the tissue cells and the latter one supplies mechanical endurance. Different from conventional methods, proposed work aims to lower the steps of application of the scaffold to the harmed tissue by not using toxic solvents, thereby, contributing to the literature from the greener synthesis respective and also determination of the optimum process parameters.

2. Literature Review

2.1. Techniques Used in Skin Tissue Engineering

2.1.1. Phase Separation

Phase separation is a multi-stage fabrication method used for many years to construct porous membranes. Two different phases exist inside a solution obtained via by non-solvent method or thermally induced phase separation (TIPS). While the former one results in heterogeneous, latter one results in homogenous pore size distribution with interconnected pores [20]. This technique enables nano-to-macro sized fibers and pore sizes (>90%). Combining with other techniques can yield efficient solutions in scaffold production (porogen leaching, electrospinning) [20]. Also, it allows controlling of pore-size and distributions. Major drawbacks of phase separation are that it requires simple but time consuming steps in addition to the toxic solvent usages and shrinkage issues with anisotropic pores. Also, mechanical strength of obtained scaffolds (natural polymers) with this technique is not sufficient for elasticity required biomedical applications. They usually suitable for compression applications [21].

Steps for TIPS briefly can be listed as:

(i) A polymer solution is prepared. Especially a well-organized non-solvent and solvent mixture is required.
(ii) Phase separation with gelation resulting in entrapped water/solvent regions of fibrous matrix.
(iii) Solvent exchange with water.
(iv) Freeze-dry.

In Figure 2.1, gelatin matrices were obtained by phase separation from gelatin solutions of aqueous and water/ethanol binary solvent system by Liu (*et al.*, 2009) [21]. Surface morphologies are very different due to interaction between gelatin and solvent molecules. In the same study, in order to construct interconnected macro pores, paraffin was used as a porogen leaching method.

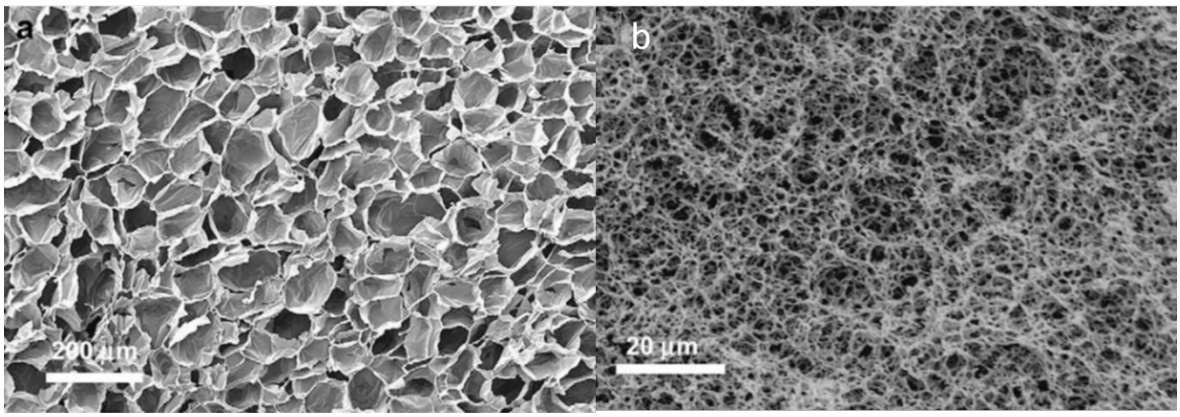

Figure 2.1. SEM micrographs of gelatin matrices a) pure water as solvent - freze-dry b) ethanol/water binary solvent – TIPS (adapted from [21].)

2.1.2. Wet-Dry Spinning

In wet-spinning technique, a polymer solution is prepared and driven by a syringe pump through the nozzle. Ejected solution due to viscous forces stays as long wires and drops inside the non-solvent coagulation bath. There can be an air gap between nozzle and coagulation bath which turns method into dry-jet wet spinning [22]. This gap allows crystalline fibers to form their organized structures and prevents precipitation at the tip of the nozzle. There are several polymers and polymer composite fiber produced with this technique like chitosan, gelatin, cellulose acetate, acrylics, etc. The advantage of this process is enabling multiple polymer blend fibers and easy incorporation of different materials. Main disadvantage is thick fibers that are on the nano scale. For instance, in industry, gelatin fibers were obtained via wet or dry-spinning method have fibers on micro-millimeter scale [23].

Also used coagulation baths are usually organic solvents which keeps toxicity concerns. But in some cases different baths are used as Kafy *et al.* (2017) produced microfibers of aligned cellulose nanofibers with wet-drying method using $CaCl_2$ to form fibers [22].

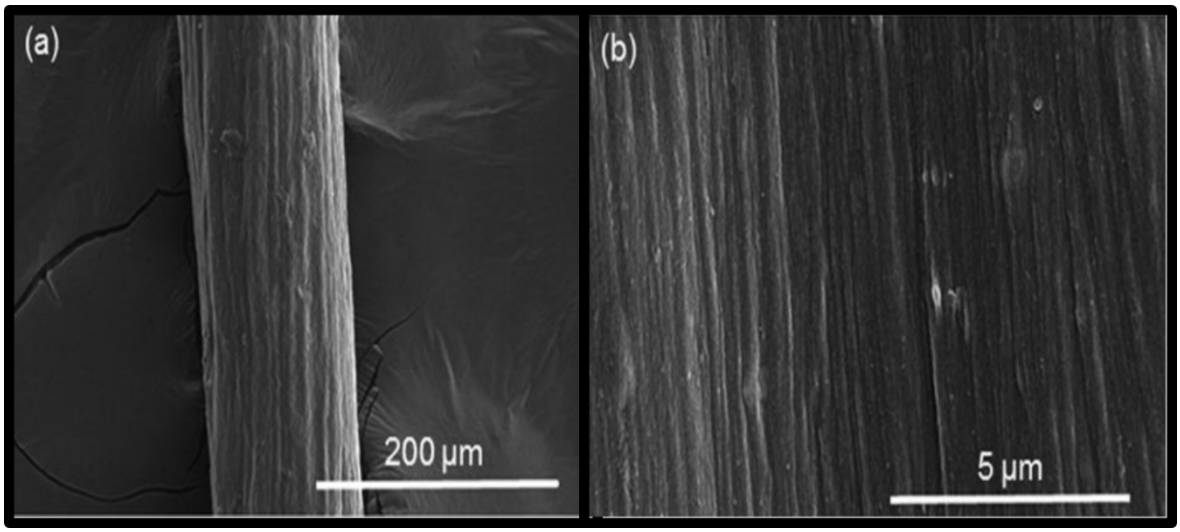

Figure 2.2. SEM micrograph of wet-spun cellulose microfiber (a) zoomed to observe aligned cellulose nanofibers. (adapted from [22] .)

2.1.3. Electrospinning

Electrospinning (ES) is an effective method for producing nano and submicron fiber. Fibers obtained from a polymer solution exposed to the high electric field are collected on a counter electrode. These fibers are used in a wide variety of fields including wound dressing [24, 25], tissue engineering [26], sensors [27], drug delivery [28, 29] and etc.

Nano-fibers are employed in many areas other than biomedical applications, especially: nanofilters [30], composite reinforcements [31], energy supplement [32], sensors [28], photovoltaics [33] and water-proof fabric [34]. In any cases, ES promises a bright future for the nanofiber based applications due to easily adjustable and convertible setups and low costs.

Interest in electrospinning is increasing due to bare advantages when compared to other alternative fiber production methods (phase separation, drawing, template synthesis, extrusion, centrifugal spinning and etc.) Figure 2.3. Since technique is being cheap, responsive and enables mimicking the nature, it is widely studied in laboratories around the world. With minor changes in the setup, many forms of surface and fiber morphologies like aligned [35], core–shell [36], porous [37], hollow [38], etc. fibers can be fabricated. Besides, degree of the pore size and fiber diameter can be controlled by optimizing applied voltage, feed rate and electrode distance or polymer concentration [39, 40].

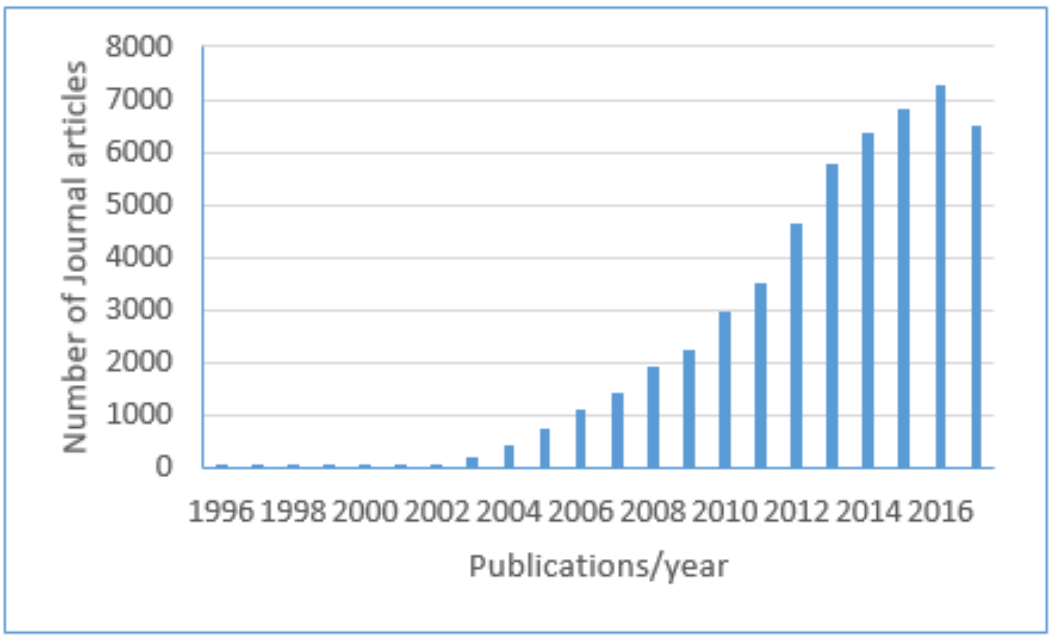

Figure 2.3. Publications containing word 'electrospin' + 'nanofiber' (summon.boun 2018 August)

There are many original methods patented and published to obtain aligned fibers. The most commonly used method is deposition on a rotating cylindrical drum. Rotational speed of (rpm) the drum is high such that electrodeposited fibers stretch and become lined up. Aligned fibers with different orientations and narrowed jet bending instability thanks to pre-placed auxiliary electrodes are also obtained with this

method [41, 42]. Aligned fibers can also be obtained by depositing on two grounded electrodes which are arranged in parallel to each other. Those two electrodes change distribution of electrical field and improve the alignment of nanofibers. However, if the produced fibers are not electrically conductive, they do not come close to each other due to not discharging the charges accumulated on the fiber and repel the neighbouring fibers. One way to obtain dense fiber meshes using a modified parallel electrode system is to collect fibers with a sliding board mechanism in between two electrodes which results in high orientation order parameter of S>97% [43]. Also applying alternating current power instead of direct current resulted in wavy fibers which opens a new way to patterned deposition morphology [44].

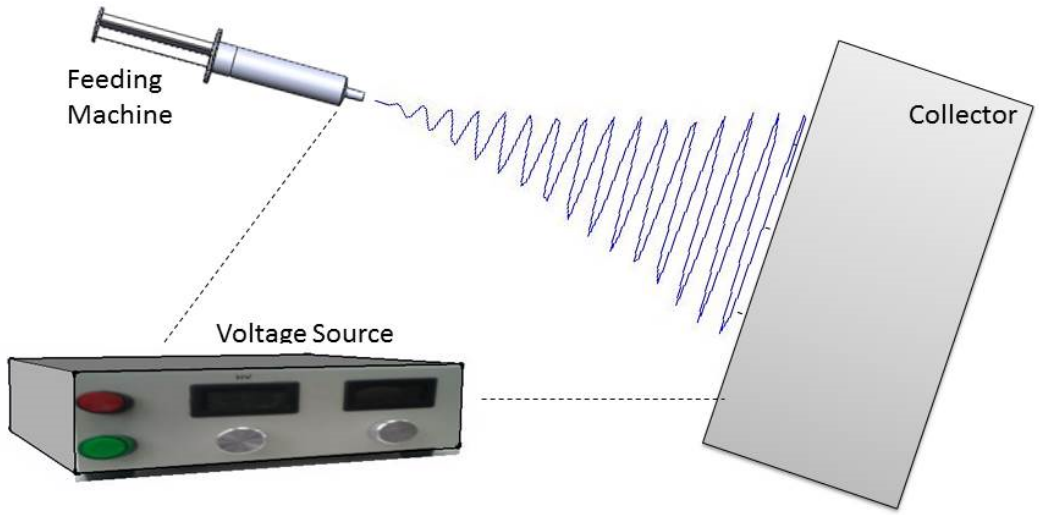

Figure 2.4. Illustration of a simple electrospin setup

Fibers in core-shell (CS) morphology can be obtained by using co-axial needles. With this method, dissimilar polymer solutions can be spun concentrically. Coaxial spinning of immiscible polymer solutions is relatively easy to achieve core-shell morphology. Solvents of the two solutions need to have approximately the same evaporation rate so that less deficient fibers will be formed. CS morphology can also be attained with different techniques like using wire electrodes circulating on the free-surface [45]. This needless method produces a faster production result than the other methods, but also brings higher voltage and evaporation problems in addition to immiscibility requirement which enforces the polymer solution density of the shell should be less than the core. Gas assisted coaxial electrospun method is an example of coaxial spinning which eliminates clogging possibility and reducing flight time. Jiang *et al.* (2014) demonstrated this technique for rapid homeostasis in liver resection [46]. Hollow fibers have been employed for different applications such as gas sensors, extractive phases and medical applications. Coaxial needle setup qualifies hollow fiber fabrication in which a sacrificed core solution will be extracted during post-process [47].

Fiber collection using a liquid counter-electrode is one of many other variants of ES. This makes it possible to produce thicker membranes and in situ coating of spun fibers benefitting from a coagulation bath [48]. What should be noted in this method is that surface tension of the liquid electrode should be arranged such that deposited fibers would sink below the surface [49]. 3D cell-fiber structure can be attained by deposition of alternating layers of human fibroblast cells and fiber on a cell-culture media [50]. In some cases, fibers which are deposited on the liquid, are pulled slowly through the liquid with the aid of a rotating cylinder to form fiber yarns [51].

The simplest ES uses a single-needle spinneret to draw the solution. The process, however, is very time consuming. Therefore, multiple jets needs to be formed in order to reduce production time from either a free surface or with the aid of nozzles [52]. The most critical issue in multiple jet ES is the interaction of path of initiated jets. Models were hypothesized or experimented to minimize and homogenize the interactions through proper design of the spinneret while taking into account the nozzle arrangement, number of nozzles, and nozzle distances [53, 54].

Instabilities of conventional electrospinning limits its applications both in mass production or experiment level. In recent years, low voltage ES has been focused to obtain devices which usually requires arranged or patterned fibrous structures. Although applying low voltage at a close distance near field electrospinning (NFES) compared to far field ES yields in desired structures, electric discharge due to close proximity of electrode and collector, fiber thickness in addition to the membrane thickness necessitates further considerations. Small diameter spinneret has limitations on the flow of the solution due to shear stress developed on the walls. Jet initiation is another tricky constraint which was overcome at low voltages by using physical objects [55] or switching high voltages at the start of the deposition to initiate fiber [56]. NFES combined with coaxial ES results in a thicker but bio-mimicked structures which makes technique more promising [57].

Obtaining fibers from natural polymers generally requires toxic or acidic solvents which deteriorates important groups of the polymers in addition to the safety considerations [57]. Definitely, the most reliable solvent is water and makes ES green [58, 59]. However, since water soluble polymers can be dissolved easily in daily operations, requires further post-treatments. Some ionic liquids [60], melt spinning process [61] can be considered as green synthesis way of ES. Both has limitations, former one results in residual material inside fibers and latter has a fiber diameter limitation of large sizes.

All in all ES is a fascinating technique to produce woven, non-woven, patterned submicron and nano fibrous structures. Recent advances on ES were motivated to improve the fiber production rates, patterned structures and safer processing methods for future improvements.

2.1.3.1. Process Parameters. Mainly parameters that are affecting the morphology of the end-product can be gathered under two distinct categories as operational and solution dependent parameters.

Table 2.1. Operational and solution dependent electrospinning parameters

Operational Parameters	**Solution dependent Parameters**
Feed Rate	Concentration
Distance	Viscosity
Voltage	Vapor Pressure
Humidity	Conductivity
Temperature	Surface Tension
Collector Type	Charge Density

Each of these parameters have contribution on the individual fiber morphology and the overall surface morphology. As example, a fiber can have different morphologies: hollow, beaded, core-shell, etc. In addition, surface of the produced specimen can have different morphologies like: porous, aligned, random, etc.

Feed rate (FR), distance and voltage are among the mostly studied parameters. Depending on the solution dependent parameters, those parameters can have diverse effects. Many researchers investigated effects of FR for needled ES. Since electric field extracts fibers from the droplet occurred at the tip, there are two limits for the fiber formation one for excess and one for low rates. In between those rates, fiber diameter, usually increases as rate increased. Below the minimum limit, solution drains too fast that it is not possible to observe a stable ES. Above the maximum available limit, electro-spray occurs such that droplets fly directly to the electrode. Actually, this phenomenon is valid for voltage as a process parameter. Apart from FR, voltage has different aspects of ES. Applied voltage can be either AC or DC, nozzle can be positive electrode while counter electrode can be negative or vice versa.

Electrode distance is another factor on the fiber morphology. It also has critical limits that determines optimum conditions by means of evaporation rate, instability region and flight time in addition to the magnitude of the Coulombic forces. However, positive direct effect of electrode distance on the fiber morphology has not been reported.

Humidity, temperature are the environmental parameters having different effects on the fiber morphology depending on the material types. For instance, humidity has no bare impact on the hydrophobic polymers while has considerable effect on hydrophilic polymers by means of changing the fiber surface and incorporating beads due to surface tension. Temperature affects fiber morphology from evaporation rates, solution viscosity and surface tension aspects. Generally, increased temperature results in lower viscosity and lower surface tension, which means smaller diameter fibers however, it also, increases evaporation rates, and faster evaporation results in faster extraction of the solvent from the jet therefore a thicker fiber forms prior to stretching of pre-mature fiber.

Collector type has effect on the deposited mesh. A drum type collector may result in the aligned fiber depending on the speed of the drum or a liquid collector may result in thicker membranes by eliminating piled up charges on each layer. A reduction in nozzle diameter results in smaller diameter fibers. However, there is another factor needs to be considered coming with nozzle diameter “coagulation” which prevents solution flow. In addition, a decrease in size may bring the problem of excess shear stress on the fluid that blocks flow again.

Solution dependent parameters are listed in Table 2.1, among all of the parameters the most detrimental parameter for a specific polymer is the solution concentration and molecular weight of the polymer. It affects intrinsic parameters, like viscosity, conductivity and surface tension properties, thereby fiber thickness. The dependence of the fiber diameter on the polymer concentration is highly related to the viscosity. A competition occurs in between viscosity which tries to keep solution together with viscoelastic forces, conductivity which determines the effect of coulombic forces causing to charge repulsion inside solution and surface tension which reduces surface area.

Vapor pressure is another effect that changes the properties of fabricated fibers. Low vapor pressure solvents evaporate faster resulting in thicker fibers as fiber creates and fiber formation process ends prior to fully developed and stretched fiber. ES also affects crystallinity and conformations of the polymers by the incorporation of low vapor pressure solvents inside the prepared solutions.

2.1.3.2. Advantages and Disadvantages of ES. A complete biomimetic scaffold has many aspects. From morphology point of view, produced scaffolds have to be organized from nano-sized fibers. Nano-sized fibers increase surface area of the scaffold, which enhances binding of cells as illustrated in Figure 2.5. ES enables the production of nano-size fibers that are mimicking the native ECM structure. ES provides many advantages in addition to the control over fiber diameter distributions. It provides a cost-effective fabrication. Aligned and non-woven meshes can be obtained in a 3d shaped fashion. Pore structures and sizes can be controlled to allow the flow of nutrients and gas permeability. Ingredients can be determined by solution types and allows many polymers from natural to synthetic that play critical role in biocompatibility, biodegradability, anti-bacterial properties, adhesion and proliferation of cells.

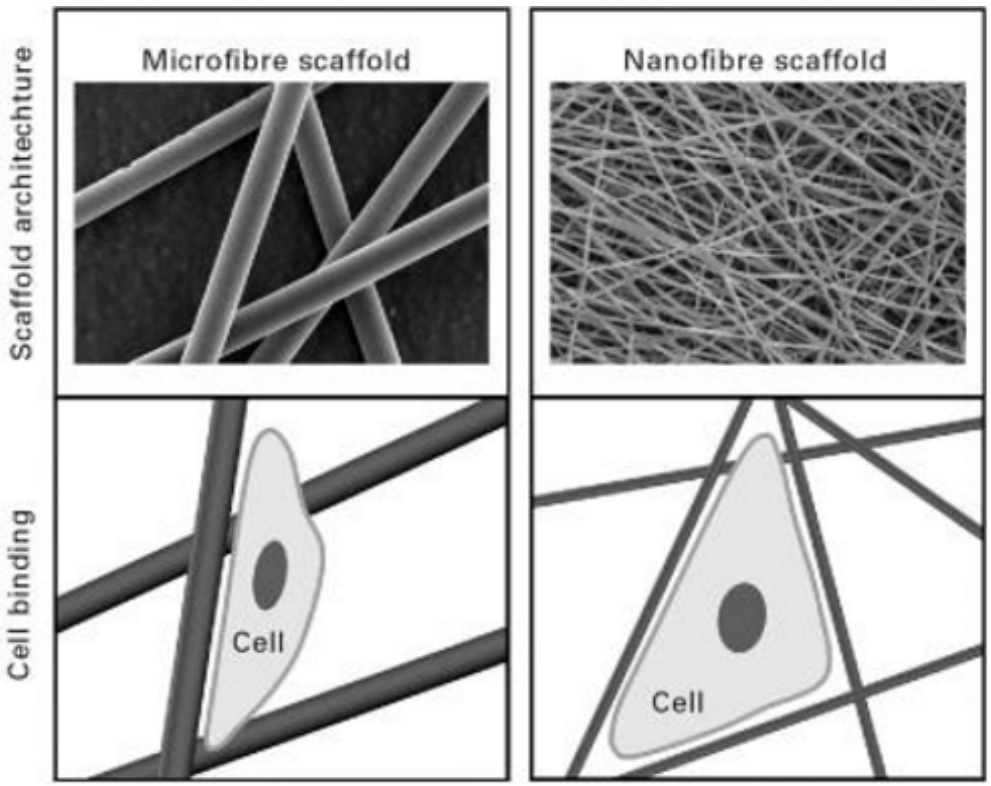

Figure 2.5. Schematic illustration of how scale affects cell binding [62].

There are some disadvantages and inabilities of this technique. Firstly, ES enables a distribution of fiber and pore sizes, it is hard to obtain specific dimensions. Although near field ES enables a large control over surface morphology of the membranes but they are very thick fibers as opposed to the conventional ES. 3D structures is hard to obtain with this technique by itself. Membrane thickness has a limit due to charge pile up on the electrode even some manipulations done on the ES setup. [20]Increased production times may not result in a proportional scaffold thickness. Thicker fibers can stick to the electrodes due to higher momentum than thinner fibers. However, they do not create a homogenous distribution. To end up 3D geometry produced membrane layers can be fused together with other techniques. Other largest challenges are used toxic solvents and crosslinking requirement due to lower mechanical strengths of the produced membranes.

2.2. Materials Used in Skin Tissue Engineering

2.2.1. Natural Polymers

2.2.1.1. Collagen. Mimicking chemical composition or morphological properties of ECM which directly leads engineers to selection of collagen based materials and fiber shaped surface morphologies as critical component and inherent morphology of the ECM. Collagen creates $\frac{3}{4}$ of dry weight of skin and up to now 29 different types of collagen exists [63]. The most abundant one is collagen I which has two $\alpha 1$ helix chains and one $\alpha 2$ chain forming 3 stranded rope like structure making up $\frac{1}{4}$ of the dry weight.

One collagen peptide chain mainly consists of glycine, proline and hydroxylproline amino acids with a helix form (Figure 2.6). They are gathered to end up a repeating sequence of (glycine-*frequently* proline - *frequently* hydroxyproline)$_n$. Helix twist was found to be sequence dependent, and a variation in this sequence may result in different recognition features [64]. $\alpha 1$and $\alpha 2$ amino acid chains having 300 nm length and 1.4 nm diameter form right-handed tropocollogen when they wrapped around each other. Amino and carboxyl groups form hydrogen bonds to keep structure stable. End terminals of helix strands (C and N terminals) are smoothened via enzymes. Those end points are called telopeptides which are the most antigenic portion of collagen. Terminals allow the once soluble collagen to become insoluble and bond with other collagen triple helixes to self-assemble into extended fibrils [65]. In Figure 2.2, cellulose nanofibers were gathered to form a hierarchical cellulose microfibers. It actually resembles to the collagen hierarchical structure. There is a huge difference where the collagen fibrils formed by tropocollagens. When they enzymatically crosslinked to each other from the terminals and created a cylindrical shaped long fibril clusters (fiber), there occurs a pattern on the surface of the fiber due to gap zone overlaps. (See Figure 2.6,e,g) Collagen fibers can be 500 nm in diameter and 500 μm in length [65].

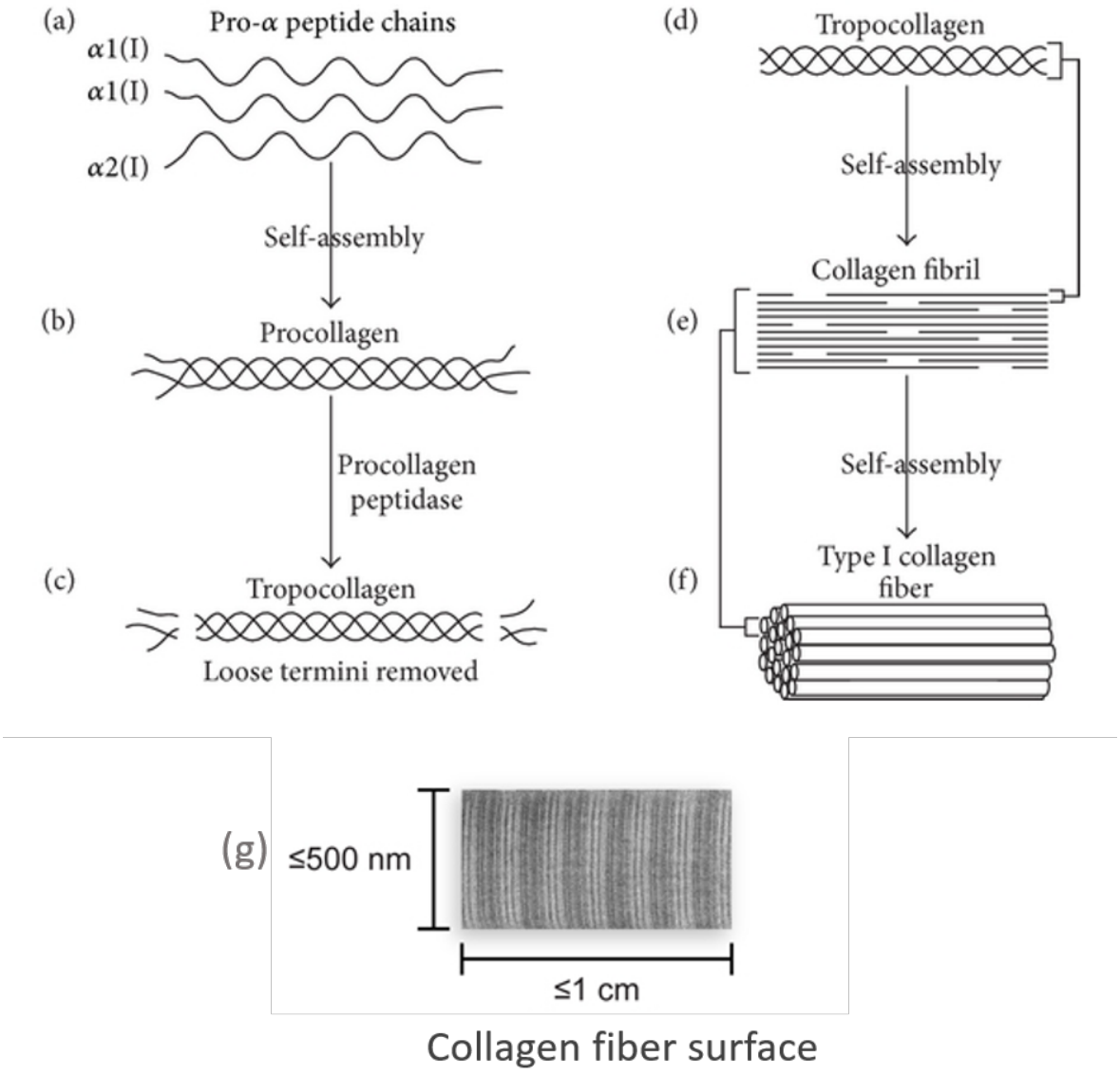

Figure 2.6. The process of type I collagen synthesis. (a) Two identical α1(I) and one α2(II) peptide chains self-assemble to form procollagen (b). (c) Procollagen peptidase removes loose termini to create a type I tropocollagen molecule (d). Tropocollagen molecules self-assemble to form a growing collagen fibril (e). Self-assembly of collagen fibrils forms a type I collagen fiber (f). Strips of overlapped regions on a collagen surface (adapted from [65].)

Collagen has been used as drug-delivery system to deliver a bio-substance to the targeted tissue in a controlled release rates. Used as sponges to absorb excaudate from the wounded area due to swelling properties. It is used also as skin substitute, bone substitute and cellular tissue substitutes [66].

2.2.1.2. Gelatin. Gelatin (GE) is a natural biopolymer derived from collagens by controlled denaturation that contains many functional groups (glycine, proline, glutamic acid, hydroxyproline, arginine, alanine, aspartic acid, and other amino acids). Gelatin obtained from an acid-treated precursor is known as Type A and alkali-treated process is known as Type B [67]. Chemical properties of different gelatins are differing depending on the source they are extracted: skin, bones, and connective tissue of animals including fish and poultry. There is no chemical relationship between vegetable gelatin and animal gelatins.

The use of gelatins instead of animal-derived collagen can reduce the risk of antigenicity and disease transmission and offer a relatively easy mass production [68]. Gelatin is derived by denaturation of collagen can be categorized as type A and B depending on the acidic or alkaline-treated precursors, respectively. They contain main functional groups of collagen and conformational organization is close to the collagen with partially denatured alfa-helix and triple helix structure. Chemical properties of different gelatins are differing depending on the source they are extracted: skin, bones, and connective tissue of animals including fish and poultry. Also treatment kind is effective on the content of gelatins, alkaline treated gelatins contain more carboxylic groups and molecular weight distributions are narrower than acidic treated ones [69]. There is no chemical relationship between gelatin obtained from vegetables and animals even fish, bovine and porcine have different amino acids [70].

Gelatin molecules can perform different levels of conformations like collagen. They can exhibit α-helix and random structures as well as triple helix conformations. Apart from collagen they can contain many forms at the same time (Figure 2.7). Used solvents highly affect conformations. Collagen D-bands cannot be observed in gelatin due to the acidic or basic treatments that cleaves peptide bonds.

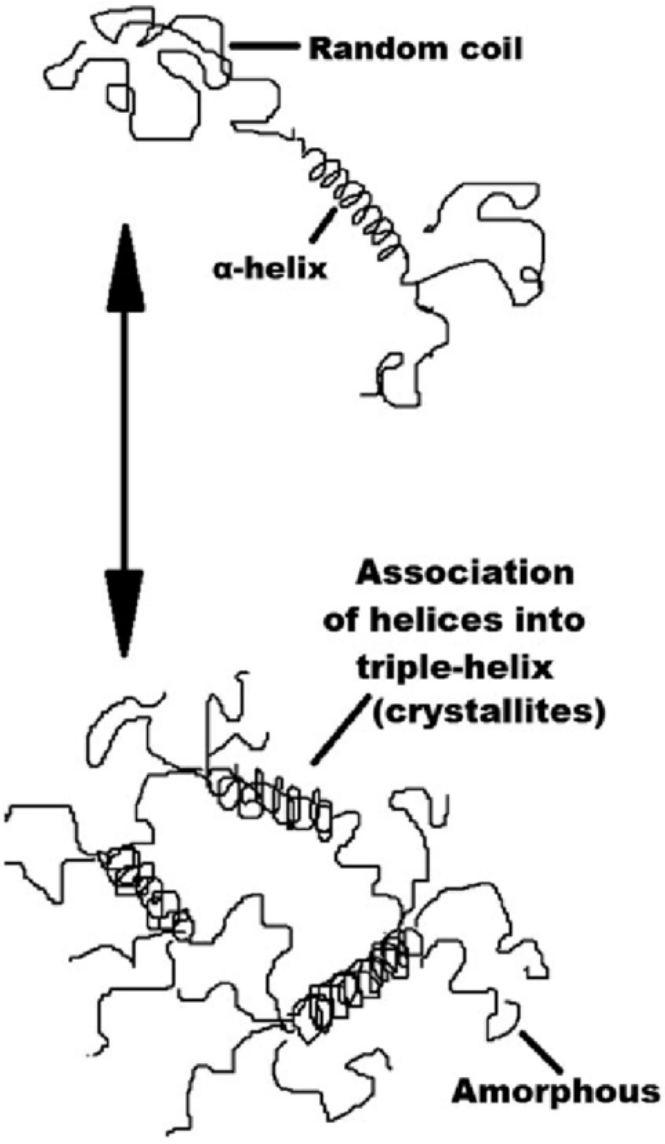

Figure 2.7. Conformational structure of Gelatin [66].

Gelatin mostly preferred in tissue engineering due to the properties of:

(i) enzymatic biodegradability and biocompatibility [64]
(ii) having peptide domains for the recognition of integrin receptors of the cells even more than collagen due to unfolded domains of gelatin, [71–73],
(iii) being highly hydrophilic due to strong polarity which promotes cell adhesion of negatively charged surfaces [74],
(iv) resemblance to the collagen type I with the triple-helix structure [75],
(v) containing carboxylic groups that leads to biocompatibility [76],
(vi) low-cost and simple preparation [71],
(vii) Easy to follow a wound healing process due to transparency under hydration [77],
(viii) Easy to dissolve in aqueous environments while collagen not [36].

Gelatin has a profound biomedical potential application area due to good film, gel, sponge, scaffold forming capabilities. Different combinations with other proteins, polysaccharides and ceramics can yield high performance scaffolds since gelatin only scaffolds have lack of mechanical strength. Gelatin is also used in drug delivery with controlled release rates.

2.2.1.3. Elastin . Elastin is one of the major component of the body ECM responsible from the elasticity and resilience of the tissues. It has the capability of self-assembly and provides biological activity that induces migration and differentiation of cells [78]. Elastin is composed of tropoelastin (pre-form of elastin) protein containing hydrophobic and hydrophilic aminoacid residues of glycine, valine, modified alanine and proline [79]. Elastin can be synthesized with the hydrolyzing of the peptide bonds or via host microorganism. Elastin by itself is a highly crosslinked polymer that limits its application. However, tropoelastin soluble and have been used in the fabrication of elastin fibers preserving the unique properties of elastin [80]. Elastin has been widely targeted to use in the modification of implant surfaces, vascular and cartilage tissue engineering [81].

2.2.1.4. Hyaluronic Acid. Hyaluronic acid (HA) is a glycosaminoglycan which is a long unbranched polysaccharide contains repetitive disaccharide sub-units. It is mostly found in skin ECM filling the interspace of soft connective tissue [82]. HA is a biodegradable and biocompatible substance, can be observed in the vicinity of increased cellular activities. HA is a polyanionic, hydrophilic polymer surface that does not promote cell attachment [83]. However, a proper combination with recognizable proteins on the surface of HA particles result in efficient results[84]. Since HA is a highly soluble material, different cross-linking procedures are required to keep gel structure stable. HA have been used in commercial products frequently, as cell deposited gel with laser drilled holes allowing keratinocytes to transfer gradually to the surface of the wound. It is used in chronic wounds, diabetic ulcer and burn wounds that are lacking proliferative cells. Other applications areas are cosmetic, drug delivery, ophthalmic surgery [84].

2.2.2. Synthetic Polymers

Synthetic polymers have been used in tissue engineering widely. They are reproducible and applicable to industrial-scale production when compared to natural polymer. It is also easy to manipulate physical and chemical properties. Synthetic polymers can be divided into two categories inorganic sub-group containing metals and ceramics and organic sub-group containing PEG (poly (ethylene glycol)), PVA (poly(vinyl alcohol)), PLA (poly (lactic acid)) etc. In this dissertation, PVA was focused on due to efficient combination with gelatin.

2.2.2.1. PVA & Electrospun PVA Nanofibers. Polyvinyl alcohol was first obtained by hydrolyzing polyvinyl acetate by Hermann and Haehnel in 1924 having the formula of $[CH_2CH(OH)]_n$. First PVA fiber fabricated via dry and wet spinning patent was taken by Hermann in 1931 [85]. It is used in biomedical area due to biodegradability and mechanical properties [86]. Lack of cell-adhesion sites needs further modification on the chemical structure or needs a blended mixture with polymers having cell binding properties. PVA has also increasable crystalline nature with the post process that gives mechanical strength to the films or scaffolds obtained from PVA included polymer

composites. Biodegradation rate is closely related to the hydrolysis and crystallinity degree [87]. Its hydrophilic nature requires crosslinking procedures to end up with water resistant materials. It has been used with other polymers and ceramics like gelatin, HA, hydroxyapatite for wound dressing to nerve guiding applications.

PVA can be dissolved inside water at around 80 ^{o}C and aqueous solution is suitable for ES. This makes it one step forward in biomedical applications where the device contact with the body due to non-toxic solvent usage.

PVA- metallic particle composite nanofibers can be used as biochemical-sensors. Noble metallic nano-particle added PVA was spun with a simple ES setup to measure changes in the H_2O_2 levels [88]. In another work, electrospun nanofibers of PVA-glucose oxidase [89] composite fibers were shown to be good candidates for enzyme immobilization and to detect glucose level. Another glucose level detecting device was proposed by Kim (*et al.*,2017). PVA was crosslinked to make insoluble substance with PAA (poly(acylic acid)) which makes ester bond unlike glutaraldehyde (a very common crosslinker of PVA which will be toxic at high concentrations) [90]. Selection of PVA is due to providing inert environment and not inducing modifications in enzymatic natures. Also spun fibers offers homogenous distribution of key metallic, ceramic substance resulting in increased electron activity from receptors to the electrodes [91]. Apart from glucose, cholesterol, triglyceride, and low density lipoprotein affinity sensing can also be achieved with metal incorporated PVA nanofibers.

PVA/chitosan meshes targeted to use in wound healing due to enhanced cell viability, proliferation and attachment of cells [92] in addition to drug delivery applications [93]. Bi-layered collagen/PVA scaffolds were aimed to use in cartilage tissue engineering that are deposited on collagen sponges with aligned and random morphologies. It was concluded that aligned PVA/collagen fibers were more favorable due to higher mechanical strengths that may be required in osteochondral repairs [94]. Ag incorporated PVA nanofibers were used in skin tissue engineering to prevent bacteria activity and shown significant decrease in E. coli (gram-positive) and S. aureus (gram-negative) bacteria activities [95].

PVA/gelatin is a good combination for tissue engineering that is tried and found it is a very good candidate for wound dressing applications [36], bone tissue engineering [96], skin regeneration [97], controlled drug release [98], vascular tissue engineering [99].

2.3. Electrospun Gelatin Nanofibers

There are various ways to produce different distinctive fiber meshes with ES on the nano scale which makes cell attachment easy due to increased surface area. Fabrication method (alkaline, acidic) and origin (bovine, porcine, fish, microorganisms) of gelatin raw powders from collagen affects characteristics of gelatin fibers. Even, solutions obtained from same solvent can possess different viscosities, conductivities and surface tensions due to polymer concentrations in addition to the environmental parameters of temperature and humidity. Those parameters change fiber diameter and porosity of the scaffold therefore, cell attachment capabilities.

Scaffolds obtained by ES requires a conductive liquid state. De-ionized or distilled water solution of gelatin is in gel state at room temperatures (23^{o}C) which makes it not-suitable for ES. Some gelatin kinds like fish gelatin can be attained in liquid state at room temperatures but obtained fibers contain large beads due to high surface tension of water. Although effect of bead is not clear from the cell viability, fiber lengths are shorter and scaffolds have weak mechanical durability.

There are very few solvents that can dissolve gelatin due to strong polarity. Therefore, first researches on the ES of gelatin focuses on organic solvents like TFE (fluorinated alcoholic solvent of 2,2,2-trifluoroethanol), [100] HFIP (1,1,1,3,3,3-hexafluoro-2-propanol) [101]. Although those solvents are successful in dissolving gelatin, they smash α-helix and partial triple helix conformation inherited from collagen histories. The resultant fibers are smooth. HFIP is less volatile than TFE having a boiling point of 59 ^{o}C, a costly chemical and contains clogging risk during fabrication at the tip of the needle. Organic solvents are usually toxic to environment and has safety issues. Dealing with these solvents requires extra attention and procedures in addition to the concerns of residual toxic elements entrapped inside the scaffolds due to strong hydro-

gen bonds in between solvent and the protein. Although *in vitro* tests results of human embryonic palatal mesenchymal cell attachment and growth are positive, their batch production requires complex post-process to eliminate toxicity risks [102].

Dimethyl sulfoxide (DMSO) is another polar aprotic alternative solvent that does not contain OH groups. Since it is hard to dissolve gelatin by itself it was used with other solvent combinations [103]. And even sometimes acetone was added to increase volatility to obtain a good binary solvent system.

Acetic and formic acids as being solvents for peptides are good alternatives to obtain as-spun nanofibers since they are not toxic as other organic solvents [104]. There are several groups that used acetic acid/water combination at different ratios to obtain smooth gelatin nanofibers usually targeted to use in biomedical applications [105, 106]. Even, it is far better than toxic and volatile solvents from health perspective of researchers, acidic solvents decomposes amino acids partially and this changes conformational structure of the gelatin fibers one more time that was inherited from the denaturation of collagen at the beginning [107].

Sizeland *et al.* (2018) showed this fact clearly in their study for pig-skin and hoki fish skin derived gelatins by using SAXS, TEM and FTIR techniques [107]. They showed that collagen d-bands were not present in acetic acid solved collagen and gelatin. Although, α-helix structure stays inside the electrospun nanofibers, hierarchical morphology was disrupted. Peak associated with triple helix structure was absent and they showed that with FTIR results, using: (i) wave number difference between Amide I and Amide II peaks (should be <100 cm^{-1} to have α-helix [108]), (ii) ratio of Amide III / peak @ 1451 cm^{-1} (value of >1 means strong triple-helix structure [109]), (iii) second derivative method of Amide I broad peak (peak @ 1660 cm^{-1} normally represents hydrogen bonds of triple-helices [110]), (iv) major band and sharp second derivative peak @ Amide II indicative of the triple helix [111]. A blue-shift of peaks were observed by Sizeland *et al.*(2018) which reveals electrospinning even inside acetic acid solution resulted in some ordered conformational changes.

Due to high acidicity and volatility, formic acid was preferred in some cases, but it has almost same effect as acetic acid and stability issues of formed solutions occur [112]. In another study, Liu *et al.* (2005) cover up that fibers obtained from acetic acid has more triple-helix structures than HFIP using circular dichroism technique [113]. Those obtained fibers were also directed to use in neural tissue engineering.

Ethanol was also used in many of the studies to increase evaporation rates and balance surface tension of the prepared solutions for ES. Ethanol by itself cannot dissolve gelatin totally, although it contains both polar and non-polar groups. It is most commonly combined with acetic acid/water, formic acid/water binary systems [114].

Relatively greener and conservative method is dissolving gelatin inside PBS / ethanol /water ternary solvent system [115]. It is possible to prevent gelling with this mixture while maintaining proper spinning characteristics. Although this is an effective method that can produce < 100 nm thick fibers, residual phosphate buffer salts require further desalination procedure and direct using of ethanol may have allergic and cytotoxic effects when used inside body as skin substitute. Also, a composite synthetic material choice will require a common solvent for both of the polymers. For example, PBS is not an option for PVA to ES, while it is a way to spin gelatin. According to the ICH guidelines (International Conference on Harmonisation of Technical Requirements for Registration of Pharmaceuticals For Human Use) [116], which is a toxicity level classification of the solvents that is used to dissolve polymers, ethanol enters into the class 3. Although class 3 allows 50 mg daily usage of ethanol, this class actually represents low toxic potential solvent class. Therefore, it is required to further detection of residual solvents inside the scaffold prepared by this benign solvent technique [117].

Cationized gelatin can be obtained by anchoring of amino groups on the surface of gelatin of Type A gelatin which has more amino groups that are promoting cell affinity. Basically carboxylic groups are turned into amino groups through chemical reactions which are proved to by having a zeta potential value of (+2.9 mV) where non-treated gelatin was (-2.1mV). Major advantage is that cationic gelatin is soluble at room temperature and even a concentration of 30-50% w/v can be spun which makes mass production possible [118]. Since preparation procedure contains acidic treatment steps helix structures were lost.

The water-based system is a very attractive method for the electrospinning of gelatin, which is a method that protects the helix structure, is reliable and provides the opportunity of production with less steps. Therefore, a cationized method could be favorable but there is a much simpler and trustable way that only elevates temperature of the environment to above gelation temperature [75]. Also, according to the ICH guidelines, since there is no other solvents used except water makes fabrication as the most reliable technique. As it is conducted in this dissertation, operation temperature is increased above gelation temperature. This gelation temperature highly depends on the concentration, origin (bovine, porcine or fish gelatin) and type (type A or type B) of the gelatin solution. A 8% w/w bovine type B gelatin/water solution gels at around 25 ^{o}C while 16% solution gels at around 30 ^{o}C (proven with zeta potential measurements) [71, 119]. Usually at 37 ^{o}C gelatin totally dissolves and weakening of intermolecular hydrogen bonds in between alfa-helix strands resulting in random coil structure will occur [120]. However this transformation is reversible, typical structure of collagen will form again when critical gelation temperature is reached (cooling down to 30^{o}C from 40 ^{o}C) where molecular network occurs. Addition of acetic acid inside water deforms triple-helix structure and no crystal peaks observable from WAXS analysis while it is possible to see pure water systems [106]. One major drawback of this technique is that within operational limits, it is not possible to produce smooth nano-fibers due to surface tension, viscosity and conductivity effects. Increasing concentration will decrease bead formation but it also has a limit for needled electrospinning that clogs at the tip of the needle. Collagen derived from bovine is not possible to dissolve inside water, however, gelatin allows at elevated temperatures. But keeping gelatin solution above gelation

temperature for long hours result in thermal degradation of ordered structure [70]. Therefore a fast method is required to produce aqueous gelatin nanofibers to keep solution as short as possible (less than half hour), which may be a multi-needle ES for high throughput mass production or free surface ES [121, 122].

Another drawback of aqueous ES is that producing thick membranes above 40 μm is not possible due to charge accumulation on the surface of the collecting electrode. Since fiber diameters are <100 nm they don't have enough momentum to override charge repulsion and stick on the surface. It is possible for thicker and conductive fibers to enforce and stick on the electrode but for thinner fibers new methodologies are required. For instance, negatively charged collecting electrode can insist flying jets to stick on the surface of positively charged and piled up fibers [123].

2.4. Composite Gelatin Electrospun Nanofibers

An ideal scaffold should be biocompatible, biodegradable and strong enough to resemble native tissue. Biodegradable scaffolds are planned to place to the target tissue in order to mimic ECM and replace with the cells and new born matrix over time. An efficient scaffold needs to contain enough porosity, fibril structures and cell recognition sites. As aforementioned, electrospun gelatin plays a critical role from porosity, cell binding surface area, recognition site perspectives. However, as-spun gelatin fibers lack mechanical strength and stability inside aqueous environments. Therefore, a composite scaffold is a good alternative that takes physical, chemical preferences from gelatin and mechanical preferences from another material usually synthetic polymers. Moreover, targeted tissues can change by type, for instance, a bone tissue requires hydroxyapatite (HAP) as key component in addition to the collagen structure [124]. Thus, addition of hydroxyapatite inside denaturized version of collagen – gelatin – is a clever way to mimic host tissue [125].

Electrospun gelatin composite scaffolds can be classified into three categories by composition: (i)inorganic nano-particle-gelatin, (ii) natural polymer-gelatin and (iii) synthetic polymer-gelatin composite scaffolds. Actually, all other combinations are also possible like gelatin-natural polymer-synthetic polymer-inorganic nano-particle.

Metal oxide addition is used to increase anti-bacterial skills of fabricated fiber scaffold. Conventional scaffolds and wound dressings have usually lack of anti-bacterial properties. As a trending method of increasing anti-bacterial performance, ZnO metal oxides have been inserted inside scaffolds [126]. ZnO is a FDA proven material, loading gelatin with ZnO particles enhances anti-bacterial activity.

Blend of gelatin with another polysaccharide is one of the most common combinations. Although this combination contains critical components, mechanical strength is always missing. At the same time, the water resistance of the fibers is low. Among the examples, gelatin / chitosan blend is at the forefront. Different ratio of gelatin and chitosan polymers blend requires different optimum spinning parameters which results in different fiber diameters [127].

Hild *et al.* (2014) also fabricated electrospun gelatin nanofibers combined with chitosan wet-spun microfibers. Chitosan fibers were knitted and placed as collecting electrode and gelatin nanofibers deposited on it. With this way, they produced macropores which allows nutrition delivery and high mechanical strength due to knitted and large fiber diameter sizes [128].

A multi material blend of gelatin/hydroxyapatite/chitosan/graphene oxide was synthesized by Gao *et al.* (2016) using co-electrospinning technique [129]. Graphene oxide were used owing to excellent antibacterial properties and prevent infection while hydroxyapatite used due to cell signaling for bone cells.

Heparin is an anticoagulant glycosamine. It is widely used in damaged areas to inhibit thrombin and fibrin activation thereby preventing drug delivery problems. Wang *et al.* (2013) examined the possibility of the heparin loaded gelatin nanofibers for vas-

cular tissue engineering purposes. Heparin addition to the gelatin acetic acid solution decreased viscosity and increased conductivity, tremendously. Effect on the average fiber diameter of the solution parameters was also apparent by reducing diameter from ∼1000 nm down to ∼200 nm [130].

Nanofiber meshes from HA and gelatin blend were obtained by Li *et al.* (2006) from N,N-dimethylformamide (DMF) /water solvent mixture. Various blend ratios were trained to find out optimum ratio [131]. DMF functioned as surfactant without appreciable effect on the viscosity and conductivity which influenced fiber diameter. In another study, HA/gelatin composite membranes prepared more or less with the same technique, in vivo analysis were conducted and positive output verified with a commercial chitosan based gel for wound healing purposes [132].

Beadless gelatin-silk fibers were synthesized from formic acid by Chomachayi (*et al.*,2018). Addition of gelatin decreased pure silk fiber mechanical properties. Optimum concentration of gelatin was found to be 10% wt/wt inside the blend. Thyme essential oil and doxycycline monohydrate were loaded inside fibers as antibacterial agents [133].

Collagen coated gelatin nanofibers were synthesized by Janani (*et al.*,2017). Gelatin nanofibers were electrospun from glacial acetic acid solvent followed by crosslinking with aqueous glutaraldehyde solution. After this cross-linked membrane inserted inside acetic acid dissolved collagen bath and Riboflavin photochemical cross linker were used to create bonds between gelatin and collagen layers. Obtained membranes were used as to mimic the secondary sites of breast cancer [134].

Synthetic polymers in tissue engineering have been used usually for their unique elasto-plastic properties. Natural polymers do not possess that much strength at nanoscale productions. Also, synthetic polymers were used in ES due to effects on the solution parameters that permits smooth nanofibers. Mostly used biocompatible polymers are : PVA, poly (caprolactone) (PCL), poly (urethane) (PU), poly (ethylene oxide) (PEO), poly (lactic acid) (PLA), poly (lactic-co-glycolic acid) (PLGA), nylon6, PAN (polyacrylonitrile) . In Table 2.2, targeted tissues for synthetic blends were listed.

PVA-Gelatin blend is one of the most studied combination due to biodegradability and biocompatibility of the PVA. However, gelatin and PVA inside water is not miscible when pH is around 7 [135]. Therefore, a direct water solution spinning method is questionable from the composite scaffold perspective. Huang *et al.* (2016) prepared Gelatin/PVA blend solutions firstly, preparing deionized water solutions, separately [136]. And slowly added HCl inside the solutions to change pH and thereby, allowing a mixture followed by heating to 120 ^{o}C. They found out binding of cells via integrin to the RGD sequence of gelatin is more effective than orientation of the fibers on the cellular behavior.

Linh *et al.* (2011) studied Gelatin/PVA blend for different mixing ratios inside acetic acid solution. They used acetic acid / water system to dissolve gelatin obtained from porcine skin and showed the applicability of bone tissue engineering by using osteoblast cells. They also proposed methanol as physical cross-linker [96].

Table 2.2. ES gelatin blends with other polymers or critical ceramics and targeted applications

Electrospun gelatin blends	**Target Tissue, Application**	**References**
Gelatin - PVA	Skin, Drug delivery, Bone	[136–139]
Gelatin – PU	Wound Dressing, Drug Delivery	[140, 141]
Gelatin – PCL	Drug Delivery, General	[142, 143]
Gelatin – PEO -Chitosan	Wound Dressing	[144]
Gelatin - PLA	Bone, Nerve repair	[145, 146]
Gelatin - PLGA	Bone, Stem cell, Drug Delivery	[147–149]
Gelatin – nylon6	Wound Dressing	[150]
Gelatin – PLGA - nHAP	Bone	[151]

2.5. Core-Shell Electrospun Nanofibers

ES is a facile technique to produce nanofibers having various morphologies. One of them is the core-shell morphology. It allows to create nested cylinders at the nano-scale. This technique in fact, is a way of coating nanofibers. Coating material usually comprise of materials that can bind cells or provide differentiation and other cell activities. Since shell (natural polymer) by itself is relatively weak in mechanical strength and fast in degradation rates, early loss of structural integrity when subjected to the body fluid, may hinder cell activities [152]. Also, first interaction of the cell has a vital importance, surface of the membrane has to be compatible with the cells.

Coaxial ES is one way to obtain core-shell structures in which two nested needles are supplied with two different polymer solutions. Same parameters of simple ES is valid in here too. Except, a proper combination of solutions is necessary. For instance, a highly volatile solvent used inside the core solution ends in a ribbon like fibers due to compression of outer shell polymer fibers through the free spaces. Therefore, usually, same solvent or same evaporation rates has been selected and used as for core and shell polymers [153]. Moreover, it is possible that both polymers may mix at the tip of the nozzles. To prevent mixing, immiscible solvents are required. But it is not necessary if one can control outlets of the nozzles such that immediate jet formation occurs. Diffusion times of miscible solutions is much higher than the jet flying durations. So, usually a sharp boundary occurs in between two polymers even solutions are miscible. Other parameters like voltage, feed rates are needed to be arranged to fabricate stable fibers. Eccentricity of the needles is another key parameter to control fiber morphology for miscible polymers.

This technique has also been used to perform non-spinnable solutions to induce fiber shapes or preventing toxicity of organic solvents by preparing emulsion from core polymer with non-toxic solvents. Shell polymer enforces a fiber shape on the core polymer. Controlled release of drugs and enzymes are performed by this technique. Lysozyme enzyme was loaded inside PLGA fibers by Tiwari (*et al.*, 2012). Time dependent activity of (aqueous) lysozyme – (chloroform + DMF) solved PLGA core-

shell was higher than monolithic fibers which are prone to burst release of proteins [154]. Also in the same study, (acetic acid + water) gelatin and bovine serum albumin inserted inside the PLGA to exhibit electrospinning of high concentrations of proteins.

Medicinal herbs (Aloe vera) were incorporated inside PCL/chitosan/keratin blend fibers by Zahedi (*et al.*, 2019). Aloe vera has antibacterial and wound healing properties comprised of many vitamins, anti-oxidants, enzymes and minerals [155]. Used shell polymers are well-known polymers for wound dressing applications.

Burst release of antibacterial-agents like silver is a problem in monolithic fiber. Core-shell methodology was used to solve this problem by Khodkar (*et al.*, 2017). PCL as shell polymer and silver added PVA was used as core material to control release rates [156]. Another study was conducted by Song *et al.* (2013), same polymers were used as core and shell but collagen inside core and HAp was added shell to increase osseointegration [157].

Fibroblasts are not wanted inside bone during remodeling process since they can grow on hard tissues faster than on soft tissues that will fill the defect sites and prevent bone modelling [158]. Tang *et al.* (2016) prepared a scaffold for guided tissue regeneration combining drug release and bone growth properties. PLGA/HAp - collagen/amoxicillin core-shell nanofibers were synthesized from HFIP solvent. Amoxicillin were released in a controlled fashion while core-structure prevented fibroblast exertion inside the scaffold.

Shell thickness determined the rate of release in core-shell fibers were shown by Yu *et al.* (2014) that used PCL/PEG while core diameter determines the stiffness of the fibers [159]. PCL and gelatin core-shell combination were benefitted to pH controlled drug release by Sang (*et al.*,2018). [160]They used HFIP as solvent to prepare both precursor solutions. Drexler *et al.* (2011) also used same polymers and solvents to observe the core effect on the stiffness of the material. Produced coaxial fibers, however, have average diameter above 1 μm which can be considered as on the micron scale [161].

Gelatin-PVA core-shell nanofibers were obtained by Merkle (*et al.*, 2015; 2014 ;2013). [99, 162–164]. Merkle *et al.* (2015) proved the usage of core-shell PVA-Gelatin membranes from hemocompatibility, vascular tissue engineering, modulation of platelet activation perspectives. They obtained PVA solution from ethanol and deionized water while gelatin solution was prepared from ethanol added PBS solution. Reason for ethanol to usage is to balance evaporation rates of both solutions and minimize fiber deficiencies [163]. Effect of feed rates ratios were revealed and optimized process conditions were reported by Merkle *et al.* (2015) from bioactivity and mechanical strength. They found out that stiffness is a dominating factor on platelet deposition and activation [99].

2.6. Crosslinking Methods for Non-Woven Nanofiber Meshes

As-spun gelatin fibers are mechanically weak and water soluble. Therefore, application on the places where body fluid is present usually requires cross-linked scaffolds. There are three main crosslinking procedures for gelatin based scaffolds: physical, enzymatic and chemical crosslinking.

Dehydrothermal treatment (DHT), pulsed inductively coupled plasma (PLS) and UV radiation are among the physical treatment methods. Gelatin fibers were crosslinked with DHT by increasing environment temperature to 140 ^{o}C and kept mats at that temperature for 48 hours [165]. PLS method is the treatment of the surface of the mat by plasma at low pressures[165]. UV method is the treatment of the membrane surface with UV source at different durations. Generally, physical treatments are not effective and incase of water treatment, fibers degrade faster than other methods. Since gelatin does not contain photo initiators, UV by itself is not effective, however, bonding it with methacrylate which is a photopolymerizable biomaterial to the amine-containing groups of gelatin is an effective way to crosslink gelatin fibers[166]. This technique can be combined with in situ crosslinking or post crosslinking with immersing mats inside a non-solvent like ethanol and following UV irradiation on the surface [166]. Gelatin and phenylazide-conjugated poly(acrylic acids) were also in situ crosslinked with UV by azido activation which enables sub-surface crosslinking [167].

E-beam and gamma radiations were also used to cross-link gelatin sheets but this technique changes physical and chemical properties of the materials by inducing reactive intermediates and ions. Electron beam was exerted on the gelatin sheets at different dosages by Lee *et al.* (2017) from 10 kGy to 600 kGy [168]. Although, cell proliferation assays are positive, this technique is not used frequently due to residue problems.

Transglutaminase (TG) enzymes cross-link proteins by inducing covalent bond in between glutamine and lysine amino acids which develops more resistant membranes [169].TG has been used as tissue adhesive in hydrogel industry. Recently, with the discovery of microbial TG, this method become a cost effective method to cross-link gelatin based substances. They do not need calcium ions to be activated, as opposed to the animal originated TGs [170]. Since it is a natural cross-linker cytotoxicity is very low compared to other techniques. However, as TG and gelatin both can dissolve inside water, crosslinking of fibers without losing structure is not an easy task. Using ethanol/water mixture is also not a solution due to enzymatic activity loss [171]. Taylor *et al.* (2017) showed various crosslinking procedures on the composite gelatin fibers [172]. They used PBS as solvent for TG at 12% concentration and gelatin fibers directly soaked inside the solution. (Only published results were for tensile strength properties, micro graphs displaying surface morphology were not published.)

(EDC) 1-ethyl-3-(3-dimethyl-aminopropyl)-1- carbodiimide hydrochloride has been used in collagen fibril crosslinking widely, relatively less toxic to glutaraldehyde which is the most used cross-linker. This chemical establishes amide bonds between carboxylic and amino groups. It is a zero-length crosslinker. One of the main advantages of zero-length crosslinkers is that there will be no toxic residual after degradation of the biomaterial. (by product of urea) [173] EDC / (NHS) N- hydroxysuccinimide coupling system is another safer combination for chemical crosslinking method used in collagen crosslinking to increase the efficiency [174]. Obtained residuals are water soluble and clinically identified as safe.

Using aldehydes as formaldehyde [175], glutaraldehyde [36, 97], glyceraldehyde [175], dextran aldehydes [176] and genipin [106] are other mostly used chemical crosslinking methods. Among them, glutaraldehyde is the far most used crosslinker for peptides and it is proven not to be toxic when used at low amounts or cross-linked with glutaraldehyde vapor. Aldehydes can form linkages in between amide, hydroxyl and carboxyl groups of gelatin aminoacids [177]. Carboxyl groups of glutaraldehyde bonds with amine and hydroxyl groups of gelatin. Although, schematic was for carboxymethylcellulose and gelatin, same groups are present in gelatin and PVA. GA crosslinking occurs in between PVA molecules by inserting acetal bridges as depicted in Figure 2.9.

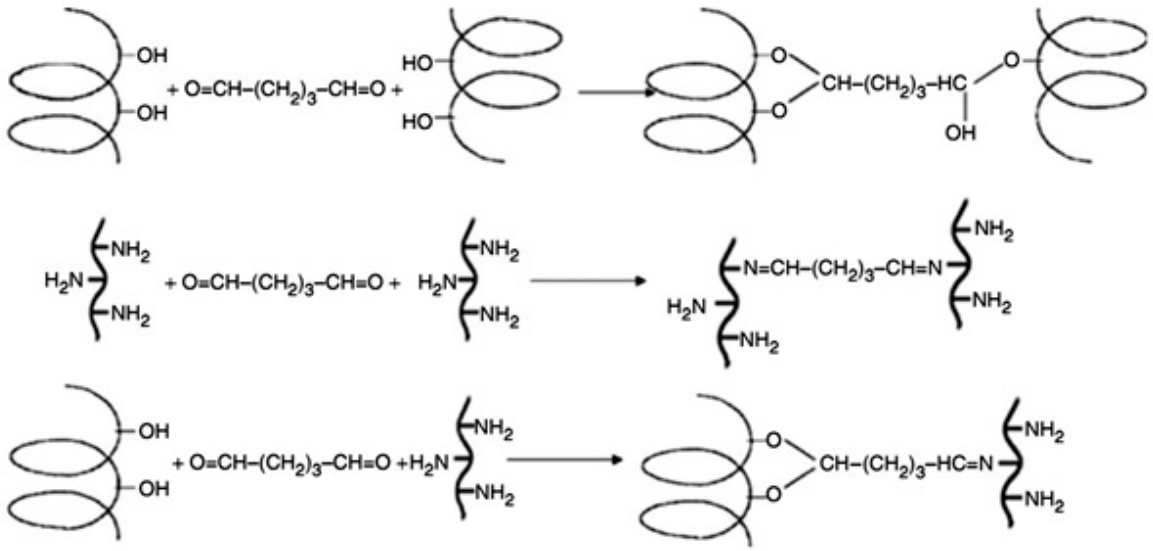

Figure 2.8. Crosslinking reactions with glutaraldehyde occurring in carboxymethylcellulose -Gelatin mixture. (Adapted from [178].)

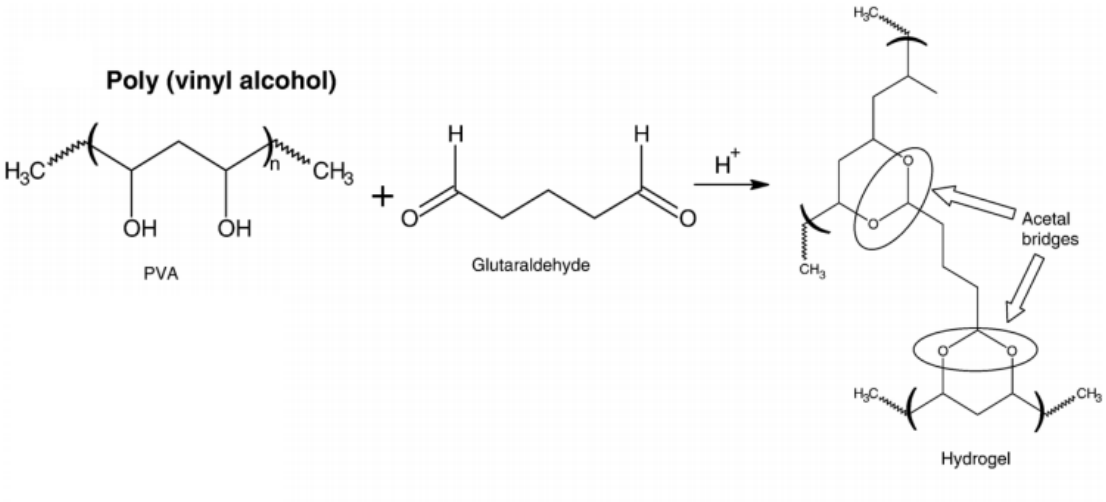

Figure 2.9. Crosslinking reaction with GA occuring in PVA solution [179].

3. MATERIALS AND METHODS

Polyvinyl alcohol (PVA, 86-89 % hydrolyzed, average molecular weight 88,000 g/mol) was obtained from ZAG Chemicals. Bovine Type-B gelatin (Bloom 200) was obtained from Merck in powder form. Glutaraldehyde (25% in H_2O), lysozyme, acetic acid and PBS were purchased from Sigma Aldrich. Deionized water was used throughout all ES experiments.

3.1. ES Setup

A flat stationary counter electrode wrapped with aluminum foil having 10x10 cm rectangular shape was used as collector. Two syringe pumps with adjustable feed rates were operated to drive 5 ml syringes that contain solutions of gelatin and PVA. Voltage was supplied with a high voltage supplier having a resolution of 100 V. Heating done with a hot air blowing gun inside a closed chamber which has higher dielectric constant Teflon covers to prevent leakages. Targeted temperature was maintained by a PID controlled custom-made system. An Arduino based microcontroller was used to check humidity and temperature. For pure PVA and gelatin solutions 18 gauge needles were used. Coaxial needles were used to obtain core-shell nanofibers. Custom-made coaxial needle setup was done by arranging two cannula needles. Nozzle diameters are 14g is outside nozzle and 18g is inner nozzle. This combination is the best remains are not suitable for flow due to high viscosity of PVA which creates shear stress between needle wall and the fluid.

Table 3.1. Needle dimensions and corresponding gauge values

Gauge	**Outer Diameter**	**Inner Diameter**	**Wall Thickness**
14	2.108	1.600	0.254
16	1.651	1.194	0.229
18	1.270	0.838	0.216

All of the concentrations of prepared solutions were stated as wt/wt. Unless it is stated, temperature of the cabin was elevated to 40 ^{o}C to eliminate gelling phenomenon, thereby nanofibers can be obtained via ES. However, gelatin only fibers have beaded morphology due to surface tension and viscosity effects.

Aqueous PVA solutions (8% wt/wt) were prepared first by charging PVA in deionized water slowly at ambient temperature, then allowing to swell for 10 min followed by heating up to 80 °C and keeping solution at that temperature and concentration for an hour. After then obtaining a transparent solution, heating stopped and solution kept at room temperature till the application. Mixing should not be pursued due to rheopectic nature of PVA.

3.2. Crosslinking of PVA/Gelatin Core-Shell Nanofibers

Cross-linking procedure was conducted after extraction of fiber mats from aluminum foil by placing all fibers inside a sealed desiccator with 5% wt/wt glutaraldehyde in ethanol vapor for 24h which was proven to be non-toxic at this level according to literature [180, 181].

If a letter “c” put before sampleID as c1P1G, it means same process parameters with 1P1G but cross-linked under glutaraldehyde vapor. Abbreviations starting with letter “a” for a sampleID mean gelatin fibers obtained from acetic acid solutions.(see Appendix)

Table 3.2. Sample IDs of the spun fiber mats

SampleID	Concentraion (wt/wt)		Feed Rate (ml/h)		Voltage (kV)	Temperature (°C)
	PVA	Gelatin	PVA	Gelatin		
1P	8%	-	0.1	-	15	40
4P1G	8%	8%	0.4	0.1	15	40
3P1G	8%	8%	0.3	0.1	15	40
1P1G	8%	8%	0.1	0.1	15	40
1P2G	8%	8%	0.1	0.2	15	40
1P3G	8%	8%	0.1	0.3	15	40
1P4G	8%	8%	0.1	0.4	15	40
1G	-	8%	-	0.1	15	40
1G12	-	12%	-	0.1	15	40
1G16	-	16%	-	0.1	15	40
1G	-	8%	-	0.1	15	40
1GF0.4V20	-	8%	-	0.4	20	40
1GF0.4V15		8%		0.4	15	40
1GF0.4V10		8%		0.4	10	40
1G1PV12.5	8%	8%	0.1	0.1	12.5	40
1G1PV15	8%	8%	0.1	0.1	15	40
1G1PV17.5	8%	8%	0.1	0.1	17.5	40
1PF0.2	8%	-	0.2	-	15	40
1PF0.4	8%	-	0.4	-	15	40
1GT25	-	8%	-	0.1	15	25
1GT30	-	8%	-	0.1	15	30
1GT35	-	8%	-	0.1	15	35

3.3. Characterization

3.3.1. FTIR

A FTIR spectrum was completed by using spectrometer (Thermo Scientific Nicolet 380) to gather bonding structure of pure PVA, gelatin, and core–shell fibers with crosslinked mats. FTIR spectra were obtained at room temperature within the range of 4000 to 500 cm−1 using 64 scans with a resolution of 2 cm−1. Vibrational frequencies have effect on the absorption amount of the applied wave, thereby chemical structure can be identified.

3.3.2. DSC

Melting, denaturation, dehydration temperatures of the samples were identified by using differential scanning calorimetry (DSC), (Seteram Instrumentation Labsys Evo) using 10 mg samples under nitrogen flow with 10 °C/min heating rate from 25 to 250 °C.

3.3.3. Mechanical Tests

Tensile strength and fracture elongation values were evaluated using universal tensile testing machine (Llyod LF Plus) equipped with a 250 N load cell. Speed of the moving head was adjusted to 3mm/min to give constant deformation rate. All of the experiments were conducted at room temperature and relative humidity of 50%. At least seven rectangular strips were cut for each group including crosslinked pure and core shell fibers. Strips were 60 mm in length and 20 mm in width. Strip holders were centered and samples attached carefully, giving a 10 mm distance in between two clamped portions. Since mats were soft that can be destructed with a micrometer, thickness of the samples were determined by optical microscopy by placing in between two glass plates Figure 3.1.

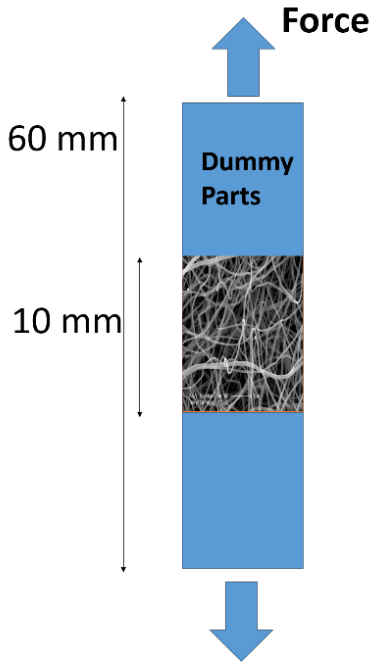

Figure 3.1. Mechanical Test specimen Dummy parts were from grinding papers.

3.3.4. SEM

Size, shape and surface morphology of the nanofibers were imaged by SEM (Philips XL30) having a chamber pressure of under 1 x 10^{-5} Pa and using a beam voltage of 10 kV. All samples were sputter-coated with Pt prior to SEM imaging. ImageJ software was used to analyze fiber diameter distribution and pore sizes. More than 100 random fibers were used for each group and more than 30 random pores analyzed to detect average pore size.

3.3.5. TEM

TEM analysis was performed with a JEOL-ARM 200 CFEG operating at 200 kV. Images were taken in STEM mode using HAADF detector. Fibers were cut into small pieces and soaked inside potassium permanganate in ethanol solution to distinguish core and shell boundaries. A single drop was placed on 300 μm mesh size Cu grids that are coated with carbon from one side. Cu grid was inserted inside oxygen plasma

for 5 minutes before loading inside the microscope chamber. EDS (Energy Dispersive Spectroscopy) analysis was also performed under the same device by shifting to EDS mode.

3.3.6. Rheology

Rheology analysis was performed with (Brookfield DV-III Ultra) a cone plate rheometer device with temperature control. Plate with 3 ^{o} angle were used to measure viscosity at a speed of 5 rpm. Data were collected at every 15 seconds and average of the viscosity values were plotted to understand the behavior of polymers during and before electrospinning.

3.3.7. Water Contact Angle

Samples were placed parallel to the camera stage and a sessile-drop of deionized water dropped on the samples. Water contact angles of crosslinked specimens in air were measured with a goniometer (KSV-CAM 101). More than five measurements were conducted at different locations and mean values were calculated.

3.3.8. Biodegradation

Enzymatic in vitro degradation tests were accomplished by preparing 0.01 M PBS solution containing 0.1 mg/mL of lysozyme. Crosslinked samples were cut into 50 mm x 50 mm squares; initial weights were recorded and soaked inside the prepared PBS. Every individual member has its own petri dish inside the incubator that is kept at 37 ^{o}C. Weights were measured at 24, 48, 72 and 336 hours. For every 24 hours period, samples were taken outside the dishes; washed with distilled water and prepared enzymatic solution re-fed. Samples rinsed, dried and weighted at the specified time points to measure weight losses. Used formula to calculate percentage loss is:

$$\mathbf{w}\% = \frac{w_i - w_f}{w_i} \times 100 \tag{3.1}$$

where w% is the percentage loss and w_i, w_f are initial and final weight of the samples.

4. RESULTS AND DISCUSSION

In this work, unless otherwise it is stated gelatin and PVA solutions have 8% (wt/wt) concentrations inside deionized water.

4.1. Effect of Time, Concentration and Temperature on the Viscosity of the Solutions

Since PVA and gelatin have different rheologic properties under load and temperature, preparing solutions has critical importance. For instance, keeping solutions at constant temperature for long time alters viscosities of the solutions. Rheology analysis was conducted to control and understand the change in viscosity of the gelatin solution which has a complex nature due to inherent conformational structures like random coil, α helical, ß-sheet and triple helix etc. Also PVA is a rheopectic fluid that is viscosity of the solution increases with time when shear was applied on it. Therefore, preparation of the solutions should be very precise. To point out, when preparing PVA solutions, deionized water is heated to 90 ^{o}C. At this temperature, stirring of PVA continues in order to have a homogenous solution. But, as can be seen from the rheology data (Figure 4.2, Figure 4.3) PVA tends to have an increasing viscosity profile with the stirring of magnetic stirrer inside. PVA solution should not be kept under stirring over night or for long time, which causes different viscosities and thereby different fiber sizes. If a narrow band of fiber diameter distribution is required then it is necessary to have the same history of the solutions.

In Figure 4.1, temperature dependencies of different gelatin solutions can be seen where gelatin viscosity plotted as a function of temperature. As it is expected, higher concentration yields a higher viscosity. Viscosity of the solutions did not change too much in between 35 ^{o}C to 40 ^{o}C, however, a sharp decrease can be easily observed after 30 ^{o}C. Gelatin having higher concentration have a better capability to create hydrogen bonds and capture water below gelation temperature. Although, 37 ^{o}C is known for gelation temperature, it highly depends on the concentration and molecular weight of the gelatin. Therefore, even at lower temperatures below 30 ^{o}C it is possible to obtain homogenous gelatin solution.

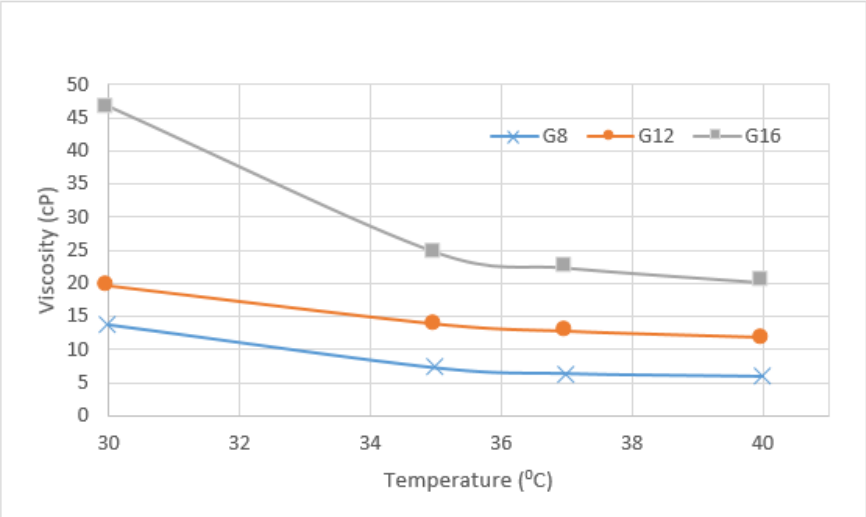

Figure 4.1. Temperature dependency of gelatin viscosity for different solution concentration values.

A linear decrease of PVA solution can be depicted from Figure 4.2. Increasing temperature from 30 to 40 ^{o}C resulted in an decrease in viscosity from 170 to 130 cP. A wide range of viscosity values can be achieved with the change of temperature. In Figure 4.2 at data points there are blurred dots indicating small changes in temperatures during experiments.

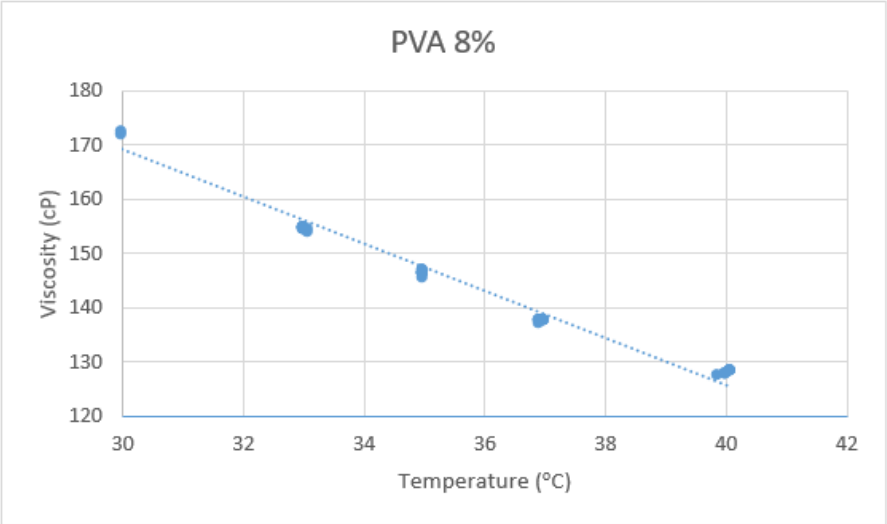

Figure 4.2. Temperature dependency of PVA viscosity for 8% PVA in deionized water.

Time dependency of the polymer solutions is important in the development of a reliable electrospinning experiment. For instance, as can be seen from Figure 4.3, a 5 hours long viscosity measurement tests were conducted in order to see the changes in rheologic properties of the solutions. For the first half an hour PVA solution has almost a constant viscosity. As rotating disc on the fluid continues, PVA hardens linearly. Approximately 30% change of viscosity value was observed.

Viscosity values of gelatin had also increased. Another 30% change after 5 hours can be observed from the graph. It is important to note that, this increase is not as is PVA. This can be originated from sophisticated nature of gelatin secondary structures. Helix conformation could have turned into random structures, gradually.

Due to polarities of PVA and gelatin solutions, it is expected to have a homogenous blend of PVA and gelatin solutions, however, under neutral conditions, inside aqueous environments they are immiscible solutions [135]. Figure 4.4 shows gelatin and PVA solutions mixture at 40^{o}C. Both solutions were heated to 40 ^{o}C and mixed in another tube. Since PVA has lower density, it moves upwards immediately after mixing. (Note to the bubbles inside the mixture) Two solutions are immiscible; in

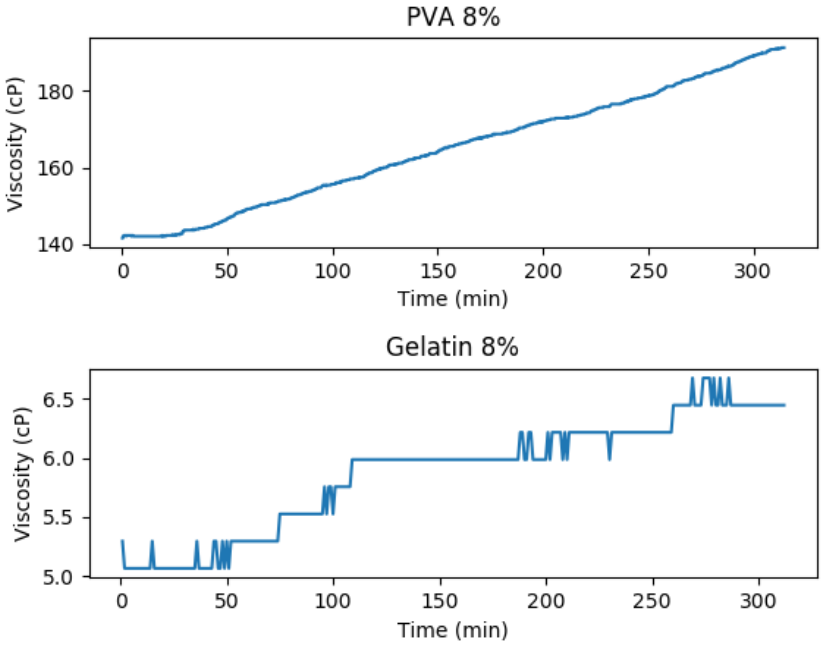

Figure 4.3. Time Dependencies of both PVA and gelatin solution at 37 ^{o}C.

fact, they create a flat interface this makes both solutions most suitable candidates to fabricate core-shell morphology [182].This property enables coaxial electropinning even though eccentricity of the needles were shifted.

4.2. Effect of Process Parameters on the Fiber Morphology

Morphology of electrospun fibers and created mesh of fibers depends on the process parameters. Those parameters were investigated in the literature thoroughly. However, gelatin dissolved inside pure water and core-shell elecrospun PVA/Gelatin dissolved inside water cases were not investigated. This work tries to reveal the effect of process parameters such as voltage, feed rate, concentration and temperature on the fiber morphology thereby on the mechanical strength and surface characteristics. Also, it is tried to show the secondary structures of gelatin with ES.

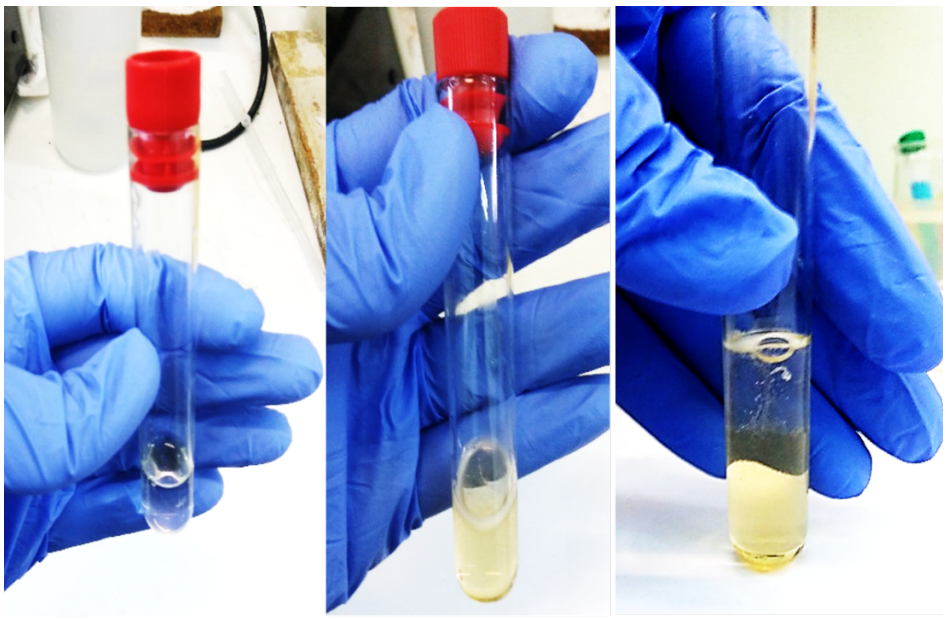

Figure 4.4. Left to right: 8%PVA solution, 8%Gelatin solution, Mixture of gelatin and PVA solution, immediately after mixing.

4.2.1. Voltage

Keeping other parameters same and looking for the morphology change as a function of voltage resulted in Figure 4.5. Concentration was 8% in deionized water, feed rate was 0.4 ml/hour electrode distance was 15 cm and 3 different voltages supplied to the solution and observed macro graphs (foils) on the left. Circles on the figures are the places where 100000X zoom occurred where the right column shows figures of SEM. Arrows indicate localized droplets. It is interesting to observe that having higher voltages diminished the droplets on the foil. Almost no fiber is observed on the lowest voltage (10 kV). Thickness of the fibers was well below 50 nm such that this can be observed from the SEM figures. Although applied 20kV diminished a concentrated zone of droplets, droplets get smaller and spread to a wide area. Besides, at lower and higher voltages small sized fibers formed and burn out when electron beam exerted on them. Shining spots on SEM figures indicates this phenomenon even though fibers were coated with gold prior to analysis. 15kV voltage resulted in a stable fiber morphology.

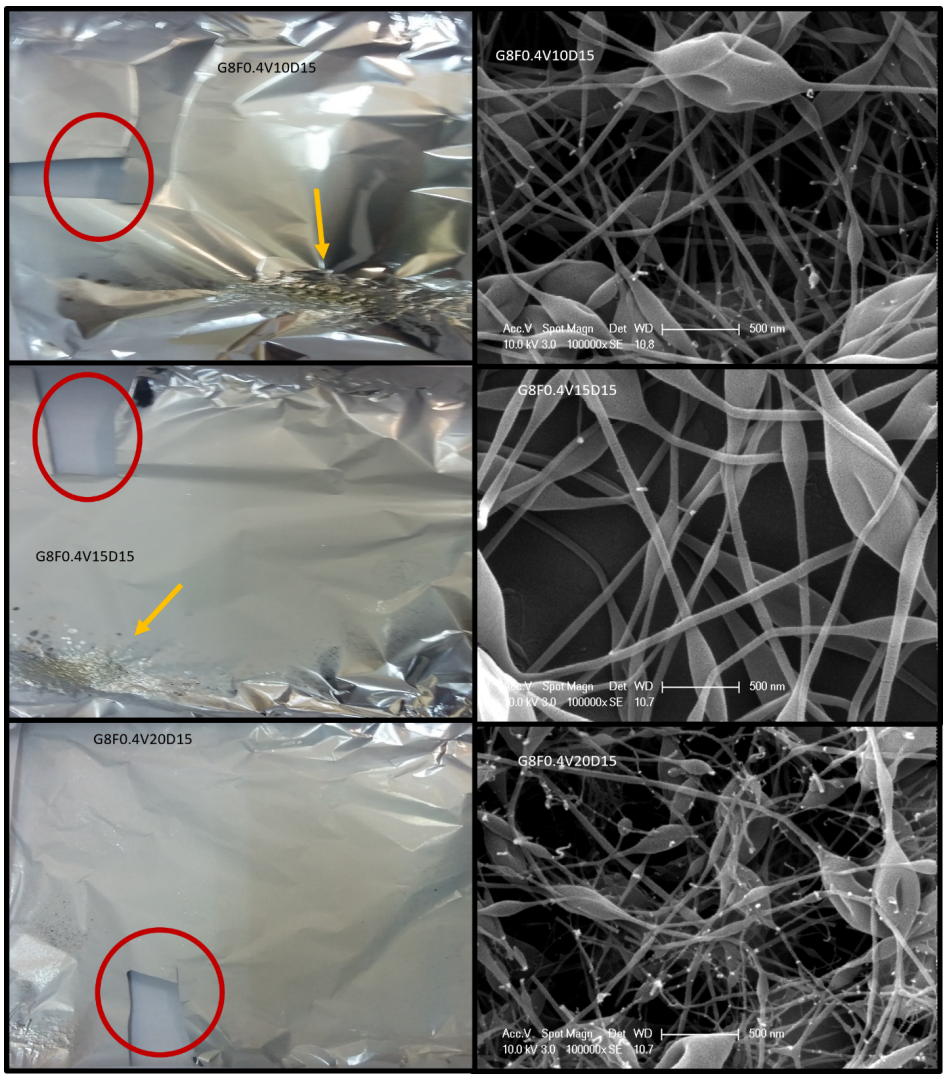

Figure 4.5. Left: Deposited Fibers on Aluminum Foil, Right: 100000X zoom on the *circled* area: %8Gelatin, Feed rate of 0.4 ml, electrode distance of 15 cm, temperature 40 voltage Top: 10kV (1GF0.4V10) Middle:15kV bottom:20kV.

Effect of voltage on Gelatin 8% inside water can be detected by looking at Figure 4.6. Fibers for different voltages can be fabricated. Through 10kV to 20kV, morphology of beads transforms into larger beads. Conversely, diameter of the fibers that are adjacent to the beads are larger in 10 kV and gets smaller when the applied voltage increased. Surface of 1GF0.4V20 membrane is full of with large droplets and spun beaded fibers are under those large droplets. 1GF0.4V15 exhibits no droplets with proper beads due to competition in between surface tension and viscosity.

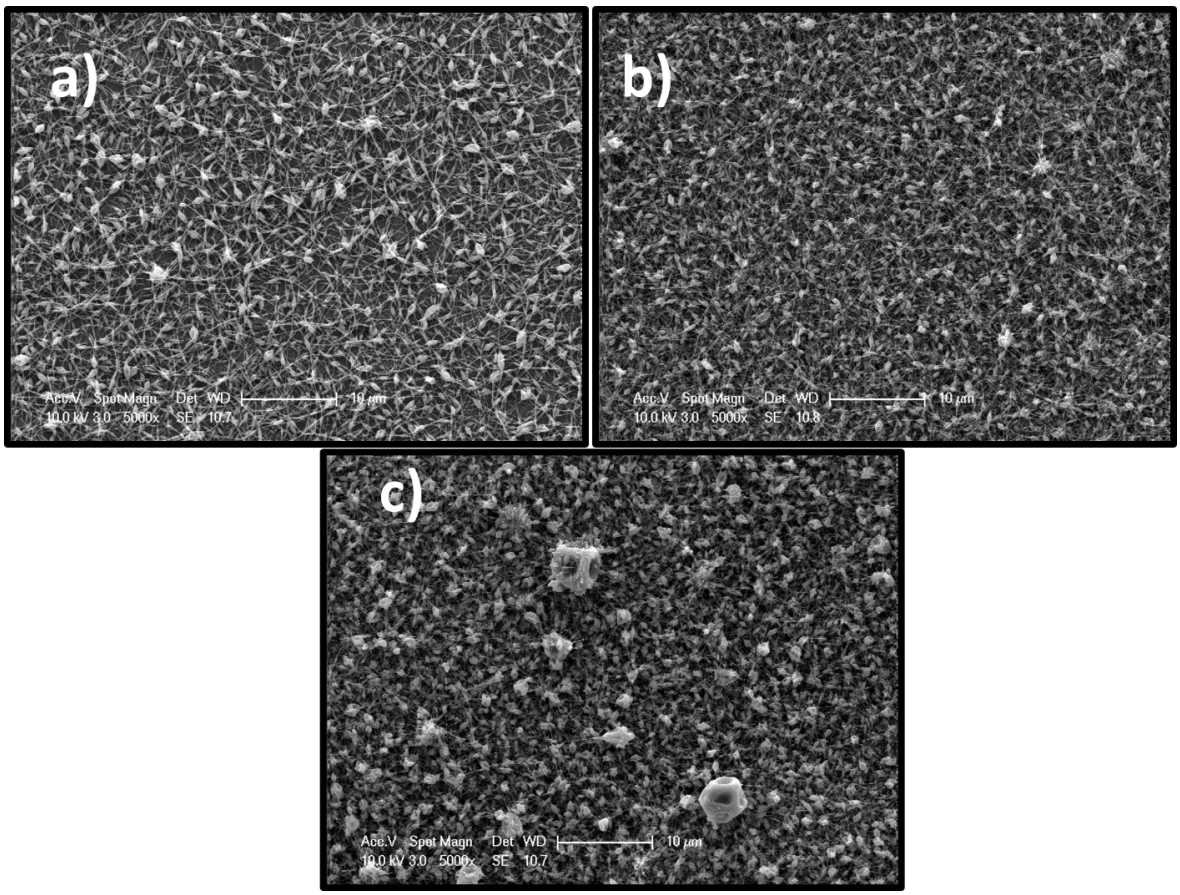

Figure 4.6. Effect of voltage on the Gelatin nanofibers obtained from deionized water, %8Gelatin, Feed rate of 0.4 ml, distance of 15 cm 5000X a) 10kV(1GF0.4V10) b)15 kV (1GF0.4V15) c)20 kV (1GF0.4V20)

Core-shell morphology can be obtained with voltages in between 12.5 to 17.5 kVs at 15 cm and feed rates of 0.1 ml/hour for both solutions as shown in Figure 4.7. Three different voltages at constant other parameters exhibited different surface morphologies. The lowest voltage of 12.5 kV has very thick nanofibers on top and smaller diameters of other fibers at the bottom. This is due to lack of required coulombic forces to extract fibers to eject at the same time. When applied voltages are low a Taylor cone could not be formed as for single solution. Bubble at the tip grows and when charges get enough to push jet, it ejects. At 17.5 kV beaded morphologies formed due to lack of time to create smooth fibers. As strength of the field is higher than the other cases they are susceptible to environmental conditions to initiate an instability. At 15 kV the optimum shape of the fiber bundles were seen. They did not exhibit any beaded morphology or any individual gelatin or PVA fiber characteristics.

As stated above, PVA was one of the most studied polymers from ES perspective. Effect of voltage on the fiber diameter were investigated recently by Rodoplu and Mutlu, (2012) increasing voltages resulted in the fiber diameter reduction when other parameters kept constant [183].

4.2.2. Feed Rate

Keeping viscosity same, feed rate has one of the most important effect on the fiber diameter [184]. There is an optimum flow rate which creates a balance in between solution dispense and the jet formation at the tip. Below that rate, solution does not form a continuous Taylor cone. Figure 4.8 is of 8%PVA solution (a) has 0.1 ml/h and (b) has 0.2 ml/h reveals that fact where both fiber diameters are very close to each other even though latter one is twofold faster than the former one. Fibers have 219 and 207 nm diameter as can be read from Table 4.1, respectively. Optimum flow rate for single PVA 8% was 0.2 ml/hour at that conditions. Further increasing to 0.4 ml/h resulted in 386 nm thick fibers. (Figure 4.8 c). These results are compatible with the literature concluded that a slight change in feed rate within the range of the continuous fiber formation results in huge deviations at fiber diameter size and distribution [185].

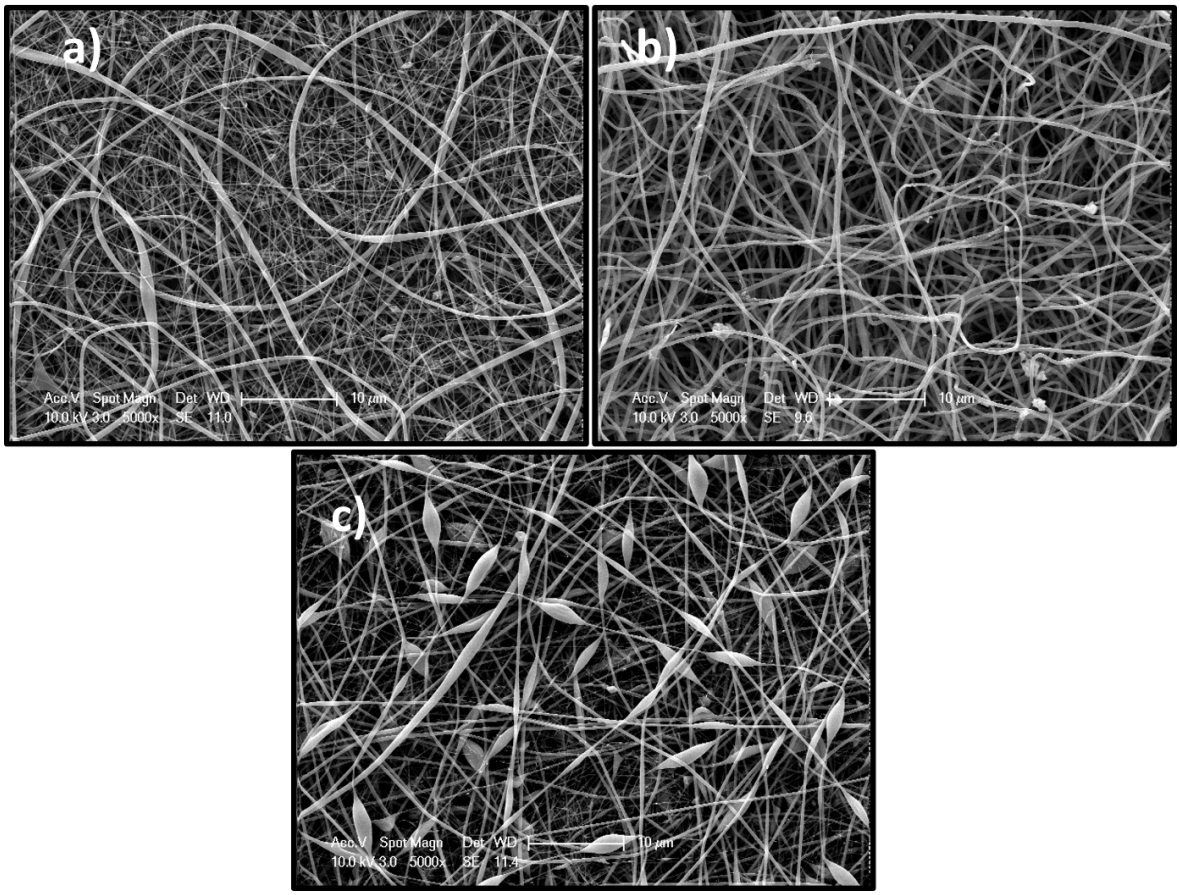

Figure 4.7. Effect of voltage on the core-shell nanofibers %8 PVA-%8 Gelatin electrode distance is 15cm feed rates of both solutions was 0.1 ml/h a) V12.5 (1G1PV12.5),b) V15 (1G1PV15),c) V17.5 (1G1PV17.5).

For Gelatin different 0.1, 0.2 and 0.4 ml/h conditions were also tried and it is observed that above 0.1 ml/h dispensed solution directly sprays on the foil without producing fibers. This dictates that allowable gelatin spinning range has a very narrow band close to 0.1 ml/h for voltage 15 kV, distance 15 cm and temperature 40 ^{o}C.

Table 4.1. Mean fiber diameter values with standart deviations for three different feed rates of 0.1 ml/hour, 0.2 ml/hour and 0.4 ml/hour of PVA 8% solution

V15D15T40	**Feed Rates**		
	Fp01	Fp02	Fp04
Mean(nm)	219.67	207.40	386.94
Standart Deviation (nm)	29.18	40.62	87.37

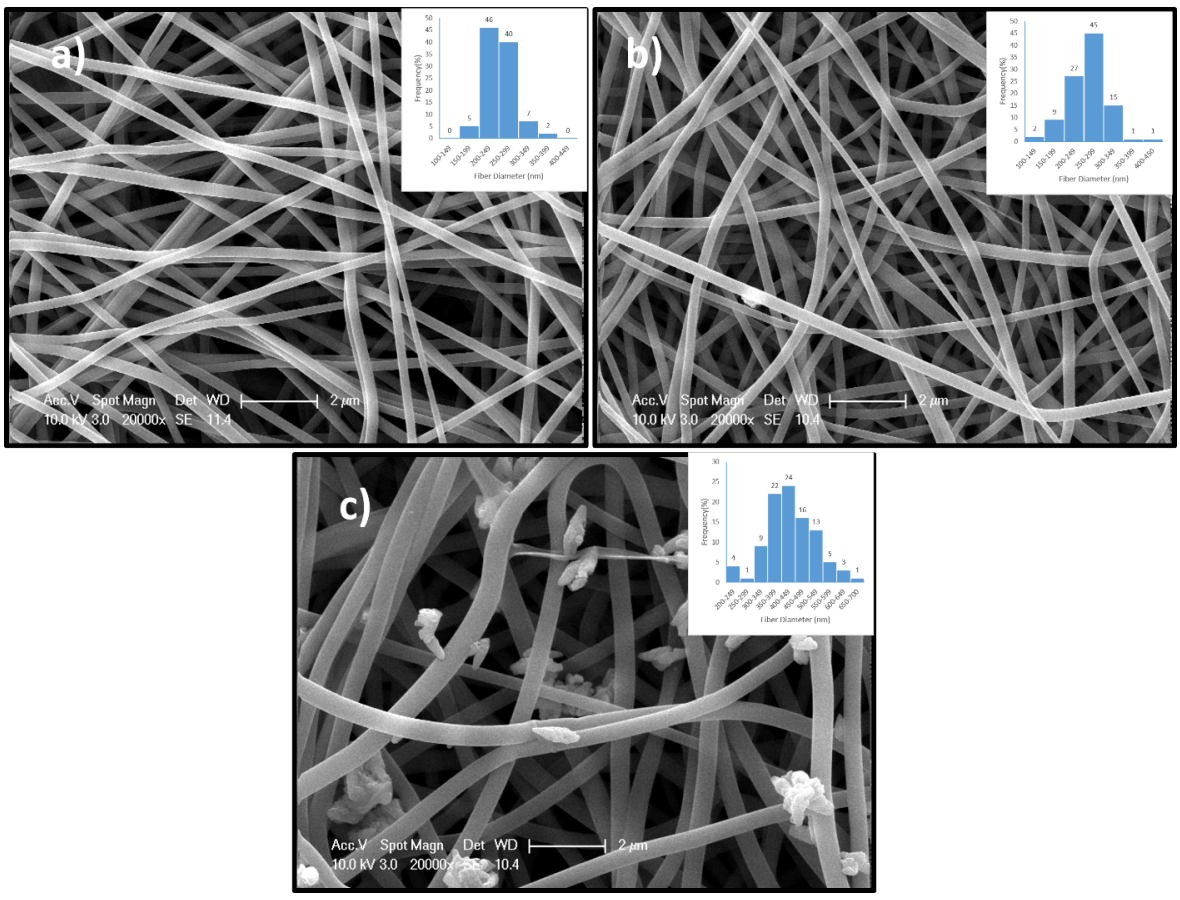

Figure 4.8. Effect of feed Rate on the PVA fibers at voltage 15kV distance 15 cm and temperaute 40 ^{o}C a)Fp01 (1P) b)Fp02((1PF0.2)) c) Fp04 ((1PF0.4)).

Gelatin smooth fibers from aqueous solvents could not be obtained with the specified conditions. Figure 4.9 shows surface of the mats that are produced at 0.4 ml/hour of PVA, 20 kV voltage amplitude, 15 cm electrode distance and 40 ^{o}C conditions while shell gelatin solution had feed rates of (a) 0.1 ml/h, (b) 0.2 ml/h, (c) 0.4 ml/h. Size of pure PVA at 0.4 ml/h had shown at Figure 4.8 (c). It has a mean diameter of 387 nm which is very thick compared to other feed rates. Even 0.1 ml/h of gelatin can coat the surface of PVA. Interestingly shell feed rate of 0.4 ml/h decreased the mean size of coaxial fibers. Increased shell feed rate enforces and stabilizes PVA fibers. Also it is claimed that there is a ratio that coating of core fiber can be possible. Above that ratio free forms of pure gelatin fibers can be observed. For instance, comparing shell feed rate of 0.4 ml/h, core feed rate of 0.4 ml/hour (Figure 4.9(c)) with core feed rate of 0.1 ml/hour (Figure 4.10 (c)) with specified process parameters, resulted in large, beaded fibers. Since a decreased feed rate of PVA lead to smaller diameter fibers at the core, adhesion of gelatin shell layer was decreased and 0.4 ml/h became excess for the 0.1 ml/h core.

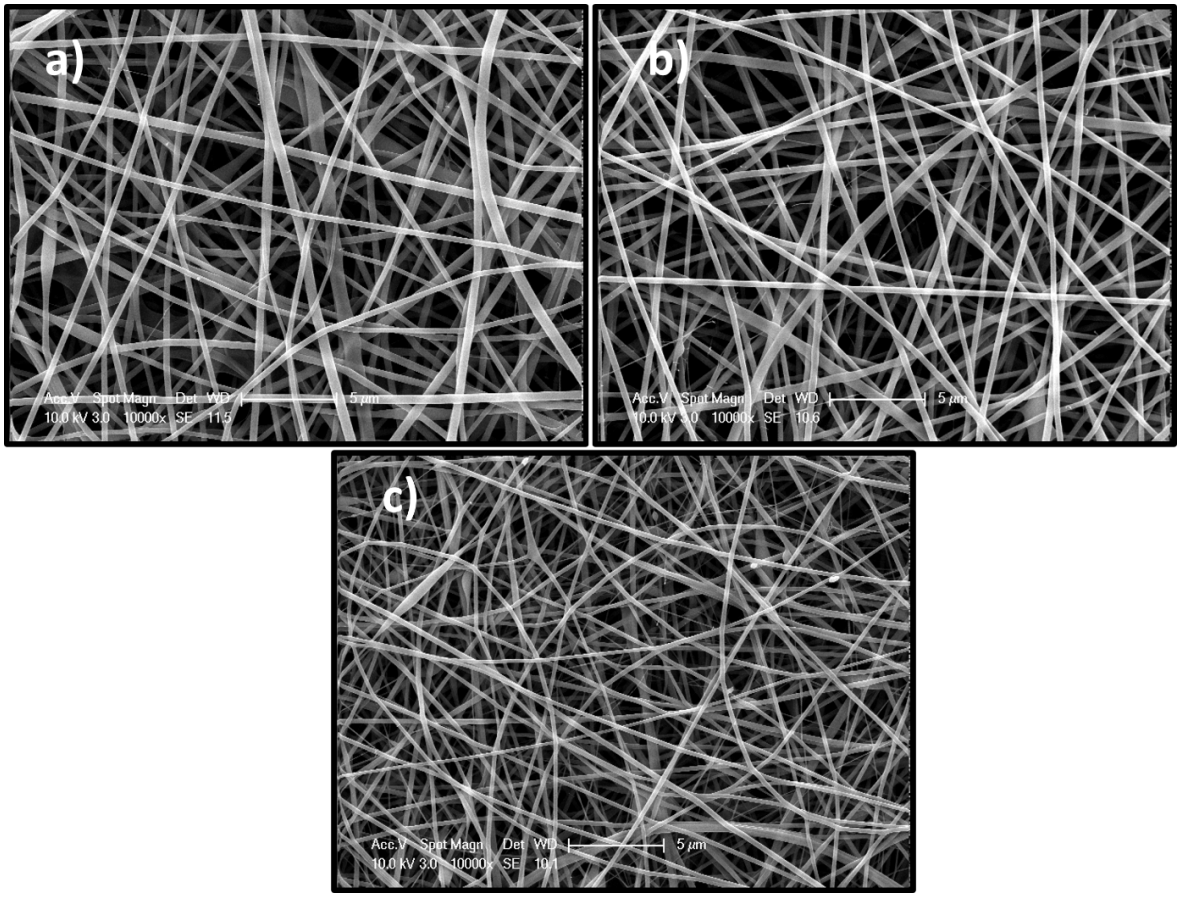

Figure 4.9. Effect of feed rate on core-shell fiber morphology. Fp0.4V20D15 a)Fg0.1 b)Fg0.2 c)Fg0.4.

Figure 4.10 (a) and (b) reveals 1:1 ratio of feed rates. Decreasing feed rates obviously decreased the mean diameter. Although case (b) is barely smaller diameter than other cases due to slow feed rates, it has very thin fibers and thick fibers at the same time. Case (a) has more smooth fibers and a narrower diameter distribution but thicker than case (b). Therefore, changing operational parameters like voltage to 15kV can make case (b) more smooth and a normalized fiber distribution.

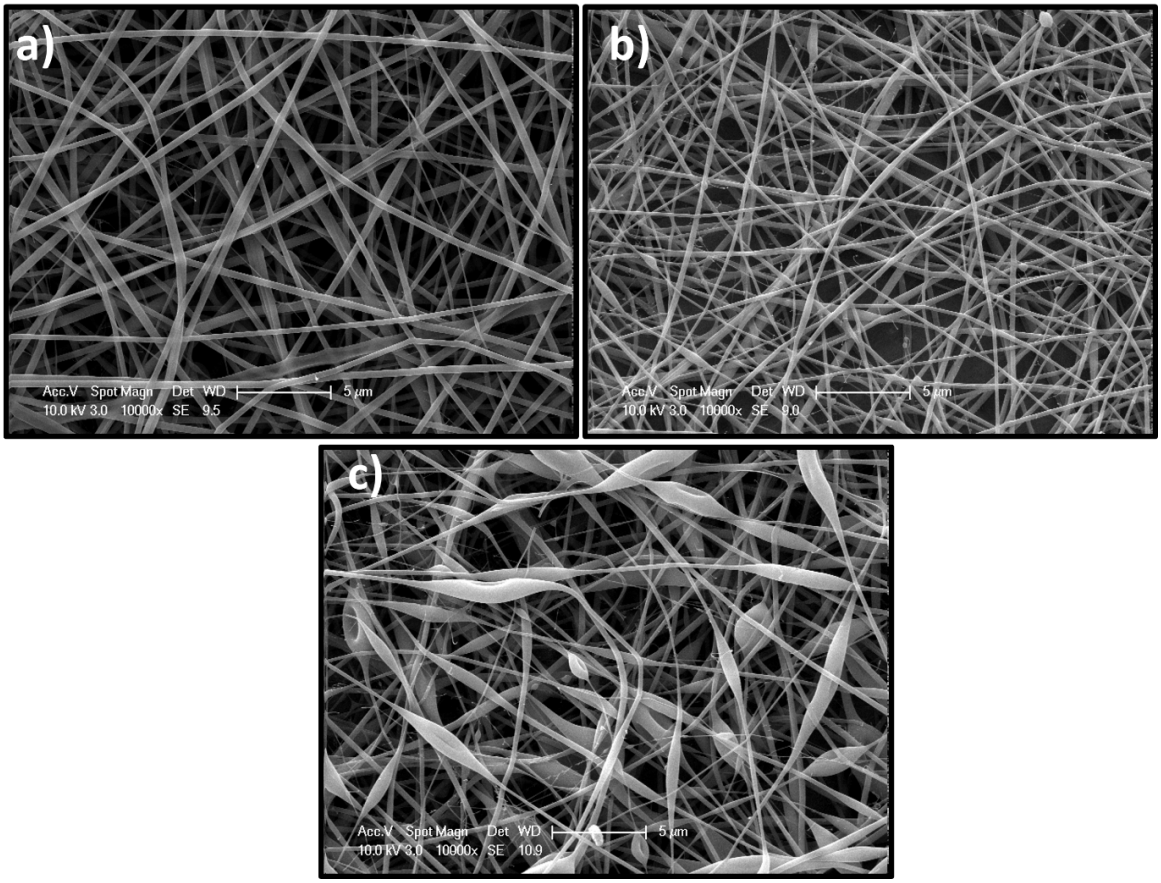

Figure 4.10. Effect of feed rate on core-shell fiber morphology voltage 20 kV distance 15 cm Temperature 40 ^{o}C a)Fp02Fg02,b) Fp01Fg01,c) Fp01Fg04.

To find out adsorption limit on PVA, feed rate ratios were changed gradually. SEM images of 4:1, 3:1, 1:1, 1:2, 1:3 and 1:4 ratios were presented in Figure 4.11.Pure PVA with 0.4 ml/h has a 387 nm mean diameter at voltage 15 kV, distance 15 cm and temperature 40 ^{o}C conditions, while 4P1G has 308 nm diameter with an apparent decrease at diameter. This identifies the effect of gelatin which has stabilizer and even creating extra stress on the core PVA and shrinks size of the PVA more. Decreasing the feed rate of PVA 0.4 to 0.1 ml/h while keeping gelatin constant at 0.1 ml/h created a decrease on the size of the nanofiber as expected since pure PVA decreases its size with decreasing feed rates. Even further increasing the ratio of gelatin resulted in a slight decrease trend at diameter values. (Figure 4.12)

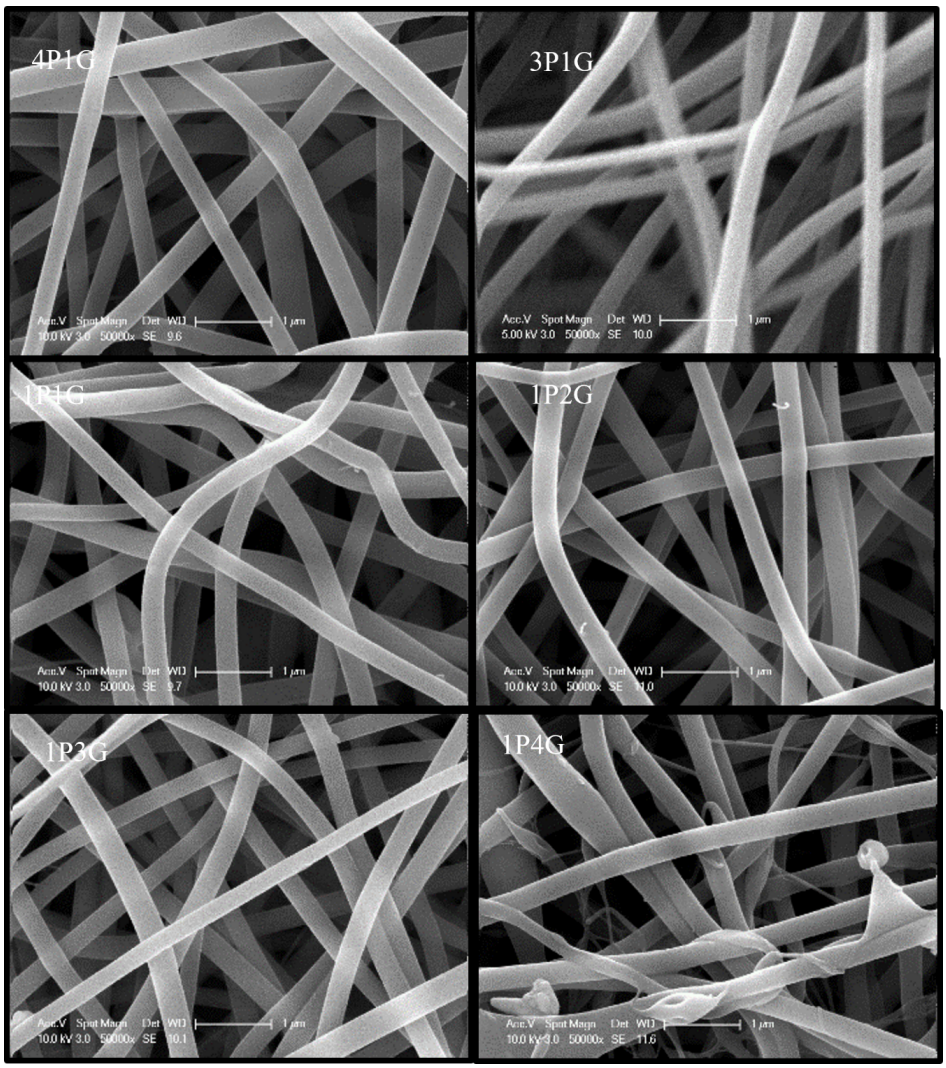

Figure 4.11. Fiber morphology wrt different feed rate ratios, process parameters are voltage 15 kV distance 15 cm and temperature 40 ^{o}C.

After 1:3 ratio extra rise resulted in free forms of gelatin as can be depicted from Figure 4.11. This indicates 1P3G as a limiting feed rate ratio for continuous smooth coating at voltage 15 kV distance 15 cm and temperature 40 ^{o}C conditions. 1P4G case effects trends of the diameter size in Figure 4.12, in fact, standard deviation is very large where diameter values are constituted from both pure gelatin and core-shell fiber diameter values. Even excluding the last case, a slight decreasing trend at the size of the fibers can be illustrated.

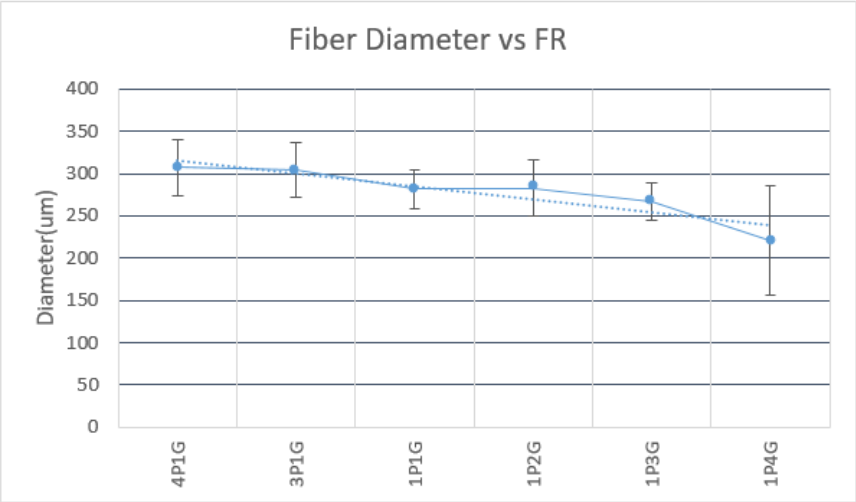

Figure 4.12. Diameter vs different feed rate ratios at voltage 15 kV distance 15 cm temperature 40 ^{o}C.

4.2.3. Concentration

By trial and error method maximum and minimum concentrations of the solutions were found. For gelatin, allowed spinning range was 8-16%. To fabricate thinner fibers lowest viscosity of the solutions that permits spinning is the first essential point. 8% concentration was the lowest limit, below which fabrication method turns into electrospray where aluminum foil is coated with wet small droplets. Gradual increasing results in fibers with larger diameters, as concentration was increased bead size decreased and fiber diameter increased. Further increase resulted in severe clogging of the solution at the tip of the needle.

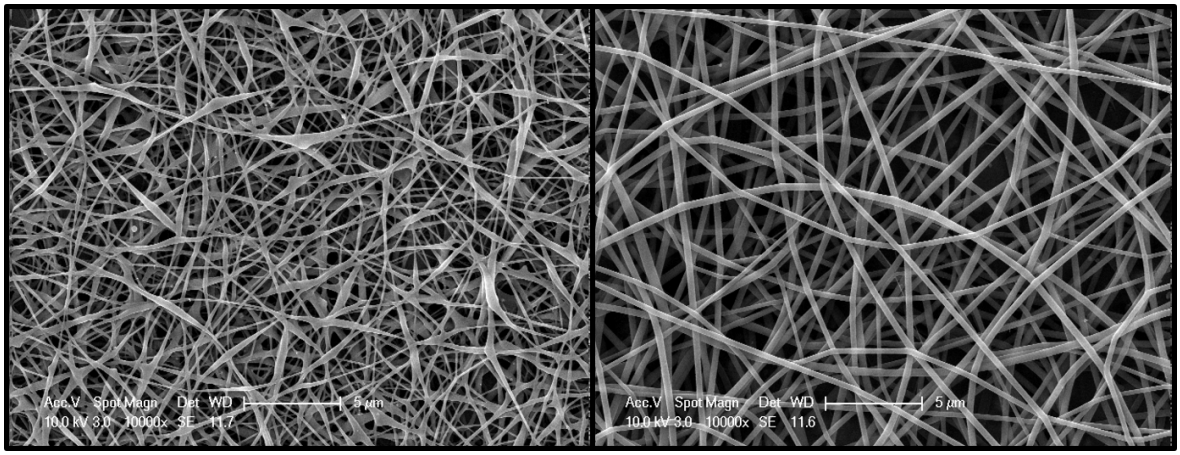

Figure 4.13. PVA fibers obtained from deionized water left 4% right 8%, feed rate of 0.1 ml/h and other process parameters voltage 15 kV distance 15 cm and temperature 40 ^{o}C.

For PVA as taken from literature and our findings it has an optimum concentration of 8% inside deionized water at 40^{o}C. 4% PVA was also achieved and SEM Figure 4.13 shows the fiber morphology. Although 4% fibers are thinner than 8% ones, they have a barbed morphology not a uniform morphology. 8% PVA concentration has a clear smooth fiber morphology.

As concentration increases gelatin fiber diameter becomes larger and beads due to instabilities decrease. %16 concentration of gelatin is physical limit for spinning it is because higher amounts results in severe clogging of the nozzle. This can be prevented by increasing nozzle diameter and increasing temperature. (Figure 4.14)

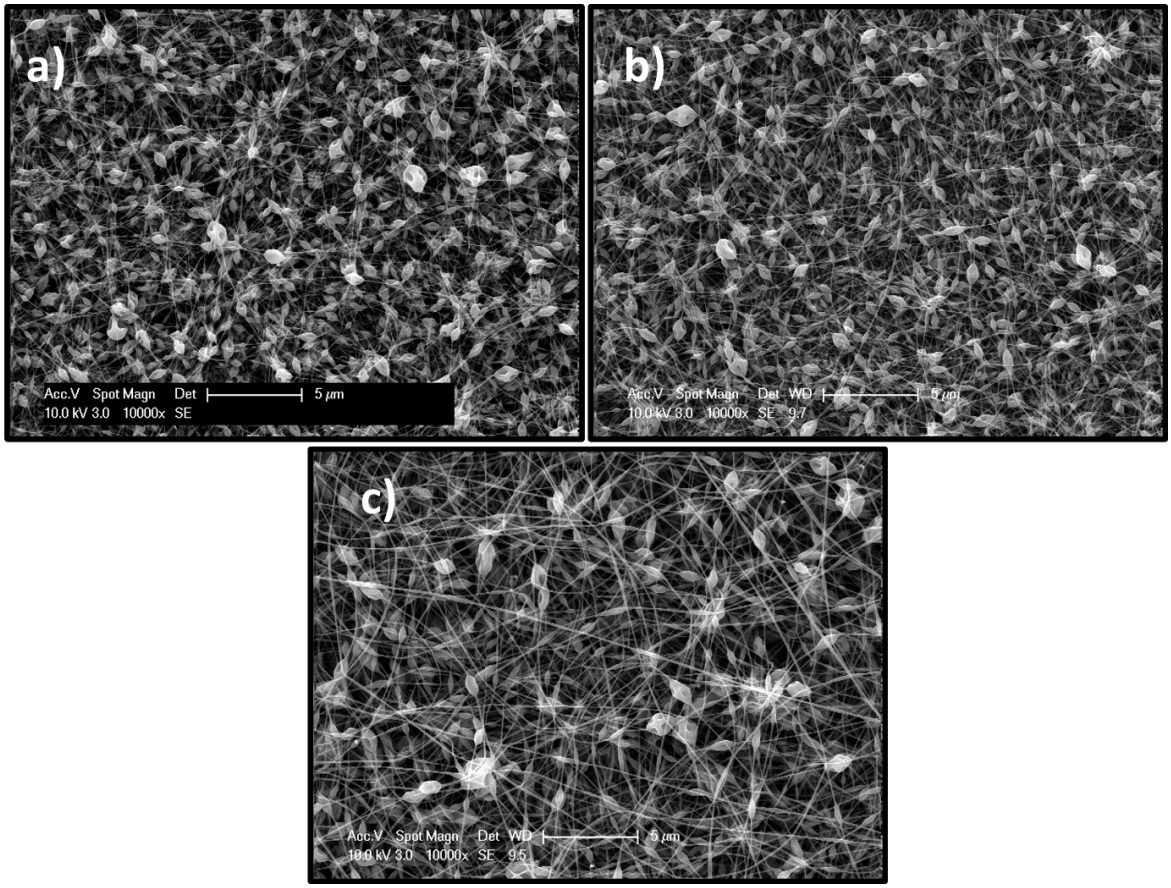

Figure 4.14. Effect of gelatin concentration on the fiber morphology a)G8,b)G12,c)G16; process parameters are voltage 15 kV distance 15 cm and temperature 40 ^{o}C and feed rate of 0.1 ml/h.

4.2.4. Temperature

Effect of temperature on the electrospun nanofibers can be detected on below figure. Increasing temperature decreases viscosity therefore a decrease at fiber diameter was expected [186], however higher temperatures leads faster evaporation which turns fibers become solid immediately after ejection from the tip of the needle. This phenomenon was also detected by different researches [187, 188].

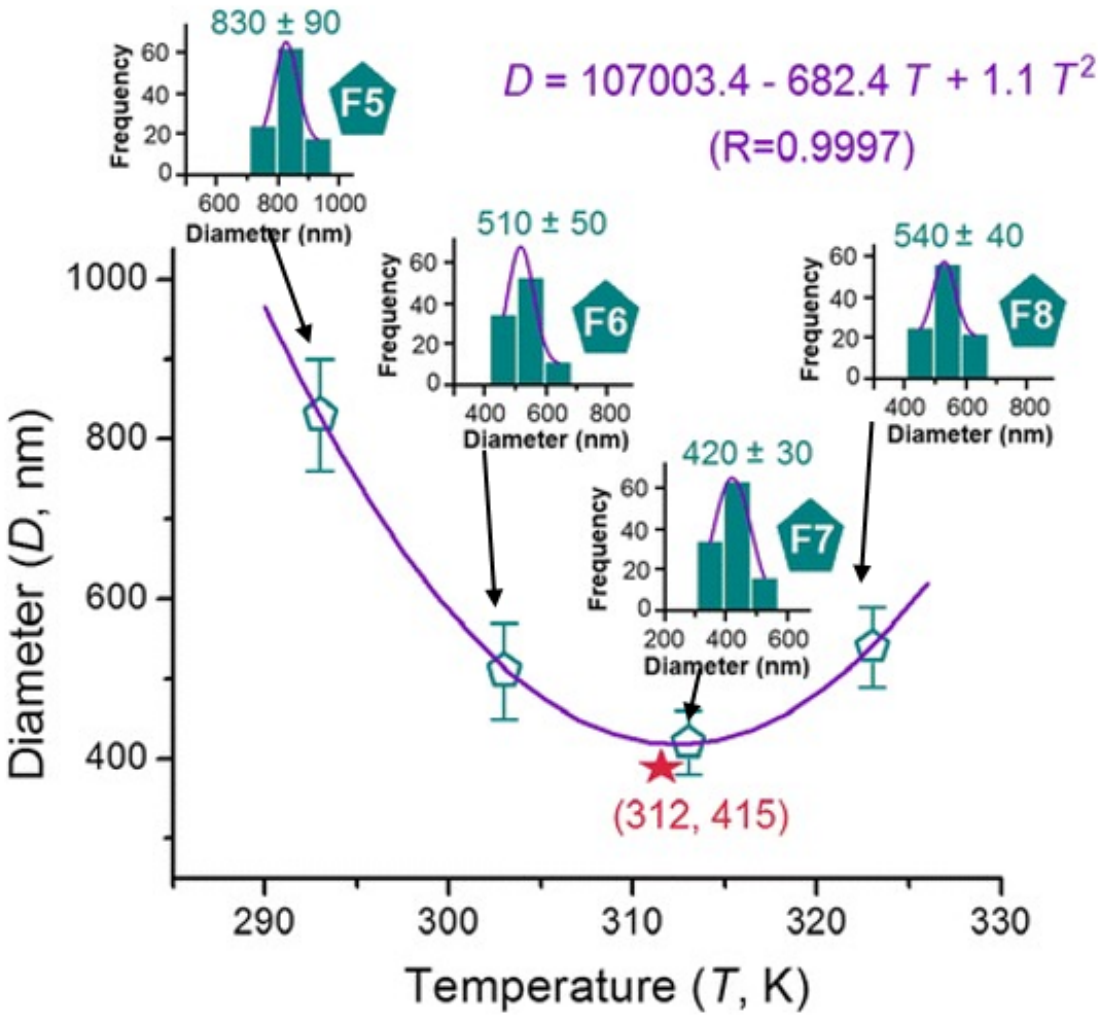

Figure 4.15. PVP(polyvinylpyrrolidone) fiber diameter wrt temperature, F5,F6,F7,F8 are the names of the experimental groups [187]

Near a liquid surface there occurs a thin layer of dense vapor layer called as Knudsen layer. Knudsen layer can be computed as [189]

$$L_c = \frac{kT_s}{\pi d^2 p_s}$$

where p_s is the saturated pressure, T_s is the temperature, d is the solvent molecular diameter, and k is the Boltzmann constant.

In the above equation, saturated pressure also depends on temperature which increases in a parabolic trend. Therefore, layer thickness (L_c) decreases with increased temperature in a linear way. Explanation of the fiber diameter change with respect to ambient temperature is lying under the tradeoff between positive effect of viscosity and negative effect of faster evaporation. Same dependency can be detected at 1G8 nanofibers. (Figure 4.16) Changing concentration and checking again the diameters wrt temperature, resulted the same issue.

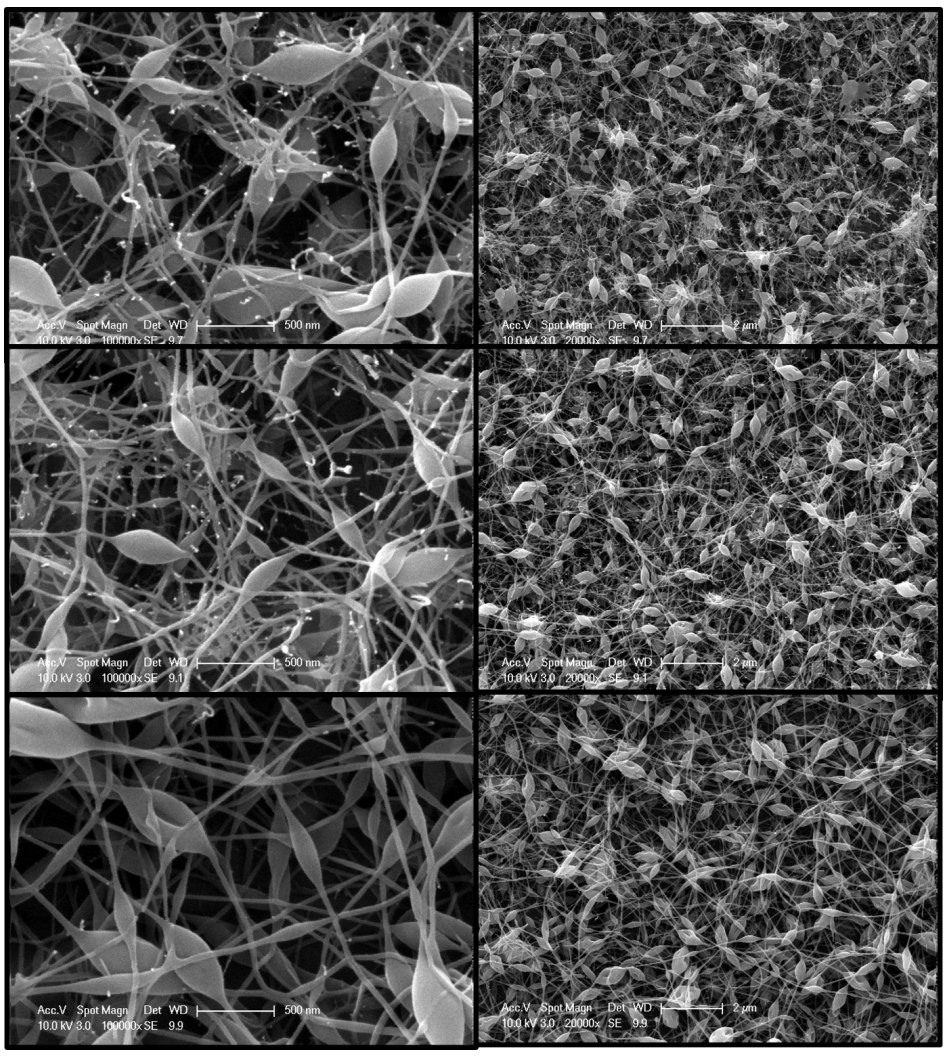

Figure 4.16. Gelatin fibers obtained at voltage 15 kV distance 15 cm 0.1 ml/h feed rate and temperature of top row:25 ^{o}C (1GT25), middle row:30 ^{o}C(1GT30), bottom row:35 ^{o}C (1GT35).(Left column zoom 100000X, right column 20000X).

Diameter of the gelatin fibers measured by taking the smooth fibers after or before the bead along deposited fiber. As Figure 4.17, reveals that increased temperature resulted in thicker fibers. This result implies that those temperature values are at the right side of the concave up parabola of diameter vs temperature graph for the specified conditions. Below 25 ^{o}C (298K) (1GT25) Gelatin at that concentration becomes a total gel that prevents fiber formation. Above 40 ^{o}C is not practical because of the fact that demanded conformation of gelatin could not be preserved. Similar results were obtained by Elliott (*et al.*, 2009) [190]. Temperature was changed from 37 to 52 ^{o}C for bovine gelatin having a bloom value of 210. Initially fiber diameter decreased with temperature and increased after reaching its minimum value due to evaporation rate.

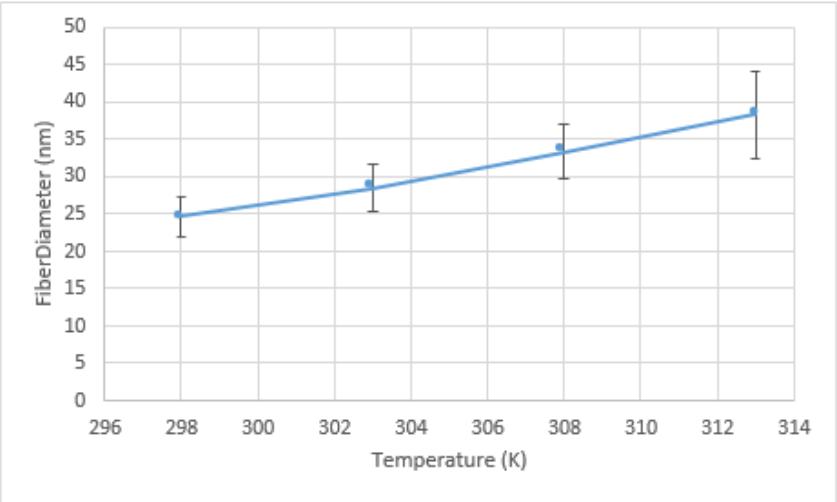

Figure 4.17. Gelatin fiber Diameters obtained from voltage 15 kV, feed rate of 0.1 ml/h, electrode distance 15 cm with respect to temperature.

4.3. Proof of Core-Shell Structure

Proof of the core-shell structure were ensured with TEM and EDS images of the 1P1G and SEM images of the 1P4G cases.

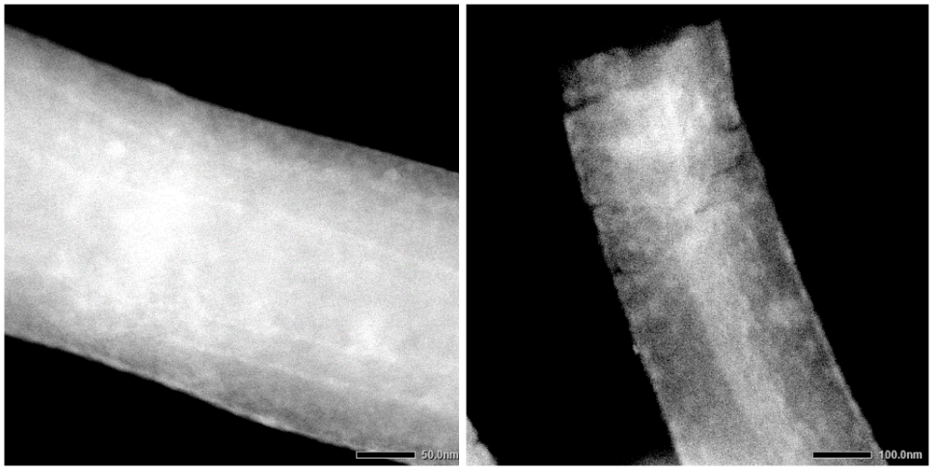

Figure 4.18. TEM figure of core-shell fibers.

Figure 4.18 displays two distinct regions of two separate fibers obtained from distinct places of the samples. In order to detect core-shell structure at TEM, potassium per manganite ethanol solution was used to increase contrast difference in between PVA and gelatin due to different affinities of gelatin and PVA on metals [191].

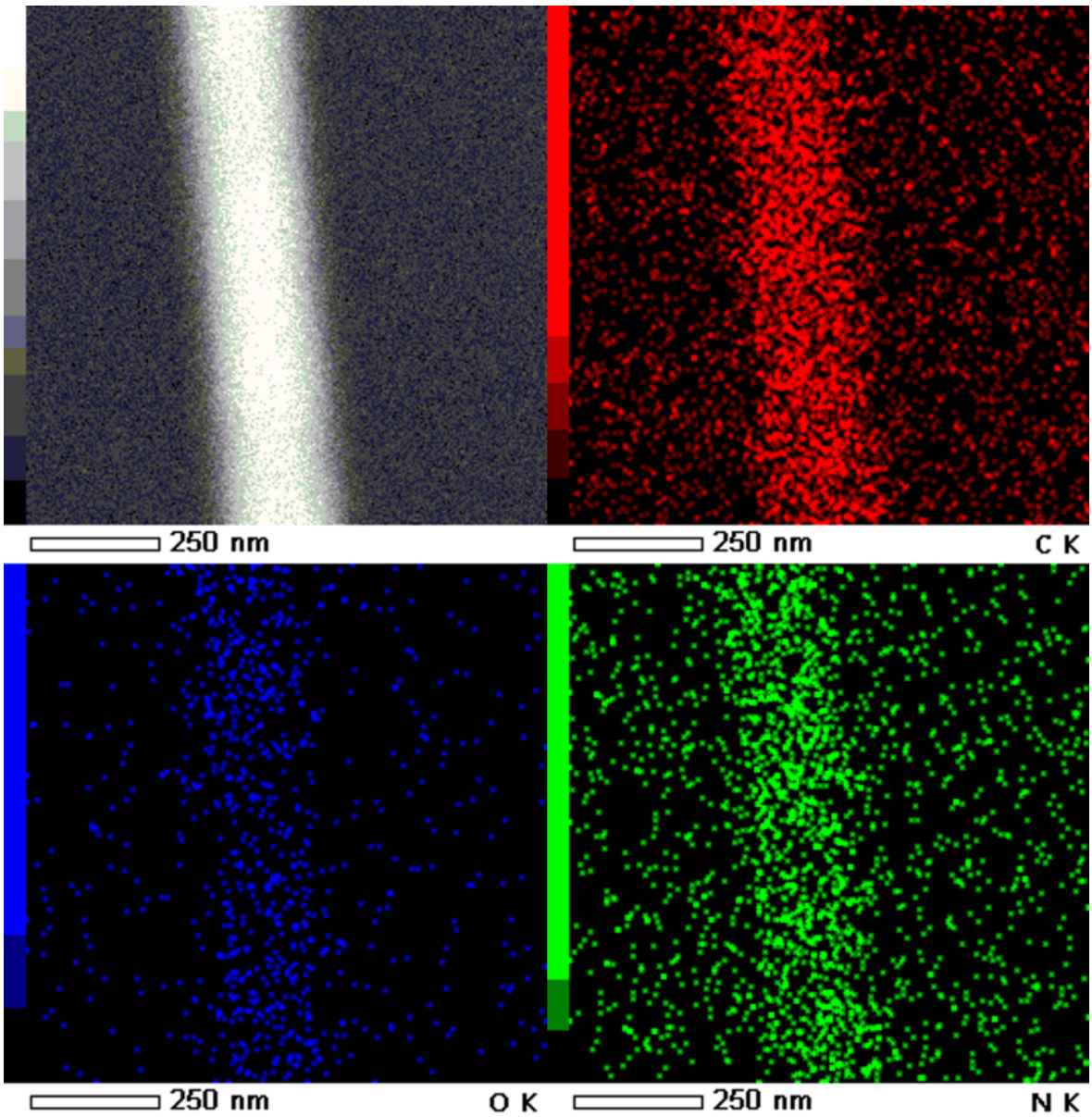

Figure 4.19. TEM EDS analysis of the samples 1P1G.

EDS analysis was performed in order to detect which element is at what point. (Figure 4.19) Since gelatin contains nitrogen and PVA does not, this element has a distinguisher property. Detecting the place of nitrogen gives information about the coating. If gelatin did not coat core PVA, then nitrogen peaks could not be observed, or they had confined to a place rather than covering hole diameter. Also EDS analysis defeated the possibility of PVA-only fibers since PVA fibers are also smooth and close

in diameter to the core-shell fibers.

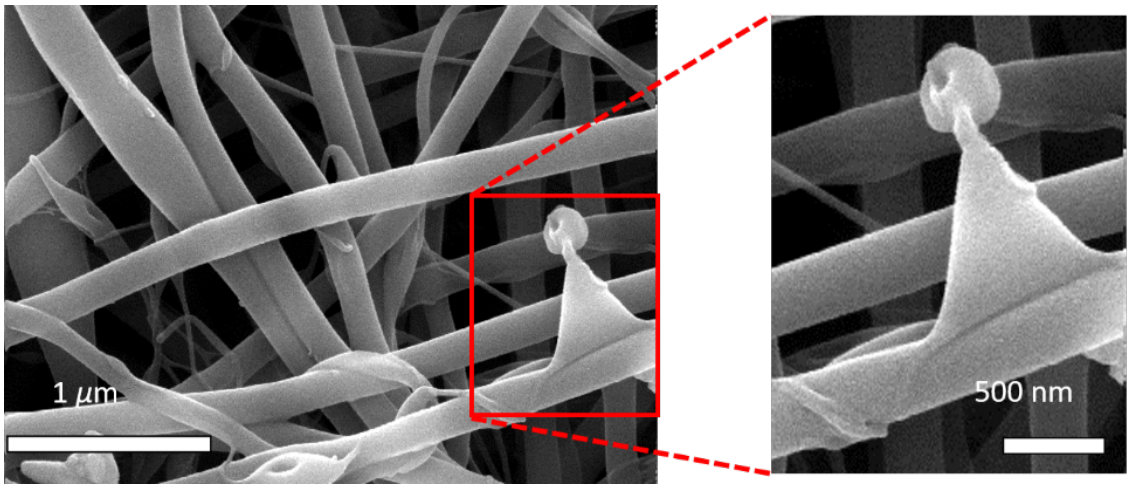

Figure 4.20. SEM image of 1P4G sample, peeled nanofiber reveals core–shell morphology [36]

In Figure 4.20 1P4G sample was shown. Characteristics of gelatin-only fibers obtained from water are beads with thin fibers and small collapsed region on the beads due to evaporation. Looking at that figure revealed an interesting result that is above coating limit of gelatin, excess part can be easily peeled off by high strength field. Under the peeled part another smooth fiber core can be detected which is PVA.

4.4. Mechanical Test Results

ASTM D882 is a standard that tensile properties of the specimens are determined by using rectangular strips of mats and are not dog bone shaped. This way there is no need to use external measuring devices to measure the elongation as the built-in displacement indicator is adequate which reduces the complexity of the setup.

Mechanical properties of the core-shell and pure PVA mats for cross-linked and non-cross-linked cases were listed in Table 4.3 having process parameters of voltage 15 kV, electrode distance 15 cm and temperature of 40 ^{o}C. Mechanical tests of pure gelatin mats were excluded since they don't have a connected fiber distribution and

Table 4.2. Dimensions of some mechanical test specimens from literature.

Article	**Width**	**Thickness**	**Length**	**Gauge Length**	**Velocity**
[139]	4 mm			20 mm	0.5 mm/s
[57]	10 mm	0.05 mm	30 mm	10 mm	0.17 mm/s
[192]	10 mm			30 mm	10 mm/s
[193]	5 mm			5 mm	5 mm/s
[194]				8 mm	0.1 mm/min

are very short fiber, which made removal of the mat from aluminum foil at the form of rectangular specimen impossible. However, properties of gelatin mats can be obtained from literature which are obtained from acidic solvents that makes long fibers and made possible to test their properties. Elongation at fracture and tensile strength values acquired from literature for non-cross-linked pure gelatin are 15±3.0% and 3.7±0.5 MPa respectively [194]. For cross-linked gelatin, the two values were 4.3±0.5% and 0.48±0.20 MPa [163] respectively. Although those values were obtained at different test conditions, they were represented here for comparison. In general, crosslinking barely decreased deformation capabilities of the mats while tensile strength properties were slightly increased.

Tensile properties of gelatin-only mats were weak due to lack of water inside protein structures which is responsible for the plasticizer effect. Gelatin shell increased the strength of pure PVA due to the semi-crystal structure of PVA. During the electrospinning, crystalline nature of PVA and protein conformational structure of gelatin can be improved [163].Even at coaxial electrospinning, core solution properties can be advanced by shell solution such that PVA becomes more crystallized with the aid of gelatin resulted in higher tensile properties. (1P 2.3±0.3 MPa vs 1P2G 2.8±0.2 MPa) 1P1G was the most effected mats from crosslinking operation with nearly two times tensile property of non-crosslinked situation. (from 2.4 to 4.3 MPa) Elongation capabil-

Table 4.3. Mechanical properties of the non-crosslinked and cross-lined cases

	Non-cross-linked		**Cross-linked**	
FRR	Percent Elongation before Failure (%)	Ultimate Tensile Strength (MPa)	Percent Elongation before Failure (%)	Ultimate Tensile Strength (MPa)
1P	93.5±39.0	2.3±0.3	89.3±7.50	3.1±0.2
4P1G	137.4±12.5	3.9±0.2	77.5±5.0	4.8±0.8
1P1G	80.2±9.0	2.4±0.3	28.9±1.2	4.3±0.5
1P2G	83.0±1.1	2.8±0.2	23.9±12.7	3.9±0.6
1P4G	114.0±15.3	2.9±0.1	25.4±3.5	2.3±0.2

ities were improved wrt pure gelatin values for both cross-linked and non-cross-linked cases due to elastic properties of PVA. 1P4G mats lost their mechanical properties which could be related to the entanglement level that elevates localized stresses in addition to the free forms of short gelatin beaded fibers [195].

4.5. FTIR & DSC Results

FTIR spectra of the fabricated groups were attained to detect secondary structures of gelatin due to ES and impact of the cross-linking. Figure 4.21 shows spectra of as received gelatin powder, electrospun non-cross-linked and cross-linked gelatin, PVA and one characteristic group of core-shell fibers (1P1G).

The band rising at 3305 cm^{-1} can be attributed to amide A due to N-H stretching and the band at 3065 cm^{-1} to amide B due to C-H stretching. Also, representative gelatin peaks observed at 1643, 1536 and 1238 cm^{-1} are ascribed to amide I, amide II and amide III, respectively. The shift of the amide I peak from 1630 to 1643 cm^{-1} points to the effect of ES on the conversion of beta turn structures to more stable α helices [196] as ordered conformations increase with ES. Cross-linking exhibits an

intensification at amide I and II on FTIR spectra in any of the samples, which implies that secondary structures are mostly preserved and shows the effect of crosslinking with glutaraldehyde. Cross-linking process, creates aldimine linkage (CH=N) in between aldehyde groups of glutaraldehyde and amino groups of gelatin. (Figure 2.8) The characteristic transmittance of the aldimine appears at 1450 cm^{-1} deeper for cross-linked samples [197].

Electrospinning of gelatin inside deionized water can be performed at elevated temperatures to prevent gelation. Depending on the concentration of the gelatin solution temperature of the gelation phenomenon exhibits from 25^oC to 37^oC. Above this gelation temperature ordered conformation of the protein turns into random profile, to prevent thermal degradation a multi nozzle system was used to finish the process within a short time at the required temperature. Preserved position of amide I peak at 1643 cm^{-1} in the gelatin containing electrospun samples ensures existence of α-helix structures.

Band around 3320 cm^{-1} for 1P refers to the stretching of O-H. Peak around 2930 cm^{-1} can be linked to the vibrational band of C-H stretching from alkyl groups [179]. Also strong peak around 1733 cm^{-1} attributed to the stretching of C=O. General effect of crosslinking on PVA is the broadening of O-H [179].

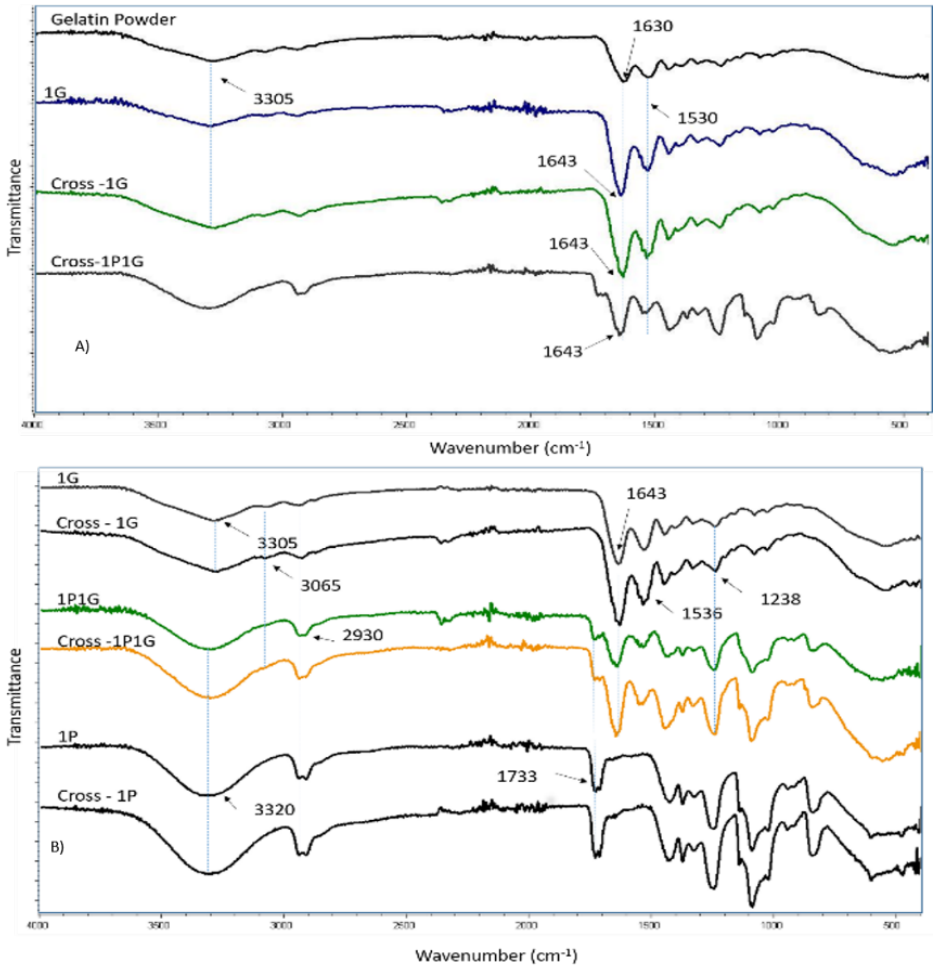

Figure 4.21. FTIR spectra of gelatin,PVA, core-shell and crosslinked groups.

DSC analysis of the same groups were also performed to understand natures of gelatin and PVA, effect of cross-linking and ES. Non-cross-linked and cross-linked of selected 4 groups were presented in Figure 4.22. Around $\sim 75^{o}$C water associated evaporation enthalpy difference broadened the peak at that point which is attributed to helix to coil transition for gelatin containing groups [198]. Transitional groups of 1P1G and 1P4G in between pure PVA and gelatin contains both characteristic properties of polymers. They carry denaturation peak (Td) of gelatin and melting peak (Tm) of PVA [199].

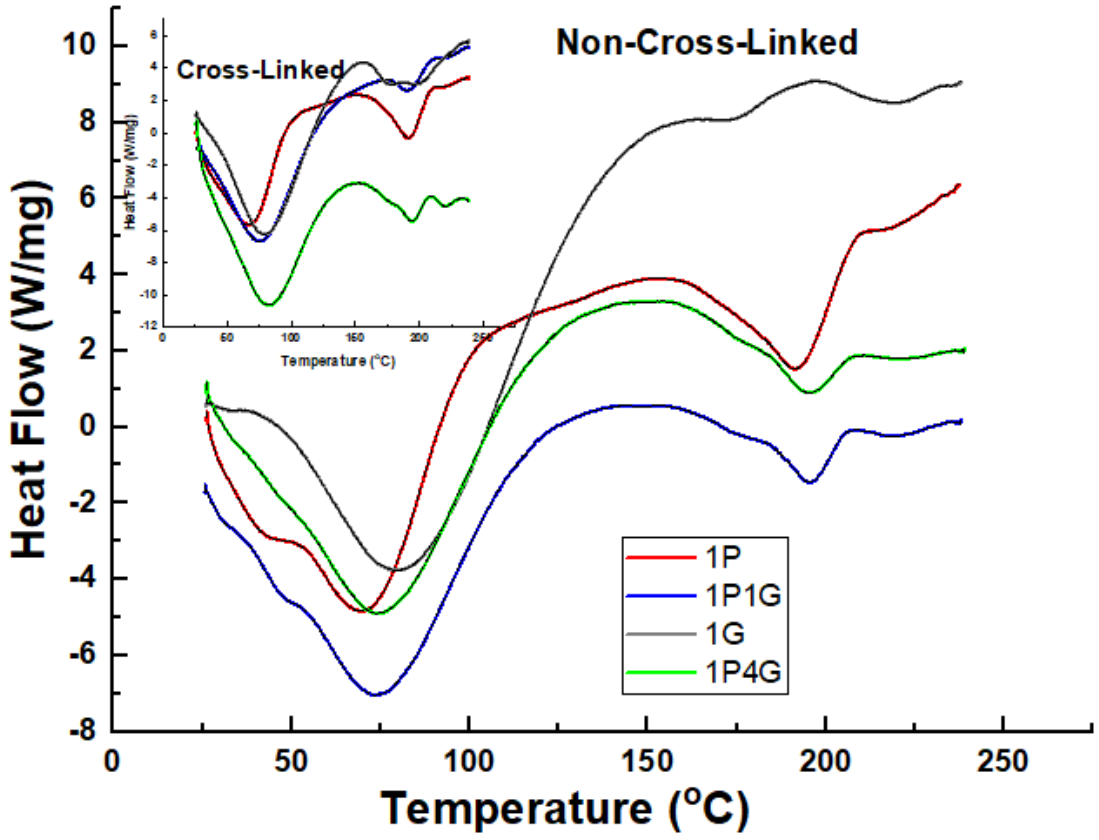

Figure 4.22. DSC curves of gelatin,PVA and core-shell groups.

Melting and denaturation temperatures of 1P, 4P1G, 1P1G, 1P2G, 1P4G and 1G were listed at Table 4.4. In Figure 4.22 only two case of the core-shell groups was plot due to similarities. Td shifted through the peak of 1G as gelatin concentration was increased in core-shell groups. (69^{o}C to 75^{o}C) Melting temperature did not display any significant difference. Miscibility of two polymers can be detected by the merge of melting points [200]. Also cross-linking smoothened the curves and shifted denaturation temperatures of gelatin-dominated samples to the right [201]. A bare effect of cross-linking can be noticed by focusing on the change of endothermic peak value of 1P4G group. Its value doubled while other cases did not alter that much. This could be arousing from crosslinking of PVA –OH groups and carboxylic groups of gelatin. (Figure 2.9) Considering SEM image of 1P4G and 1P1G cases, (see Figure 4.11,Figure

4.12) 1P4G contains some irregular structures like beads and peeled branched fibers while 1P1G does not contain such structures. Therefore, in 1P4G case glutaraldehyde has the ability to connect PVA and gelatin more due to having more free surface area.

Table 4.4. Melting (Tm) and denaturation (Td) temperatures of cross-linked and non-cross-linked (normal) groups obtained via DSC measurements (Note: For 1P Td is dehydration temperature)

	Non-Cross-linked		**Cross-linked**	
	Td	**Tm**	**Td**	**Tm**
1P	69.93	191.6	64.76	192.1
4P1G	71.65	195.41	68	189.82
1P1G	74.3	195.68	75.12	192.7
1P2G	76.43	195.32	76.9	192.9
1P4G	75.16	195.14	82.57	194.22
1G	79	219.8	78.93	197

4.6. Water Contact Angle

Cell interactions, like adhesion and spreading with non-biological substrates are highly dependent on the surface knowledge of the membrane. Cells can easily attach on the hydrophilic interfaces [202]. Effect of crosslinking on the surface characteristics and different FRRs with different fiber diameters are analyzed with using FRR group. Cross-linking with glutaraldehyde did not change hydrophilic character of the scaffolds. ($<90^{o}$ see) There is a close relation between surface roughness which in this case fiber diameter and surface porosity.

Table 4.5. Average fiber diameter size, pore size, standard deviations and water contact angle values of samples[36]

FRR	**1P**	**4P1G**	**1P1G**	**1P2G**	**1P4G**	**1G**
Fiber Diameter (nm)	200 ± 40	307± 66	281± 45	282±66	220±130	<50
Pore Size (nm)	586±595	877±798	839±803	703±701	650±609	NA
Water Contact Angle (^{o})	47.0±2.0	70.0±3.0	60.0±5.0	63.0±4.0	65±10	41±10

It is obvious from the information that increased fiber diameter brought about reduced wettability. It was recently shown that expanded surface area upgrades inherent wettability properties of nanofibrous substrates [203]. For instance, hydrophobicity of nanofibrous membranes obtained from hydrophobic materials can be increased by increasing specific surface area which is dependent on the fiber and pore sizes [203]. Conversely, when the sesame membrane was artificially changed to exhibit hydrophilic moieties at the surface, hydrophilic response increased with the surface area [204]. PVA and gelatin displayed hydrophilic properties because of their polar functional groups, an increase in wettability was normal with smaller diameter size. 4P1G has the largest diameter, pore size and the highest water contact angle lowest wettability among other groups.

4.7. Biodegradation

Biodegradation data (Figure 4.23) shows that scaffolds made of pure gelatin (1G) fibers are the least degraded within 14 days. This shows us that cross-linking has been most effective on this group. The most important reason is that fiber diameters (∼50 nm) are about 6 times smaller than other groups (∼250 nm). This increases the surface area that the crosslinker can touch. In the opposite direction, there are PVA pure fibers. They lose about 80% from the first day. Gelatin contains more groups that can bind to glutaraldehyde [205] while PVA has only one [206]. Degradation rates generally decrease as gelatin concentration increases. However, another factor here is the lysozyme enzyme. The larger the surface pore diameter, the easier it can penetrate. Degradation rates of core-shells, generally, decrease as the gelatin rate increases due to surface area and therefore crosslinking degree although attack of the lysozyme changes degradation profile.

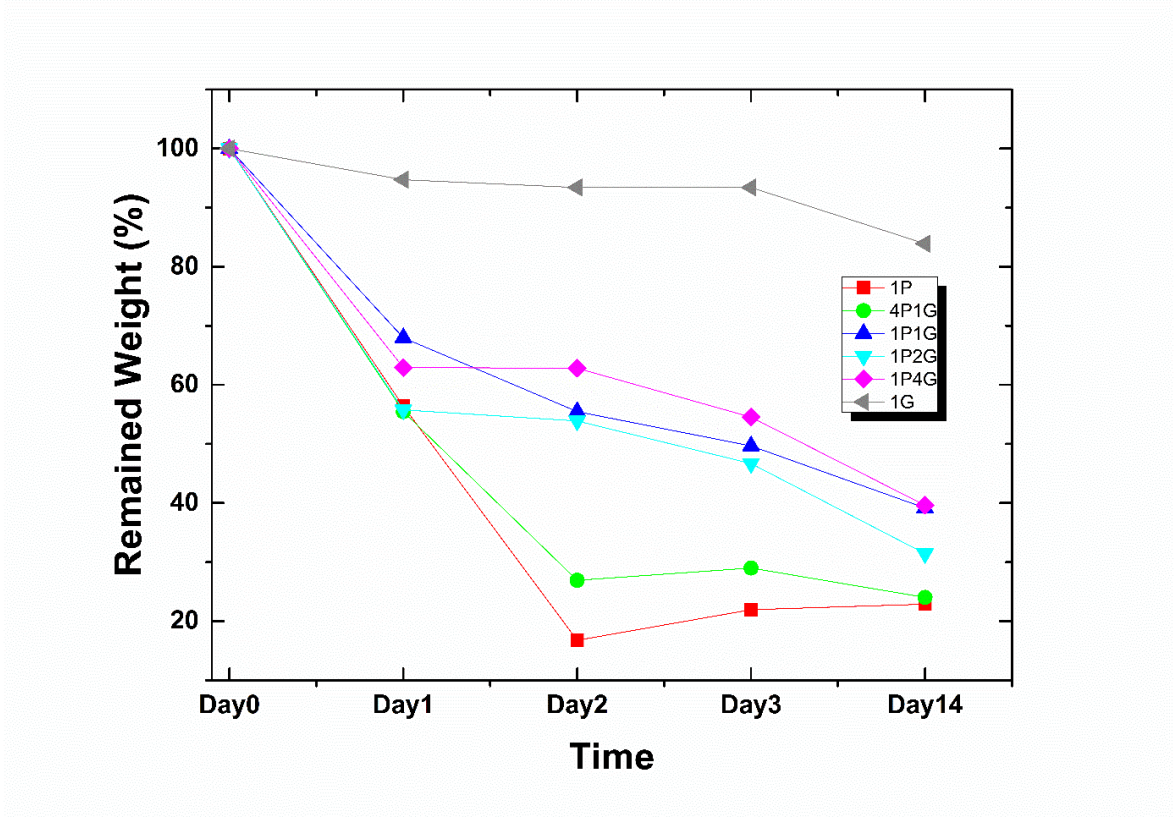

Figure 4.23. Biodegradation rates of the crosslinked samples [36].

5. CONCULUSION

In this study, it was aimed to fabricate composite, nanofiber based scaffolds without using toxic or acidic solvents. Coaxial ES, a specialized version of ES, was used in order to obtain core-shell nanofibers. PVA was used as core material that provides mechanical endurance, while gelatin was used as cell recognition material that can stimulate adhesion and proliferation of cells. PVA has been studied widely in literature by itself and it is easy to produce smooth fibers using ES. Gelatin was the focus of this dissertation, since the critical component was gelatin as a natural protein. Following conclusions were drawn from studies:

A systematic solution preparation is required due to different characteristics of both solutions under shear and temperature. PVA has rheopectic properties that will shear thicken during the preparation of the solution inside deionized water (from 140 to 180 cP). In addition, gelatin has jumps during time under elevated temperatures (from 5 to 6.5 cP). Those findings clearly states the importance of the history of the prepared solutions for electospinning.

Effect of process parameter was detrimental on the single and core-shell fiber morphology. Voltage limits at specified conditions were reported for both gelatin and core-shell nanofibers. A converse correlation in between temperature and gelatin fibers were stated due to fast evaporation rates and being premature fibers. Concentration of the solutions had bare effect on the fiber morphology. Although obtaining smooth gelatin nanofibers was not possible, 16% (wt/wt) was the closest concentration in order to fabricate a smooth gelatin nano-fiber.

Core shell fibers were obtained by feeding 8% PVA and 8% gelatin solutions from two different sources into the electric field created with 15 kV, 15 cm at 40 ^{o}C. 1:1 feed rate ratio of PVA:gelatin was found to be the most proper ratio to endup core-shell structure. 1:3 ratio has relatively more beads while 1:4 ratio contains peeled fibers. Core-shell structures were identified with TEM after than a proper solution found that has different affinities for both of the polymers.

Mechanical tests, FTIR, DSC revealed that, crosslinking increased and changed material properties significantly. Although crosslinking of pure PVA fibers were not good enough, 1P1G case has considerable improvements in tensile properties. FTIR and DSC showed the properties of the secondary ordered structures enforced by ES.

While water contact angle analysis showed hydrophilic nature even after crosslinking, biodegradation tests displayed a 14 day long degradation and tunable degradation characteristics.

REFERENCES

1. Farach-Carson, M. C., R. C. Wagner, K. L. Kiick, R. C. Wagner and K. L. Kiick, *Extracellular Matrix: Structure, Function, and Tissue Engineering Applications*, Taylor & Francis, 2016.

2. Nimčenko, T., G. Omerca, V. Varinauskas, E. Bramanti, F. Signorino and M. Cicciù, "Tooth Auto-Transplantation As An Alternative Treatment Option: A Literature Review.", *Dental Research Journal*, Vol. 10, No. 1, pp. 1–6, 2013.

3. Duan, B., M. Wang, W. Y. Zhou, W. L. Cheung, Z. Y. Li and W. W. Lu, "Three-Dimensional Nanocomposite Scaffolds Fabricated Via Selective Laser Sintering For Bone Tissue Engineering", *Acta Biomaterialia*, Vol. 6, No. 12, pp. 4495–4505, 2010.

4. Wagoner Johnson, A. J. and B. A. Herschler, "A Review Of The Mechanical Behavior Of Cap And Cap/Polymer Composites For Applications In Bone Replacement And Repair", *Acta Biomaterialia*, Vol. 7, No. 1, pp. 16–30, 2011.

5. Ravi, S. and E. L. Chaikof, "Biomaterials For Vascular Tissue Engineering.", *Regenerative Medicine*, Vol. 5, No. 1, pp. 107–20, 2010.

6. Orth, P., A. Rey-Rico, J. K. Venkatesan, H. Madry and M. Cucchiarini, "Current Perspectives In Stem Cell Research For Knee Cartilage Repair.", *Stem Cells and Cloning : Advances and Applications*, Vol. 7, pp. 1–17, 2014.

7. Groeber, F., M. Holeiter, M. Hampel, S. Hinderer and K. Schenke-Layland, "Skin Tissue Engineering — In Vivo And In Vitro Applications", *Advanced Drug Delivery Reviews*, Vol. 63, No. 4-5, pp. 352–366, 2011.

8. Harper, J. R. and D. J. McQuillan, "Extracellular Wound Matrices:A Novel Regenerative Tissue Matrix (RTM) Technology for Connective Tissue Reconstruction", *Wounds : A Compendium of Clinical Research and Practice*, Vol. 19, No. 6, pp. 163–8, 2007.

9. Watt, F. M. and H. Green, "Stratification And Terminal Differentiation Of Cultured Epidermal Cells", *Nature*, Vol. 295, No. 5848, pp. 434–436, 1982.

10. Sasaki, M., R. Abe, Y. Fujita, S. Ando, D. Inokuma and H. Shimizu, "Mesenchymal Stem Cells Are Recruited Into Wounded Skin And Contribute To Wound Repair By Transdifferentiation Into Multiple Skin Cell Type.", *Journal of Immunology (Baltimore, Md. : 1950)*, Vol. 180, No. 4, pp. 2581–7, 2008.

11. Hovav, A.-H., "Mucosal and Skin Langerhans Cells – Nurture Calls", *Trends in Immunology*, Vol. 39, No. 10, pp. 788–800, 2018.

12. Celleno, L. and F. Tamburi, *Structure and Function of the Skin*, John Wiley & Sons, Ltd, Chichester, UK, 2009.

13. Shimizu, H., *Shimizu's Dermatology*, John Wiley & Sons, Ltd, Chichester, UK, 2017.

14. Sussman, C. and B. M. Bates-Jensen, *Wound Care : A Collaborative Practice Manual for Health Professionals*, Wolters Kluwer Health/Lippincott Williams & Wilkins, 2012.

15. Golebiewska, E. M. and A. W. Poole, "Platelet Secretion: From Haemostasis To Wound Healing And Beyond.", *Blood Reviews*, Vol. 29, No. 3, pp. 153–62, 2015.

16. Huttenlocher, A. and A. R. Horwitz, "Integrins in Cell Migration", *Cold Spring Harbor Perspectives in Biology*, Vol. 3, No. 9, 2011.

17. Field, F. K. and M. D. Kerstein, "Overview Of Wound Healing In A Moist Environment.", *American Journal Of Surgery*, Vol. 167, No. 1A, pp. 2S–6S, 1994.

18. Gonzalez, A. C. d. O., T. F. Costa, Z. d. A. Andrade and A. R. A. P. Medrado, "Wound Healing - A Literature Review.", *Anais Brasileiros de Dermatologia*, Vol. 91, No. 5, pp. 614–620, 2016.

19. Leveriza-Oh, M. and T. J. Phillips, "Dressings And Postoperative Care", *Lower Extremity Soft Tissue & Cutaneous Plastic Surgery*, pp. 471–488, 2012.

20. Vaquette, C. and J. Cooper-White, "A Simple Method For Fabricating 3-D Multilayered Composite Scaffolds", *Acta Biomaterialia*, Vol. 9, No. 1, pp. 4599–4608, 2013.

21. Liu, X. and P. X. Ma, "Phase Separation, Pore Structure, And Properties Of Nanofibrous Gelatin Scaffolds", *Biomaterials*, Vol. 30, No. 25, pp. 4094–4103, 2009.

22. Kafy, A., H. C. Kim, L. Zhai, J. W. Kim, L. V. Hai, T. J. Kang and J. Kim, "Cellulose Long Fibers Fabricated From Cellulose Nanofibers And Its Strong And Tough Characteristics", *Scientific Reports*, Vol. 7, No. 1, p. 17683, 2017.

23. Yang, C. Y., C. T. Chiu, Y. P. Chang and Y. J. Wang, "Fabrication Of Porous Gelatin Microfibers Using An Aqueous Wet Spinning Process, Artificial Cells", *Blood Substitutes, and Biotechnology*, Vol. 37, No. 4, pp. 173–176, 2009.

24. Yang, Y. and H. Hu, "Spacer Fabric-Based Exuding Wound Dressing – Part II: Comparison With Commercial Wound Dressings", *Textile Research Journal*, Vol. 87, No. 12, pp. 1481–1493, 2017.

25. Venkatasubbu, G. D. and T. Anusuya, "Investigation on Curcumin Nanocomposite For Wound Dressing", *International Journal of Biological Macromolecules*, Vol. 98, pp. 366–378, 2017.

26. Holmes, B., N. J. Castro, L. G. Zhang and E. Zussman, "Electrospun Fibrous Scaffolds For Bone And Cartilage Tissue Generation: Recent Progress And Future Developments.", *Tissue engineering. Part B, Reviews*, Vol. 18, No. 6, pp. 478–86, 2012.

27. Milne, S. D., I. Seoudi, H. Al Hamad, T. K. Talal, A. A. Anoop, N. Allahverdi, Z. Zakaria, R. Menzies and P. Connolly, "A Wearable Wound Moisture Sensor As An Indicator For Wound Dressing Change: An Observational Study Of Wound Moisture And Status", *International Wound Journal*, Vol. 13, No. 6, pp. 1309–1314, 2016.

28. Luo, Y., S. Nartker, H. Miller, D. Hochhalter, M. Wiederoder, S. Wiederoder, E. Setterington, L. T. Drzal and E. C. Alocilja, "Surface Functionalization Of Electrospun Nanofibers For Detecting E. Coli O157:H7 And BVDV Cells In A Direct-Charge Transfer Biosensor", *Biosensors & Bioelectronics*, Vol. 26, No. 4, pp. 1612–7, 2010.

29. Li, W., X. Tan, T. Luo, Y. Shi, Y. Yang and L. Liu, "Preparation And Characterization Of Electrospun PLA/PU Bilayer Nanofibrous Membranes For Controlled Drug Release Applications", *Integrated Ferroelectrics*, Vol. 179, No. 1, pp. 104–119, 2017.

30. Gibson, P., H. Schreuder-Gibson and D. Rivin, "Transport Properties Of Porous Membranes Based On Electrospun Nanofibers", *Colloids and Surfaces A: Physicochemical and Engineering Aspects*, Vol. 187-188, pp. 469–481, 2001.

31. Chen, D., R. Wang, W. W. Tjiu and T. Liu, "High Performance Polyimide Composite Films Prepared By Homogeneity Reinforcement Of Electrospun Nanofibers", *Composites Science and Technology*, Vol. 71, No. 13, pp. 1556–1562, 2011.

32. Vandewal, K., W. D. Oosterbaan, S. Bertho, V. Vrindts, A. Gadisa, L. Lutsen, D. Vanderzande and J. V. Manca, "Varying Polymer Crystallinity In Nanofiber Poly(3-Alkylthiophene): PCBM Solar Cells: Influence On Charge-Transfer State Energy And Open-Circuit Voltage ", *Applied Physics Letters*, Vol. 95, No. 12, 2009.

33. Kim, F. S., G. Ren and S. a. Jenekhe, "One-Dimensional Nanostructures Of Π-Conjugated Molecular Systems: Assembly, Properties, And Applications From Photovoltaics, Sensors, And Nanophotonics To Nanoelectronics", *Chemistry of Materials*, Vol. 23, No. 3, pp. 682–732, 2011.

34. Kang, Y. K., C. H. Park, J. Kim and T. J. Kang, "Application Of Electrospun Polyurethane Web To Breathable Water-Proof Fabrics", *Fibers and Polymers*, Vol. 8, No. 5, pp. 564–570, 2007.

35. Cirillo, V., V. Guarino, M. A. Alvarez-Perez, M. Marrese and L. Ambrosio, "Optimization Of Fully Aligned Bioactive Electrospun Fibers For "In Vitro" Nerve Guidance", *Journal of Materials Science: Materials in Medicine*, Vol. 25, No. 10, pp. 2323–2332, 2014.

36. Sengor, M., A. Ozgun, G. Corapcioglu, M. Ipekoglu, B. Garipcan, N. Ersoy and S. Altintas, "Core-Shell PVA/Gelatin Nanofibrous Scaffolds Using Co-Solvent, Aqueous Electrospinning: Toward A Green Approach", *Journal of Applied Polymer Science*, p. 46582, 2018.

37. Wagner, A., V. Poursorkhabi, A. K. Mohanty and M. Misra, "Analysis of Porous Electrospun Fibers from Poly(l -lactic acid)/Poly(3-hydroxybutyrate-co-3-hydroxyvalerate) Blends", *ACS Sustainable Chemistry & Engineering*, Vol. 2, No. 8, pp. 1976–1982, 2014.

38. Seyyed Monfared Zanjani, J., B. Saner Okan, I. Letofsky-Papst, M. Yildiz and Y. Z. Menceloglu, "Rational Design And Direct Fabrication Of Multi-Walled Hollow Electrospun Fibers With Controllable Structure And Surface Properties", *European Polymer Journal*, Vol. 62, pp. 66–76, 2015.

39. Chutipakdeevong, J., U. R. Ruktanonchai and P. Supaphol, "Process Optimization Of Electrospun Silk Fibroin Fiber Mat For Accelerated Wound Healing", *Journal of Applied Polymer Science*, Vol. 130, No. 5, pp. 3634–3644, 2013.

40. Liu, M., Y. Wang, Z. Cheng, M. Zhang, M. Hu and J. Li, "Electrospun Carboxylic-Functionalized Poly(Arylene Ether Ketone) Ultrafine Fibers", *High Performance Polymers*, Vol. 27, No. 8, pp. 939–949, 2015.

41. Arras, M. M. L., C. Grasl, H. Bergmeister and H. Schima, "Electrospinning Of Aligned Fibers With Adjustable Orientation Using Auxiliary Electrodes", *Science And Technology Of Advanced Materials*, Vol. 13, No. 3, p. 035008, 2012.

42. Kim, J. I., T. I. Hwang, L. E. Aguilar, C. H. Park and C. S. Kim, "A Controlled Design of Aligned and Random Nanofibers for 3D Bi-functionalized Nerve Conduits Fabricated via a Novel Electrospinning Set-up", *Scientific Reports*, Vol. 6, No. 1, p. 23761, 2016.

43. Pokorny, M. and V. Velebny, "Collection Method For Extra Aligned Nanofibers Deposited By Electrospinning", *Review of Scientific Instruments*, Vol. 82, No. 5, p. 055112, 2011.

44. Zhu, Z., X. Chen, Z. Du, S. Huang, D. Peng, J. Zheng and H. Wang, "Fabricated Wavy Micro/Nanofiber via Auxiliary Electrodes in Near-Field Electrospinning", *Materials and Manufacturing Processes*, Vol. 31, No. 6, pp. 707–712, 2016.

45. Flores, A., G. C. Rutledge and K. M. Forward, "Production Of Core/Shell Fibers By Electrospinning From A Free Surface Terms Of Use Production Of Core/Shell Fibers By Electrospinning From A Free Surface", *Chemical Engineering Science*, Vol. 104, pp. 250–259, 2013.

46. Jiang, K., Y.-Z. Long, Z.-J. Chen, S.-L. Liu, Y.-Y. Huang, X. Jiang and Z.-Q. Huang, "Airflow-Directed In Situ Electrospinning Of A Medical Glue Of Cyanoacrylate For Rapid Hemostasis In Liver Resection ", *Nanoscale*, Vol. 6, pp. 7792–7798, 2014.

47. Rezvani, O., M. H. Hedeshi and H. Bagheri, "Polyamide/Titania Hollow Nanofibers Prepared By Core–Shell Electrospinning As A Microextractive Phase In A Fabricated Sandwiched Format Microfluidic Device", *Journal of Chromatography A*, Vol. 1528, pp. 1–9, 2017.

48. Zheng, Y., J. Miao, N. Maeda, D. Frey, R. J. Linhardt and T. J. Simmons, "Uniform Nanoparticle Coating Of Cellulose Fibers During Wet Electrospinning", *J. Mater. Chem. A*, Vol. 2, No. 36, pp. 15029–15034, 2014.

49. Salehi, M. and F. Bastami, "Characterization of Wet-electrospun Poly (ϵ-caprolactone)/Poly (L-lactic) Acid with Calcium Phosphates Coated with Chitosan for Bone Engineering", *Regeneration, Reconstruction, & Restoration*, Vol. 1, No. 2, pp. 69–74, 2016.

50. Yang, X., J. D. Shah and H. Wang, "Nanofiber Enabled Layer-By-Layer Approach Toward Three-Dimensional Tissue Formation", *Tissue Engineering Part A*, Vol. 15, No. 4, pp. 945–956, 2009.

51. Olsson, R. T., R. Kraemer, A. Lo´pez-Rubio, S. Torres-Giner, M. J. Ocio and J. M. Lagaro´n, "Extraction Of Microfibrils From Bacterial Cellulose Networks For Electrospinning Of Anisotropic Biohybrid Fiber Yarns", *Macromolecules*, Vol. 43, No. 9, pp. 4201–4209, 2010.

52. Salehhudin, H. S., N. Mohamad, W. Nor, L. Mahadi and A. M. Afifi, "Materials And Manufacturing Processes Multiple-Jet Electrospinning Methods For Nanofiber Processing: A Review", , 2018.

53. Theron, S., A. Yarin, E. Zussman and E. Kroll, "Multiple Jets In Electrospinning: Experiment And Modeling", *Polymer*, Vol. 46, No. 9, pp. 2889–2899, 2005.

54. Yang, Y., Z. Jia, Q. Li, L. Hou, J. Liu, L. Wang, Z. Guan and M. Zahn, "A Shield Ring Enhanced Equilateral Hexagon Distributed Multi-Needle Electrospinning Spinneret", *IEEE Transactions on Dielectrics and Electrical Insulation*, Vol. 17, No. 5, pp. 1592–1601, 2010.

55. Li, X., Z. Li, L. Wang, G. Ma, F. Meng, R. H. Pritchard, E. L. Gill, Y. Liu, Y. Yan and S. Huang, "Low-Voltage Continuous Electrospinning Patterning", *ACS Applied Materials & Interfaces*, Vol. 8, No. 47, pp. 32120–32131, 2016.

56. Huang, Y., Y. Duan, Y. Ding, N. Bu, Y. Pan, N. Lu and Z. Yin, "Versatile, Kinetically Controlled, High Precision Electrohydrodynamic Writing Of Micro/Nanofibers", *Scientific Reports*, Vol. 4, No. 1, p. 5949, 2015.

57. Li, Z., Y. Zhou, H. Yao, J. Wang, D. Wang and Q. Liu, *International Journal of Nanomedicine*, Vol. 10.

58. Sun, J., K. Bubel, F. Chen, T. Kissel, S. Agarwal and A. Greiner, "Nanofibers by Green Electrospinning of Aqueous Suspensions of Biodegradable Block Copolyesters for Applications in Medicine, Pharmacy and Agriculture", *Macromolecular Rapid Communications*, Vol. 31, No. 23, pp. 2077–2083, 2010.

59. Zhu, M., D. Hua, H. Pan, F. Wang, B. Manshian, S. J. Soenen, R. Xiong and C. Huang, "Green Electrospun And Crosslinked Poly(Vinyl Alcohol)/Poly(Acrylic Acid) Composite Membranes For Antibacterial Effective Air Filtration", *Journal of Colloid and Interface Science*, Vol. 511, pp. 411–423, 2018.

60. Zavgorodnya, O., J. L. Shamshina, J. R. Bonner and R. D. Rogers, "Electrospinning Biopolymers From Ionic Liquids Requires Control Of Different Solution Properties Than Volatile Organic Solvents", *ACS Sustainable Chemistry & Engineering*, Vol. 5, No. 6, pp. 5512–5519, 2017.

61. Bubakir, M. M., H. Li, W. Wu, X. Li, S. Ma and W. Yang, "Applications Of Web Produced By Hot Air Assisted Melt Differential Electrospinning Method", *IOP Conference Series: Materials Science and Engineering*, Vol. 64, No. 1, p. 012052, 2014.

62. Bosworth, L. A. and S. Downes, *Electrospinning for Tissue Regeneration*, Woodhead Publishing Series in Biomaterials, Elsevier Science, 2011.

63. Chattopadhyay, S. and R. T. Raines, "Review Collagen-Based Biomaterials For Wound Healing.", *Biopolymers*, Vol. 101, No. 8, pp. 821–33, 2014.

64. Kawai, K., S. Suzuki, Y. Tabata, Y. Ikada and Y. Nishimura, "Accelerated Tissue Regeneration Through Incorporation Of Basic Fibroblast Growth Factor-Impregnated Gelatin Microspheres Into Artificial Dermis.", *Biomaterials*, Vol. 21, No. 5, pp. 489–99, 2000.

65. Kruger, T. E., A. H. Miller and J. Wang, "Collagen Scaffolds In Bone Sialoprotein-Mediated Bone Regeneration", *TheScientificWorldJournal*, Vol. 2013, p. 812718, 2013.

66. Sajkiewicz, P. and D. Kołbuk, "Electrospinning Of Gelatin For Tissue Engineering – Molecular Conformation As One Of The Overlooked Problems", *Journal of Biomaterials Science, Polymer Edition*, Vol. 25, No. 18, pp. 2009–2022, 2014.

67. Williams, P. A. and G. O. Phillips, *Handbook of Hydrocolloids*, Vol. 2nd, Elsevier, GB, 2009.

68. Monzack, E. L., K. J. Rodriguez, C. M. McCoy, X. Gu and K. S. Masters, *Natural Materials in Tissue Engineering Applications*, Springer Vienna, Vienna, 2011.

69. Schrieber, R. and H. Gareis, *From Collagen to Gelatine*, Wiley-VCH Verlag GmbH & Co. KGaA, Weinheim, Germany, 2007.

70. America, G. G. M. I. O., *Gelatin Handbook*, Tech. Rep. 888, GMIA, 2019.

71. Ko, C.-L., Y.-C. Tien, J.-C. Wang and W.-C. Chen, "Characterization Of Controlled Highly Porous Hyaluronan/Gelatin Cross-Linking Sponges For Tissue Engineering", *Journal of the Mechanical Behavior of Biomedical Materials*, Vol. 14, pp. 227–238, 2012.

72. Zaman, M. H., "Understanding The Molecular Basis For Differential Binding Of Integrins To Collagen And Gelatin.", *Biophysical Journal*, Vol. 92, No. 2, pp. L17–19, 2007.

73. Ruoslahti, E., "Rgd And Other Recognition Sequences For Integrins", *Annual Review of Cell and Developmental Biology*, Vol. 12, No. 1, pp. 697–715, 1996.

74. Inouye, K., M. Kurokawa, S. Nishikawa and M. Tsukada, "Use of Bombyx Mori Silk Fibroin As A Substratum For Cultivation Of Animal Cells", *Journal of Biochemical and Biophysical Methods*, Vol. 37, No. 3, pp. 159–164, 1998.

75. Elliott, D. E., F. J. Davis, G. R. Mitchell and R. H. Olley, "Structure Development In Electrospun Fibres Of Gelatin", *Journal of Physics: Conference Series*, Vol. 183, p. 012021, 2009.

76. Gu, S. Y., Z. M. Wang, J. Ren and C. Y. Zhang, "Electrospinning Of Gelatin And Gelatin/Poly(L-Lactide) Blend And Its Characteristics For Wound Dressing", *Materials Science and Engineering C*, Vol. 29, No. 6, pp. 1822 – 1828, 2009.

77. Watanabe, R., R. Hayashi, Y. Kimura, Y. Tanaka, T. Kageyama, S. Hara, Y. Tabata and K. Nishida, "A Novel Gelatin Hydrogel Carrier Sheet for Corneal Endothelial Transplantation", *Tissue Engineering Part A*, Vol. 17, No. 17-18, pp. 2213–2219, 2011.

78. Daamen, W. F., J. H. Veerkamp, J. C. van Hest and T. H. van Kuppevelt, "Elastin As A Biomaterial For Tissue Engineering", *Biomaterials*, Vol. 28, No. 30, pp. 4378 – 4398, 2007.

79. Loureiro dos Santos, L., "Natural Polymeric Biomaterials: Processing and Properties", *Reference Module in Materials Science and Materials Engineering*, 2017.

80. Wise, S. G., S. M. Mithieux and A. S. Weiss, "Engineered Tropoelastin and Elastin-Based Biomaterials", *Advances in Protein Chemistry and Structural Biology*, Vol. 78, pp. 1–24, 2009.

81. Gomes, M., H. Azevedo, P. Malafaya, S. Silva, J. Oliveira, G. Silva, R. S. João Mano and R. Reis, "Natural Polymers in Tissue Engineering Applications", *Handbook of Biopolymers and Biodegradable Plastics*, pp. 385–425, 2013.

82. Chong, B. F., L. M. Blank, R. Mclaughlin and L. K. Nielsen, "Microbial Hyaluronic Acid Production", *Applied Microbiology and Biotechnology*, Vol. 66, No. 4, pp. 341–351, 2005.

83. Ji, Y., K. Ghosh, X. Z. Shu, B. Li, J. C. Sokolov, G. D. Prestwich, R. A. Clark and M. H. Rafailovich, "Electrospun Three-Dimensional Hyaluronic Acid Nanofibrous Scaffolds", *Biomaterials*, Vol. 27, No. 20, pp. 3782–3792, 2006.

84. Ghosh, K., X.-D. Ren, X. Z. Shu, G. D. Prestwich and R. A. Clark, "Fibronectin Functional Domains Coupled to Hyaluronan Stimulate Adult Human Dermal Fibroblast Responses Critical for Wound Healing", *Tissue Engineering*, Vol. 12, No. 3, pp. 601–613, 2006.

85. Sakurada, I., *Polyvinyl Alcohol Fibers*, International Fiber Science and Technology, Taylor & Francis, 1985.

86. Saxena, S. K., *Poly Vinyl Alcohol (PVA)*, Tech. Rep. 3, Chemical and Technical Assessment (CTA) 61st JECFA, 2004.

87. Gaaz, T. S., A. B. Sulong, M. N. Akhtar, A. A. H. Kadhum, A. B. Mohamad and A. A. Al-Amiery, "Properties and Applications of Polyvinyl Alcohol, Halloysite Nanotubes and Their Nanocomposites", *Molecules*, Vol. 20, No. 12, p. 22833, 2015.

88. Zhu, H., M. Du, M. Zhang, P. Wang, S. Bao, Y. Fu and J. Yao, "Facile And Green Fabrication Of Small, Mono-Disperse And Size-Controlled Noble Metal Nanoparticles Embedded In Water-Stable Polyvinyl Alcohol Nanofibers: High Sensitive, Flexible And Reliable Materials For Biosensors", *Sensors and Actuators, B: Chemical*, Vol. 185, pp. 608–619, 2013.

89. Sfakis, L., A. Sharikova, D. Tuschel, F. X. Costa, M. Larsen, A. Khmaladze and J. Castracane, "Core/Shell Nanofiber Characterization By Raman Scanning Microscopy.", *Biomedical Optics Express*, Vol. 8, No. 2, pp. 1025–1035, 2017.

90. Kim, K.-O. and B.-S. Kim, "Immobilization Of Glucose Oxidase On A PVA/PAA Nanofiber Matrix Reduces The Effect Of The Hematocrit Levels On A Glucose Biosensor", *Journal of Fiber Science and Technology*, Vol. 73, No. 1, pp. 27–33, 2017.

91. Sapountzi, E., M. Braiek, J.-F. Chateaux, N. Jaffrezic-Renault and F. Lagarde, "Recent Advances in Electrospun Nanofiber Interfaces for Biosensing Devices.", *Sensors (Basel, Switzerland)*, Vol. 17, No. 8, 2017.

92. Koosha, M. and H. Mirzadeh, "Electrospinning, Mechanical Properties, And Cell Behavior Study Of Chitosan/PVA Nanofibers", *Journal of Biomedical Materials Research Part A*, Vol. 103, No. 9, pp. 3081–3093, 2015.

93. Cui, Z., Z. Zheng, L. Lin, J. Si, Q. Wang, X. Peng and W. Chen, "Electrospinning And Crosslinking Of Polyvinyl Alcohol/Chitosan Composite Nanofiber For Transdermal Drug Delivery", *Advances in Polymer Technology*, Vol. 37, No. 6, pp. 1917–1928, 2018.

94. Lin, H.-Y., W.-C. Tsai and S.-H. Chang, "Collagen-PVA Aligned Nanofiber On Collagen Sponge As Bi-Layered Scaffold For Surface Cartilage Repair", *Journal of Biomaterials Science, Polymer Edition*, Vol. 28, No. 7, pp. 664–678, 2017.

95. Nguyen, T.-H., Y.-H. Kim, H.-Y. Song and B.-T. Lee, "Nano Ag Loaded PVA Nano-Fibrous Mats For Skin Applications", *Journal of Biomedical Materials Research Part B: Applied Biomaterials*, Vol. 96B, No. 2, pp. 225–233, 2011.

96. Linh, N. T. B. and B.-T. Lee, "Electrospinning Of Polyvinyl Alcohol/Gelatin Nanofiber Composites And Cross-Linking For Bone Tissue Engineering Application ", *Journal of Biomaterials Applications*, Vol. 27, No. 3, pp. 255–266, 2011.

97. Mahnama, H., S. Dadbin, M. Frounchi and S. Rajabi, "Preparation Of Biodegradable Gelatin/PVA Porous Scaffolds For Skin Regeneration", *Artificial Cells, Nanomedicine, and Biotechnology*, Vol. 45, No. 5, pp. 928–935, 2017.

98. Yang, D., Y. Li and J. Nie, "Preparation Of Gelatin/PVA Nanofibers And Their Potential Application In Controlled Release Of Drugs", *Carbohydrate Polymers*, Vol. 69, No. 3, pp. 538–543, 2007.

99. Merkle, V. M., P. L. Tran, M. Hutchinson, K. R. Ammann, K. DeCook, X. Wu and M. J. Slepian, "Core–Shell PVA/Gelatin Electrospun Nanofibers Promote Human Umbilical Vein Endothelial Cell And Smooth Muscle Cell Proliferation And Migration", *Acta Biomaterialia*, Vol. 27, pp. 77–87, 2015.

100. Zhang, Y., H. Ouyang, C. T. Lim, S. Ramakrishna and Z.-M. Huang, "Electrospinning Of Gelatin Fibers And Gelatin/PCL Composite Fibrous Scaffolds", *Journal of Biomedical Materials Research*, Vol. 72B, No. 1, pp. 156–165, 2005.

101. Hoveizi, E., M. Nabiuni, K. Parivar, S. Rajabi-Zeleti and S. Tavakol, "Functionalisation And Surface Modification Of Electrospun Polylactic Acid Scaffold For Tissue Engineering", *Cell Biology International*, Vol. 38, No. 1, pp. 41–49, 2014.

102. Li, M., M. J. Mondrinos, M. R. Gandhi, F. K. Ko, A. S. Weiss and P. I. Lelkes, "Electrospun Protein Fibers As Matrices For Tissue Engineering", *Biomaterials*, Vol. 26, No. 30, pp. 5999–6008, 2005.

103. Choktaweesap, N., K. Arayanarakul, D. Aht-ong, C. Meechaisue and P. Supaphol, "Electrospun Gelatin Fibers: Effect of Solvent System on Morphology and Fiber Diameters", *Polymer Journal*, Vol. 39, No. 6, pp. 622–631, 2007.

104. Akalın, G. E., H. Bedir and S. Altıntaş, *Electrospinning Of Polycaprolactone / Bovine Gelatin / Bovine Hydroxyapatite Biomimetic Composite Nanofibers*, Ph.D. Thesis, Bogazici University, 2018.

105. Butcher, A. L., C. T. Koh and M. L. Oyen, "Systematic Mechanical Evaluation Of Electrospun Gelatin Meshes", *Journal of the Mechanical Behavior of Biomedical Materials*, Vol. 69, pp. 412–419, 2017.

106. Panzavolta, S., M. Gioffrè, M. L. Focarete, C. Gualandi, L. Foroni and A. Bigi, "Electrospun Gelatin Nanofibers: Optimization Of Genipin Cross-Linking To Preserve Fiber Morphology After Exposure To Water", *Acta Biomaterialia*, Vol. 7, No. 4, pp. 1702–1709, 2011.

107. Sizeland, K. H., K. A. Hofman, I. C. Hallett, D. E. Martin, J. Potgieter, N. M. Kirby, A. Hawley, S. T. Mudie, T. M. Ryan, R. G. Haverkamp and M. H. Cumming, "Nanostructure Of Electrospun Collagen: Do Electrospun Collagen Fibers Form Native Structures?", *Materialia*, Vol. 3, pp. 90–96, 2018.

108. Nikoo, M., S. Benjakul, D. Ocen, N. Yang, B. Xu, L. Zhang and X. Xu, "Physical and Chemical Properties of Gelatin From the Skin of Cultured Amur Sturgeon (Acipenser Schrenckii)", *Journal of Applied Ichthyology*, Vol. 29, No. 5, pp. 943–950, 2013.

109. Albu, M. G., M. V. Ghica, M. Giurginca, V. Trandafir, L. Popa and C. Cotrut, "Spectral Characteristics And Antioxidant Properties Of Tannic Acid Immobilized On Collagen Drug-Delivery Systems", *Revista de Chimie*, Vol. 60, No. 7, pp. 666–672, 2009.

110. Payne, K. J. and A. Veis, "Fourier Transform Ir Spectroscopy Of Collagen And Gelatin Solutions: Deconvolution Of The Amide I Band For Conformational Studies", *Biopolymers*, Vol. 27, No. 11, pp. 1749–1760, 1988.

111. Rabotyagova, O. S., P. Cebe and D. L. Kaplan, "Collagen Structural Hierarchy and Susceptibility to Degradation by Ultraviolet Radiation.", *Materials Science & Engineering. C, Materials For Biological Applications*, Vol. 28, No. 8, pp. 1420–1429, 2008.

112. Ki, C. S., D. H. Baek, K. D. Gang, K. H. Lee, I. C. Um and Y. H. Park, "Characterization Of Gelatin Nanofiber Prepared From Gelatin-Formic Acid Solution", *Polymer*, Vol. 46, No. 14, pp. 5094–5102, 2005.

113. Liu, T., W. K. Teng, B. P. Chan and S. Y. Chew, "Photochemical Crosslinked Electrospun Collagen Nanofibers: Synthesis, Characterization And Neural Stem Cell Interactions", *Journal of Biomedical Materials Research Part A*, Vol. 95A, No. 1, pp. 276–282, 2010.

114. Chen, H.-C., W.-C. Jao and M.-C. Yang, "Characterization Of Gelatin Nanofibers Electrospun Using Ethanol/Formic Acid/Water As A Solvent", *Polymers for Advanced Technologies*, Vol. 20, No. 2, pp. 98–103, 2009.

115. Erencia, M., F. Cano, J. A. Tornero, J. Macanás and F. Carrillo, "Preparation Of Electrospun Nanofibers From Solutions Of Different Gelatin Types Using A Benign Solvent Mixture Composed Of Water/PBS/Ethanol", *Polymers for Advanced Technologies*, Vol. 27, No. 3, pp. 382–392, 2016.

116. "Impurities: Guideline For Residual Solvents Q3C(R5)", *International Conference On Harmonisation Of Technical Requirements For Registration Of Pharmaceuticals For Human Use*, Feb 2011.

117. Liverani, L., L. Vester and A. R. Boccaccini, *Biomaterials Produced via Green Electrospinning*, Springer International Publishing, Cham, 2017.

118. K, J., D. Naskar, S. C. Kundu and N. R. James, "Fabrication Of Cationized Gelatin Nanofibers By Electrospinning For Tissue Regeneration", *RSC Advances*, Vol. 5, No. 109, pp. 89521–89530, 2015.

119. Pandya, D. S., T. Arinzeh and G. Collins, "Elevated Temperature Electrospinning Of Aqueous Gelatin Solution And Crosslinking For Tissue Engineering Applications", *Proceedings of the 2010 IEEE 36th Annual Northeast Bioengineering Conference (NEBEC)*, pp. 1–2, IEEE, 2010.

120. Sajkiewicz, P. and D. Kołbuk, "Electrospinning Of Gelatin For Tissue Engineering – Molecular Conformation As One Of The Overlooked Problems", *Journal of Biomaterials Science, Polymer Edition*, Vol. 25, No. 18, pp. 2009–2022, 2014.

121. He, J. and Y. Zhou, "Multineedle Electrospinning", *Electrospinning: Nanofabrication and Applications*, pp. 201–218, 2019.

122. Bazbouz, M. B., H. Liang and G. Tronci, "A UV-Cured Nanofibrous Membrane Of Vinylbenzylated Gelatin-Poly(-Caprolactone) Dimethacrylate Co-Network By Scalable Free Surface Electrospinning", *Materials Science and Engineering: C*, Vol. 91, pp. 541–555, 2018.

123. Liu, L. and Y. A. Dzenis, "Analysis Of The Effects Of The Residual Charge And Gap Size On Electrospun Nanofiber Alignment In A Gap Method", *Nanotechnology*, Vol. 19, No. 35, p. 355307, 2008.

124. Ipekoglu, M. and S. Altintas, *Production Of Antibacterial Hydroxyapatite*, Ph.D. Thesis, Bogazici University, 2011.

125. Salifu, A. A., C. Lekakou and F. H. Labeed, "Electrospun Oriented Gelatin-Hydroxyapatite Fiber Scaffolds For Bone Tissue Engineering", *Journal of Biomedical Materials Research Part A*, Vol. 105, No. 7, pp. 1911–1926, 2017.

126. Chen, Y., W. Lu, Y. Guo, Y. Zhu and Y. Song, "Electrospun Gelatin Fibers Surface Loaded Zno Particles As A Potential Biodegradable Antibacterial Wound Dressing.", *Nanomaterials (Basel, Switzerland)*, Vol. 9, No. 4, 2019.

127. Dhandayuthapani, B., U. M. Krishnan and S. Sethuraman, "Fabrication And Characterization Of Chitosan-Gelatin Blend Nanofibers For Skin Tissue Engineering.", *Journal Of Biomedical Materials Research. Part B, Applied Biomaterials*, Vol. 94, No. 1, pp. 264–72, 2010.

128. Hild, M., G. Toskas, D. Aibibu, G. Wittenburg, H. Meissner, C. Cherif and R.-D. Hund, "Chitosan/Gelatin Micro/Nanofiber 3D Composite Scaffolds For Regenerative Medicine", *Composite Interfaces*, Vol. 21, No. 4, pp. 301–308, 2014.

129. Gao, Y., Y. Wang, Y. Wang and W. Cui, "Fabrication Of Gelatin-Based Electrospun Composite Fibers For Anti-Bacterial Properties And Protein Adsorption", *Marine Drugs*, Vol. 14, No. 10, 2016.

130. Wang, H., Y. Feng, Z. Fang, R. Xiao, W. Yuan and M. Khan, "Fabrication And Characterization Of Electrospun Gelatin-Heparin Nanofibers As Vascular Tissue Engineering", *Macromolecular Research*, Vol. 21, No. 8, pp. 860–869, 2013.

131. Li, J., A. He, C. C. Han, D. Fang, B. S. Hsiao and B. Chu, "Electrospinning of Hyaluronic Acid (HA) and HA/Gelatin Blends", *Macromolecular Rapid Communications*, Vol. 27, No. 2, pp. 114–120, 2006.

132. Ebrahimi-Hosseinzadeh, B., M. Pedram, A. Hatamian-Zarmi, S. Salahshour-Kordestani, M. Rasti, Z. B. Mokhtari-Hosseini and M. Mir-Derikvand, "In Vivo Evaluation Of Gelatin/Hyaluronic Acid Nanofiber As Burn-Wound Healing And Its Comparison With Chitoheal Gel", *Fibers and Polymers*, Vol. 17, No. 6, pp. 820–826, 2016.

133. Dadras Chomachayi, M., A. Solouk, S. Akbari, D. Sadeghi, F. Mirahmadi and H. Mirzadeh, "Electrospun Nanofibers Comprising Of Silk Fibroin/Gelatin For Drug Delivery Applications: Thyme Essential Oil And Doxycycline Monohydrate Release Study", *Journal of Biomedical Materials Research Part A*, Vol. 106, No. 4, pp. 1092–1103, 2018.

134. Janani, G., M. M. Pillai, R. Selvakumar, A. Bhattacharyya and C. Sabarinath, "An In Vitro 3D Model Using Collagen Coated Gelatin Nanofibers For Studying Breast Cancer Metastasis", *Biofabrication*, Vol. 9, No. 1, p. 15016, 2017.

135. Su, R., J. Su, K. Wang, D. Chen, C. Yang and Q. Fu, "Phase Behavior And Properties Of Polyvinyl Alcohol/Gelatin Blends With Novel Ph-Dependence", *Journal of Polymer Science Part B: Polymer Physics*, Vol. 47, No. 3, pp. 239–247, 2009.

136. Huang, C.-Y., K.-H. Hu, Z.-H. Wei, D. Qin, Y. Xia, G. M. Whitesides, K. Sheets, S. Wunsch, C. Ng, A. S. Nain, R. Dersch, T. Liu, A. K. Schaper, A. Greiner, J. H. Wendorff, E. Zussman, A. Theron, A. L. Yarin, B. Sundaray, V. Subramanian, T. S. Natarajan, P. Katta, M. Alessandro, R. D. Ramsier, G. G. Chase, Y. S. Choi, H. Akin, N. Hasirci, X. K. Li, Y. Wan, Y. Wang, G. Cheng, K. Yao, E. J. Chong, H. Nagahama, C. Weis, J. Pelipenko, N. T. B. Linh, Y. K. Min, H.-Y. Song, B. T. Lee, C. Yang, X. Wu, Y. Zhao, L. Xu, S. Wei, C. G. Anene-Nzelu, J. M. Dang, K. W. Leong, C. Ayres and E. C. Filippi-Chiela, "Comparison Of Cell Behavior On Pva/Pva-Gelatin Electrospun Nanofibers With Random And Aligned Configuration", *Scientific Reports*, Vol. 6, p. 37960, 2016.

137. Yang, D., Y. Li and J. Nie, "Preparation Of Gelatin/PVA Nanofibers And Their Potential Application In Controlled Release Of Drugs", *Carbohydrate Polymers*, Vol. 69, No. 3, pp. 538–543, 2007.

138. N.T.B., L., P. A.R., L. B.-Y. and L. B.-T., "Bilayer Electrospun Poly(Vinyl Alcohol)-Gelatin Mat And Biphasic Calcium Phosphate-Pectin-Gelatin Hydrogel For Application In Bone Hemorrhage", *Journal of Bioactive and Compatible Polymers*, Vol. 30, No. 4, pp. 424–435, 2015.

139. Linh, N. T. B., Y. K. Min, H.-Y. Song and B.-T. Lee, "Fabrication Of Polyvinyl Alcohol/Gelatin Nanofiber Composites And Evaluation Of Their Material Properties", *Journal of Biomedical Materials Research Part B: Applied Biomaterials*, Vol. 95B, No. 1, pp. 184–191, 2010.

140. Safikhani, M. M., A. Zamanian, F. Ghorbani, A. Asefnejad and M. Shahrezaee, "Bi-Layered Electrospun Nanofibrous Polyurethane-Gelatin Scaffold With Targeted Heparin Release Profiles For Tissue Engineering Applications", *Journal of Polymer Engineering*, Vol. 37, No. 9, pp. 933–941, 2017.

141. Kim, S. E., D. N. Heo, J. B. Lee, J. R. Kim, S. H. Park, S. H. Jeon and I. K. Kwon, "Electrospun Gelatin/Polyurethane Blended Nanofibers For Wound Healing", *Biomedical Materials*, Vol. 4, No. 4, p. 044106, 2009.

142. Lim, Y. C., J. Johnson, Z. Fei, Y. Wu, D. F. Farson, J. J. Lannutti, H. W. Choi and L. J. Lee, "Micropatterning And Characterization Of Electrospun Poly(-Caprolactone)/Gelatin Nanofiber Tissue Scaffolds By Femtosecond Laser Ablation For Tissue Engineering Applications", *Biotechnology and Bioengineering*, Vol. 108, No. 1, pp. 116–126, 2011.

143. Gong, M., C. Chi, J. Ye, M. Liao, W. Xie, C. Wu, R. Shi and L. Zhang, "Icariin-Loaded Electrospun PCL/Gelatin Nanofiber Membrane As Potential Artificial Periosteum", *Colloids and Surfaces B: Biointerfaces*, Vol. 170, pp. 201–209, 2018.

144. Barchuk, M., P. Čapková, Z. Kolská, J. Matoušek, D. Poustka, L. Šplíchalová, O. Benada and M. Munzarová, "Structure And Surface Properties Of Chitosan/PEO/Gelatin Nanofibrous Membrane", *Journal of Polymer Research*, Vol. 23, No. 2, p. 20, 2016.

145. Kim, H.-W., H.-S. Yu and H.-H. Lee, "Nanofibrous Matrices Of Poly(Lactic Acid) And Gelatin Polymeric Blends For The Improvement Of Cellular Responses", *Journal of Biomedical Materials Research Part A*, Vol. 87A, No. 1, pp. 25–32, 2008.

146. Farzamfar, S., F. Esmailpour, M. Rahmati, A. Vaez, M. Mirzaii, B. Garmabi, A. Shayannia, E. Ebrahimi, H. Vahedi and M. Salehi, "Poly-lactic Acid/Gelatin Nanofiber (PLA/GTNF) Conduits Containing Platelet-Rich Plasma for Peripheral Nerve Regeneration", *International Journal of Health Studies*, Vol. 3, No. 2, 2017.

147. Meng, Z., Y. Wang, C. Ma, W. Zheng, L. Li and Y. Zheng, "Electrospinning Of PLGA/Gelatin Randomly-Oriented And Aligned Nanofibers As Potential Scaffold In Tissue Engineering", *Materials Science and Engineering: C*, Vol. 30, No. 8, pp. 1204–1210, 2010.

148. Mehrasa, M., M. A. Asadollahi, K. Ghaedi, H. Salehi and A. Arpanaei, "Electrospun Aligned PLGA And PLGA/Gelatin Nanofibers Embedded With Silica Nanoparticles For Tissue Engineering", *International Journal of Biological Macromolecules*, Vol. 79, pp. 687–695, 2015.

149. Wei, J., J. Hu, M. Li, Y. Chen and Y. Chen, "Multiple Drug-Loaded Electrospun PLGA/Gelatin Composite Nanofibers Encapsulated With Mesoporous Zno Nanospheres For Potential Postsurgical Cancer Treatment", *RSC Adv.*, Vol. 4, No. 53, pp. 28011–28019, 2014.

150. Panthi, G., N. A. M. Barakat, P. Risal, A. Yousef, B. Pant, A. R. Unnithan and H. Y. Kim, "Preparation And Characterization Of Nylon-6/Gelatin Composite Nanofibers Via Electrospinning For Biomedical Applications", *Fibers and Polymers*, Vol. 14, No. 5, pp. 718–723, 2013.

151. Li, D., H. Sun, L. Jiang, K. Zhang, W. Liu, Y. Zhu, J. Fangteng, C. Shi, L. Zhao, H. Sun and B. Yang, "Enhanced Biocompatibility Of PLGA Nanofibers With Gelatin/Nano-Hydroxyapatite Bone Biomimetics Incorporation", *ACS Applied Materials & Interfaces*, Vol. 6, No. 12, pp. 9402–9410, 2014.

152. Bertram, U., D. Steiner, B. Poppitz, D. Dippold, K. Köhn, J. P. Beier, R. Detsch, A. R. Boccaccini, D. W. Schubert, R. E. Horch and A. Arkudas, "Vascular Tissue Engineering: Effects of Integrating Collagen into a PCL Based Nanofiber Material", *BioMed Research International*, Vol. 2017, pp. 1–11, 2017.

153. Nguyen, T. T. T., C. Ghosh, S.-G. Hwang, N. Chanunpanich and J. S. Park, "Porous Core/Sheath Composite Nanofibers Fabricated By Coaxial Electrospinning As A Potential Mat For Drug Release System", *International Journal of Pharmaceutics*, Vol. 439, No. 1-2, pp. 296–306, 2012.

154. Tiwari, S. K. and S. Venkatraman, "Electrospinning Pure Protein Solutions In Core-Shell Fibers", *Polymer International*, Vol. 61, No. 10, pp. 1549–1555, 2012.

155. Zahedi, E., A. Esmaeili, N. Eslahi, M. A. Shokrgozar and A. Simchi, "Fabrication and Characterization of Core-Shell Electrospun Fibrous Mats Containing Medicinal Herbs for Wound Healing and Skin Tissue Engineering", *Marine Drugs*, Vol. 17, No. 1, p. 27, 2019.

156. Khodkar, F. and N. Golshan Ebrahimi, "Preparation And Properties Of Antibacterial, Biocompatible Core–Shell Fibers Produced By Coaxial Electrospinning", *Journal of Applied Polymer Science*, Vol. 134, No. 25, 2017.

157. Song, W., X. Yu, D. C. Markel, T. Shi and W. Ren, "Coaxial PCL/PVA Electrospun Nanofibers: Osseointegration Enhancer And Controlled Drug Release Device", *Biofabrication*, Vol. 5, No. 3, p. 035006, 2013.

158. Villar, C. C. and D. L. Cochran, "Regeneration of Periodontal Tissues: Guided Tissue Regeneration", *Dental Clinics of North America*, Vol. 54, No. 1, pp. 73–92, 2010.

159. Yu, H., Y. Jia, C. Yao and Y. Lu, "PCL/PEG Core/Sheath Fibers With Controlled Drug Release Rate Fabricated On The Basis Of A Novel Combined Technique", *International Journal of Pharmaceutics*, Vol. 469, No. 1, pp. 17–22, 2014.

160. Sang, Q., H. Li, G. Williams, H. Wu and L. M. Zhu, "Core-shell poly(lactide-co-ϵ-caprolactone)-Gelatin Fiber Scaffolds As Ph-Sensitive Drug Delivery Systems", *Journal of Biomaterials Applications*, Vol. 32, No. 8, pp. 1105–1118, 2018.

161. Drexler, J. and H. Powell, "Regulation Of Electrospun Scaffold Stiffness Via Coaxial Core Diameter", *Acta Biomaterialia*, Vol. 7, No. 3, pp. 1133–1139, 2011.

162. Merkle, V. M., D. Martin, M. Hutchinson, P. L. Tran, A. Behrens, S. Hossainy, J. Sheriff, D. Bluestein, X. Wu and M. J. Slepian, "Hemocompatibility Of Poly(Vinyl Alcohol)-Gelatin Core-Shell Electrospun Nanofibers: A Scaffold For Modulating Platelet Deposition And Activation", *ACS Applied Materials and Interfaces*, Vol. 7, No. 15, pp. 8302–8312, 2015.

163. Merkle, V. M., L. Zeng, M. J. Slepian and X. Wu, "Core-Shell Nanofibers: Integrating The Bioactivity Of Gelatin And The Mechanical Property Of Polyvinyl Alcohol", *Biopolymers*, Vol. 101, No. 4, pp. 336–346, 2014.

164. Merkle, V., L. Zeng, W. Teng, M. Slepian and X. Wu, "Gelatin Shells Strengthen Polyvinyl Alcohol Core–Shell Nanofibers", *Polymer*, Vol. 54, No. 21, pp. 6003–6007, 2013.

165. Ratanavaraporn, J., R. Rangkupan, H. Jeeratawatchai, S. Kanokpanont and S. Damrongsakkul, "Influences Of Physical And Chemical Crosslinking Techniques On Electrospun Type A And B Gelatin Fiber Mats", *International Journal of Biological Macromolecules*, Vol. 47, No. 4, pp. 431–438, 2010.

166. Aldana, A. A., L. Malatto, M. A. U. Rehman, A. R. Boccaccini and G. A. Abraham, "Fabrication Of Gelatin Methacrylate (Gelma) Scaffolds With Nano- And Micro-Topographical And Morphological Features.", *Nanomaterials (Basel, Switzerland)*, Vol. 9, No. 1, 2019.

167. Lin, W.-H. and W.-B. Tsai, "In situ UV-Crosslinking Gelatin Electrospun Fibers For Tissue Engineering Applications", *Biofabrication*, Vol. 5, No. 3, p. 35008, 2013.

168. Lee, J. B., Y.-G. Ko, D. Cho, W. H. Park and O. H. Kwon, "Modification And Optimization Of Electrospun Gelatin Sheets By Electron Beam Irradiation For Soft Tissue Engineering", *Biomaterials Research*, Vol. 21, No. 1, p. 14, 2017.

169. Coussons, P. J., N. C. Price, S. M. Kelly, B. Smith and L. Sawyer, "Transglutaminase Catalyses The Modification Of Glutamine Side Chains In The C-Terminal Region Of Bovine Beta-Lactoglobulin.", *The Biochemical Journal*, Vol. 283 (Pt 3), No. Pt 3, pp. 803–6, 1992.

170. Kieliszek, M. and A. Misiewicz, "Microbial Transglutaminase And Its Application In The Food Industry. A Review.", *Folia Microbiologica*, Vol. 59, No. 3, pp. 241–50, 2014.

171. Cui, L., G. Du, D. Zhang, X. Fan and J. Chen, "Stability And Conformational Changes Of Transglutaminase From Streptomyces Hygroscopicus In Ethanol–Aqueous Medium", *Process Biochemistry*, Vol. 43, No. 8, pp. 887–891, 2008.

172. Taylor, B. L., A. Limaye, J. Yarborough and J. W. Freeman, "Investigating Processing Techniques For Bovine Gelatin Electrospun Scaffolds For Bone Tissue Regeneration", *Journal of Biomedical Materials Research Part B: Applied Biomaterials*, Vol. 105, No. 5, pp. 1131–1140, 2017.

173. Rose, J., S. Pacelli, A. Haj, H. Dua, A. Hopkinson, L. White and F. Rose, "Gelatin-Based Materials in Ocular Tissue Engineering", *Materials*, Vol. 7, No. 4, pp. 3106–3135, 2014.

174. Meng, L., O. Arnoult, M. Smith and G. E. Wnek, "Electrospinning Of In Situ Crosslinked Collagen Nanofibers", *Journal of Materials Chemistry*, Vol. 22, No. 37, p. 19412, 2012.

175. Kim, Y. J. and O. H. Kwon, "Crosslinked Gelatin Nanofibers and their Potential for Tissue Engineering", *Key Engineering Materials*, Vol. 342-343, pp. 169–172, 2009.

176. Jalaja, K., D. Naskar, S. C. Kundu and N. R. James, "Potential Of Electrospun Core–Shell Structured Gelatin–Chitosan Nanofibers For Biomedical Applications", *Carbohydrate Polymers*, Vol. 136, pp. 1098–1107, 2016.

177. Farris, S., J. Song and Q. Huang, "Alternative Reaction Mechanism For The Cross-Linking Of Gelatin With Glutaraldehyde", *J. Agric. Food Chem*, Vol. 58, pp. 998–1003, 2010.

178. Asma, C., E. Meriem, B. Mahmoud and B. Djaafer, "Physicochemical Characterization Of Gelatin-Cmc Composite Edibles Films From Polyion-Complex Hydrogels", *Journal of the Chilean Chemical Society*, Vol. 59, No. 1, pp. 2279–2283, 2014.

179. Mansur, H. S., C. M. Sadahira, A. N. Souza and A. A. Mansur, "FTIR Spectroscopy Characterization Of Poly (Vinyl Alcohol) Hydrogel With Different Hydrolysis Degree And Chemically Crosslinked With Glutaraldehyde", *Materials Science and Engineering: C*, Vol. 28, No. 4, pp. 539–548, 2008.

180. Destaye, A. G., C.-K. Lin and C.-K. Lee, "Glutaraldehyde Vapor Cross-linked Nanofibrous PVA Mat with in Situ Formed Silver Nanoparticles", *ACS Applied Materials & Interfaces*, Vol. 5, No. 11, pp. 4745–4752, 2013.

181. Zhu, B., W. Li, N. Chi, R. V. Lewis, J. Osamor and R. Wang, "Optimization of Glutaraldehyde Vapor Treatment for Electrospun Collagen/Silk Tissue Engineering Scaffolds", *ACS Omega*, Vol. 2, No. 6, pp. 2439–2450, 2017.

182. Li, D. and Y. Xia, "Direct Fabrication Of Composite And Ceramic Hollow Nanofibers By Electrospinning", *Nano Letters*, Vol. 4, No. 5, pp. 933–938, 2004.

183. Rodoplu, D. and M. Mutlu, "Effects of Electrospinning Setup and Process Parameters on Nanofiber Morphology Intended for the Modification of Quartz Crystal Microbalance Surfaces", *Journal of Engineered Fibers and Fabrics*, Vol. 118, 2012.

184. Veerabhadraiah, A., S. Ramakrishna, G. Angadi, M. Venkatram, V. Kanivebagilu Ananthapadmanabha, N. M. Hebbale NarayanaRao and K. Munishamaiah, "Development Of Polyvinyl Acetate Thin Films By Electrospinning For Sensor Applications", *Applied Nanoscience*, Vol. 7, No. 7, pp. 355–363, 2017.

185. Zhang, C., X. Yuan, L. Wu, Y. Han and J. Sheng, "Study On Morphology Of Electrospun Poly(Vinyl Alcohol) Mats", *European Polymer Journal*, Vol. 41, No. 3, pp. 423–432, 2005.

186. Butcher, A. L., C. T. Koh and M. L. Oyen, "Systematic Mechanical Evaluation Of Electrospun Gelatin Meshes", *Journal of the Mechanical Behavior of Biomedical Materials*, Vol. 69, pp. 412–419, 2017.

187. Yang, G.-Z., H.-P. Li, J.-H. Yang, J. Wan and D.-G. Yu, "Influence of Working Temperature on The Formation of Electrospun Polymer Nanofibers.", *Nanoscale research letters*, Vol. 12, No. 1, p. 55, 2017.

188. Wang, C., H.-S. Chien, K.-W. Yan, C.-L. Hung, K.-L. Hung, S.-J. Tsai and H.-J. Jhang, "Correlation Between Processing Parameters And Microstructure Of Electrospun Poly(D,L-Lactic Acid) Nanofibers", *Polymer*, Vol. 50, No. 25, pp. 6100–6110, 2009.

189. Gusarov, A. V. and I. Smurov, "Gas-Dynamic Boundary Conditions Of Evaporation And Condensation: Numerical Analysis Of The Knudsen Layer", *Physics of Fluids*, Vol. 14, No. 12, pp. 4242–4255, 2002.

190. Elliott, D. E., F. J. Davis, G. R. Mitchell and R. H. Olley, "Structure Development In Electrospun Fibres Of Gelatin", *Journal of Physics: Conference Series*, Vol. 183, p. 012021, 2009.

191. Zhou, Z., W. Xu, D. He, J. Fan, F. Yu and F. Ren, "Solid[U+2010]State Grafting Of Succinic Anhydride Onto Poly(Vinyl Alcohol)", *Journal of Applied Polymer Science*, Vol. 103, No. 2, pp. 848–852, 2007.

192. Huang, Z. M., Y. Z. Zhang, S. Ramakrishna and C. T. Lim, "Electrospinning And Mechanical Characterization Of Gelatin Nanofibers", *Polymer*, Vol. 45, pp. 5361–5368, 2004.

193. Huang, G. P., S. Shanmugasundaram, P. Masih, D. Pandya, S. Amara, G. Collins and T. L. Arinzeh, "An Investigation Of Common Crosslinking Agents On The Stability Of Electrospun Collagen Scaffolds", *Journal of Biomedical Materials Research - Part A*, Vol. 103, No. 2, pp. 762–771, 2015.

194. Linh, N. T. B. and B. T. Lee, "Electrospinning Of Polyvinyl Alcohol/Gelatin Nanofiber Composites And Cross-Linking For Bone Tissue Engineering Application", *Journal of Biomaterials Applications*, Vol. 27, No. 3, pp. 255–266, 2012.

195. Liu, X., Y. Won and P. X. Ma, "Porogen-Induced Surface Modification Of Nano-Fibrous Poly(L-Lactic Acid) Scaffolds For Tissue Engineering", *Biomaterials*, Vol. 27, No. 21, pp. 3980–3987, 2006.

196. Zha, Z., W. Teng, V. Markle, Z. Dai and X. Wu, "Fabrication Of Gelatin Nanofibrous Scaffolds Using Ethanol/Phosphate Buffer Saline As A Benign Solvent", *Biopolymers*, Vol. 97, No. 12, pp. 1026–1036, 2012.

197. Nguyen, T.-H., B.-T. Lee, T.-H. Nguyen and B.-T. Lee, "Fabrication And Characterization Of Cross-Linked Gelatin Electro-Spun Nano-Fibers", *Journal of Biomedical Science and Engineering*, Vol. 03, No. 12, pp. 1117–1124, 2010.

198. Samouillan, V., F. Delaunay, J. Dandurand, N. Merbahi, J.-P. Gardou, M. Yousfi, A. Gandaglia, M. Spina and C. Lacabanne, "The Use Of Thermal Techniques For The Characterization And Selection Of Natural Biomaterials.", *Journal of functional biomaterials*, Vol. 2, No. 3, pp. 230–48, 2011.

199. Linh, N. T. B., Y. K. Min, H.-Y. Song and B.-T. Lee, "Fabrication Of Polyvinyl Alcohol/Gelatin Nanofiber Composites And Evaluation Of Their Material Properties", *Journal of Biomedical Materials Research Part B: Applied Biomaterials*, Vol. 95B, No. 1, pp. 184–191, 2010.

200. Xiao, C.-D., X.-C. Shen and L. Tao, "Modified Emulsion Solvent Evaporation Method For Fabricating Core–Shell Microspheres", *International Journal of Pharmaceutics*, Vol. 452, No. 1-2, pp. 227–232, 2013.

201. Chen, H.-C., W.-C. Jao and M.-C. Yang, "Characterization Of Gelatin Nanofibers Electrospun Using Ethanol/Formic Acid/Water As A Solvent", *Polymers for Advanced Technologies*, Vol. 20, No. 2, pp. 98–103, 2009.

202. Dowling, D. P., I. S. Miller, M. Ardhaoui and W. M. Gallagher, "Effect Of Surface Wettability And Topography On The Adhesion Of Osteosarcoma Cells On Plasma-Modified Polystyrene", *Journal of Biomaterials Applications*, Vol. 26, No. 3, pp. 327–347, 2011.

203. Huang, F., Q. Wei, Y. Cai and N. Wu, "Surface Structures And Contact Angles Of Electrospun Poly(Vinylidene Fluoride) Nanofiber Membranes", *International Journal of Polymer Analysis and Characterization*, Vol. 13, No. 4, pp. 292–301, 2008.

204. Huang, F. L., Q. Q. Wang, Q. F. Wei, W. D. Gao, H. Y. Shou and S. D. Jiang, "Dynamic Wettability And Contact Angles Of Poly(Vinylidene Fluoride) Nanofiber Membranes Grafted With Acrylic Acid", *Express Polymer Letters*, Vol. 4, No. 9, pp. 551–558, 2010.

205. Phromsopha, T. and Y. Baimark, "Preparation of Starch/Gelatin Blend Microparticles by a Water-in-Oil Emulsion Method for Controlled Release Drug Delivery", *International Journal Of Biomaterials*, Vol. 2014, p. 829490, 2014.

206. Figueiredo, K. C. S., T. L. M. Alves and C. P. Borges, "Poly(Vinyl Alcohol) Films Crosslinked By Glutaraldehyde Under Mild Conditions", *Journal of Applied Polymer Science*, Vol. 111, No. 6, pp. 3074–3080, 2009.

APPENDIX A:

A.1. Gelatin Fibers Obtained From Acetic Acid/Deionized Water Solution

Acetic acid and deionized water was used as solvent at 3/1 ratio to prepare 8% gelatin solution. Operational conditions were: feed rate at 0.1 ml/h, electrode distance 15 cm, voltage 15 kV and environmental conditions were 40 ^{o}C and a relative humidity level of below 44.

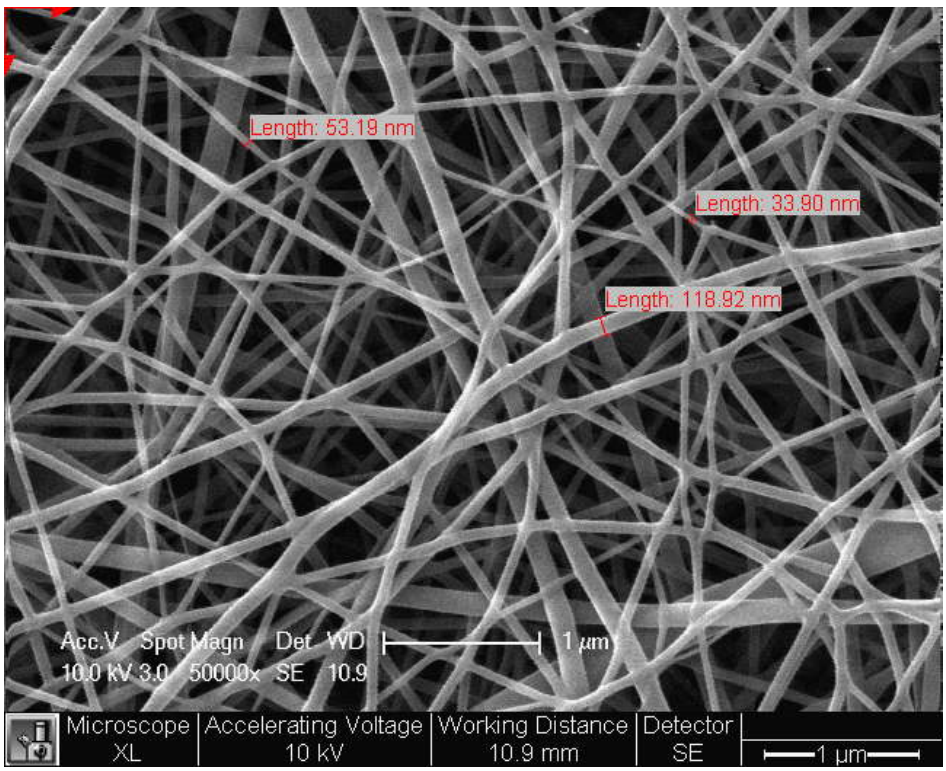

Figure A.1. ES of gelatin dissolved in acetic acid 50000X.

ES of pure aqueous gelatin exhibits beaded morphology vastly due to high surface tension. Those beads are the non-uniform parts which will raise stress for the body cells that prevents adhesion and proliferation on them. Acetic acid has been used to dissolve gelatin for the fabrication of uniform fibers. Although fibers of acetic acid and water combinations display uniform structures, they contain acetic acid peaks in FTIR analysis which will have negative effect on the cell proliferation.

Also, acid-induced degradation rates of acidic solvent and natural polymer combination is high as stated in the literature.

As can be depicted from Figure A.1, as spun nanofibers constituted from secondary jet branches departed from primary jet. This can be detected by focusing on the conjunction points of at least 3 branches.

A.2. Electrode Distance

Effect of electrode distance on the fiber morphology was not significant for core-shell nanofibers. Ki *et al.* (2009) also tested four different electrode distance and concluded that electrode distance does not have any effect on the fiber diameter.[187]

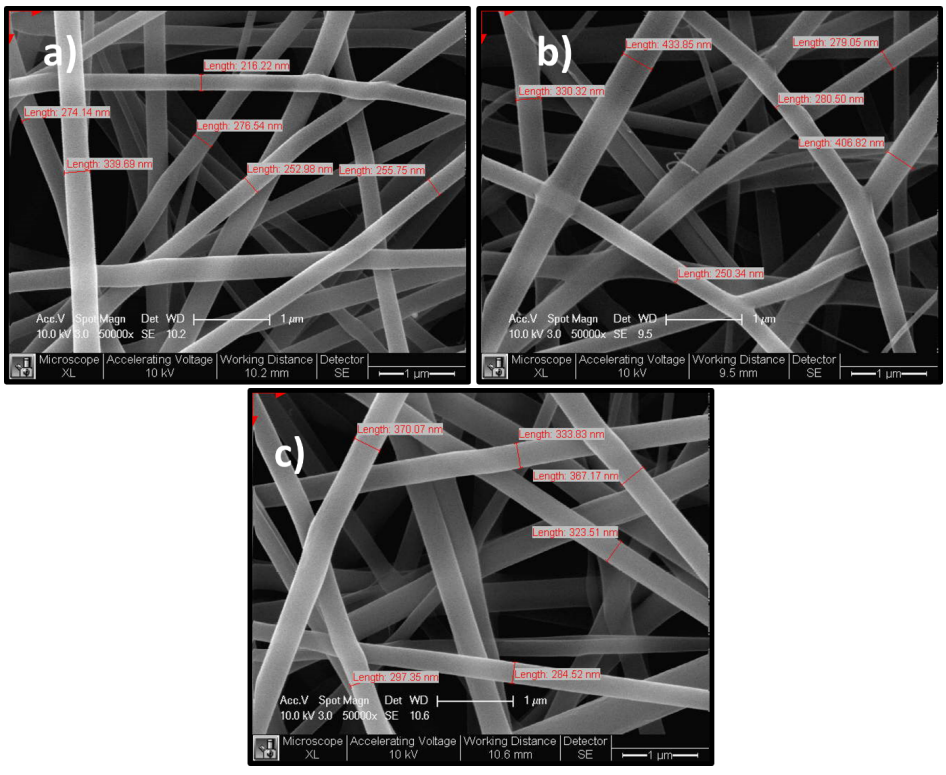

Figure A.2. Electrode Distance effect on the fiber size distance a)10 cm b) 15 cm c) 20 cm, at voltage 20 kV, PVA feed rate 0.2 ml/h, gelatin feed rate of 0.2 ml/h and temperature 40 ° C.